AN INVESTIGATION INTO THE CRITICAL DOMAINS AND FUNCTION OF XMI-ER1 DURING XENOPUS DEVELOPMENT

YOELLA TEPLITSKY

AN INVESTIGATION INTO THE CRITICAL DOMAINS AND FUNCTION OF XMI-ER1 DURING XENOPUS DEVELOPMENT

By

© YOELLA TEPLITSKY

A thesis submitted to the

School of Graduate Studies

in partial fulfillment of the

requirements for the degree of

Master of Science

Division of Basic Medical Science
Faculty of Medicine
Memorial University of Newfoundland

October 2003

St. John's Newfoundland

Your file Votre référence
ISBN: 0-612-99121-0
Our file Notre référence
ISBN: 0-612-99121-0

Abstract

The FGF signal transduction pathway has been linked to many events that occur throughout vertebrate development. Model systems, such as the amphibian *Xenopus laevis*, have been used to define numerous components of this signalling cascade. One such discovery was *Xmi-er1*, a maternally derived immediate-early gene in the FGF pathway thought to act in transcriptional regulation. The purpose of this project was to further characterize the activity of XMI-ER1 in the developing *Xenopus* embryo and to explore how this activity relates to its molecular structure.

Over-expression of *Xmi-er1* resulted in truncations along the anteroposterior axis. These abnormalities first become apparent during gastrulation. Analysis of tissue development using antibodies demonstrated that both mesodermal and neural tissues are affected by *Xmi-er1* over-expression, yet differentiation still occurs in the most severe cases. In FGF-induced mesoderm induction, this event was partially inhibited in the presence of excess XMI-ER1. No analogous inhibition was observed with mesoderm induction by activin. Also suppressed was part of the expression pattern of the early mesodermal marker, *brachyury*. Subsequent examination of the various domains present in the protein implicated a proline-rich region in the over-expression activities of XMI-ER1 throughout development, however the investigation failed to connect both the SANT domain and the ELM2 domain to this effect. Overall, these results indicate that XMI-ER1 functions in some FGF-related cellular activities, such as mesoderm induction, but

that its role may not be limited to this pathway. This function appears to be dependent upon the proline-rich region.

Acknowledgements

First and foremost I would like to thank my supervisor, Dr. Laura Gillespie, for all her help, support, and guidance. I feel as though I have grown and learned so much in my three years here and that this began the day I started working with you. The wonderful experience that I have gained here would not be the same were it not for your part in it. Thank you.

I also wish to thank my committee members, Dr. Gary Paterno and Dr. Ken Kao, for guiding me through this project and for showing me the true value of what it means to be a graduate student. I will forever remember your wisdom and commitment. Thanks.

I would like to express my utmost gratitude to the wonderful people in the Terry Fox Labs. To Paula, Corinne, and Yuan, thank you so much for all your help, for always having an answer to my questions, for complying with my recycling wishes and dry ice requests, and for always being there in times of need, of which there were many. I loved working with each of you and have learned so much from you, both in the lab and out. To Rebecca, Artee, Janine, Gord, Ding, Marianne, Tina, Ivy, Blue, Kelly, and Phil, thanks for your help and for putting up with my music and singing and antics. It's been fun. Because of you, I will always remember my time here with a smile.

I would also like to thank my family and especially parents for all their support, their love, and for always being willing to visit me no matter how far away I stray - whether it's the rugged wilderness of Newfoundland, the rainforests of Costa Rica, or the hot deserts of Israel.

And last but not least, I would like to thank my friends, both near and far. To Erin, for encouraging me to go to grad school and for being such a great role model. To Showsh, Jenn, and Aimee, for remaining so close in my heart that I have never felt like we were more than five minutes away from each other. And to Paula, Cory, Cole, and Chase. Thanks for giving me a family when mine was so far away. I will never forget how kind you have been to me. When people speak of how nice Newfoundlanders are, it is most certainly you that they have in mind. Here's to the memories.

Table of Contents

List of Figures

List of Tables

List of Abbreviations

A	animal
aa	amino acid
AP	alkaline phosphatase
AP-GAM	alkaline phosphatase goat anti-mouse
ATP	adenosine triphosphate
BA:BB	benzyl alcohol: benzyl benzoate
β-gal	beta galactosidase
BMB	Boehringer Mannheim blocking buffer
BMP	bone morphogenic protein
BSA	bovine serum albumin
C	celsius
cRNA	complementary ribonucleic acid
DAI	dorso-anterior index
DEPC	diethyl pyrocarbonate
DNA	deoxyribonucleic acid
dNTP	deoxyribonucleotide phosphate
DV	dorsovegetal
ECM	extracellular matrix
EDTA	ethylenediamine tetraacetic acid
EGTA	ethylene glycol-bis-N,N,N',N'-tetraacetic acid
ELM2	EGL-27 and MTA1 homology domain 2
FGF	fibroblast growth factor
FGFR	fibroblast growth factor receptor
g	grams
GFP	green florescent protein
GSK	glycogen synthase kinase
HCG	human chorionic gonadotrophin
HDAC	histone deacetylase
HRP	horseradish peroxidase
IU	international units
Ig	immunoglobulin
L	litre
LB	Luria-Bertani
M	molar
MAB	maleic acid buffer
MAPK	mitogen activated protein kinase
MAPKK	MAP kinase kinase
MBT	mid-blastula transition
MEKK	MEK kinase
μg	microgram

µl	microlitre
MI-ER1	mesoderm induction early response 1
mg	milligram
ml	millilitre
mM	millimolar
mRNA	messenger ribonucleic acid
N/A	not applicable
NAM	normal amphibian medium
ng	nanogram
nl	nanolitre
NLS	nuclear localization signal
O	organizer
PAGE	polyacrylamide gel electrophoresis
PBS	phosphate buffered saline
PBSA	phosphate buffered saline amphibian
PBSAT	PBSA + 0.1% Tween-20
PCR	polymerase chain reaction
PI3K	phosphoinositide 3 kinase
PKC	protein kinase C
PLCγ	phospholipase C gamma
RNA	ribonucleic acid
RNAi	RNA interference
rpm	revolutions per minute
RTK	receptor tyrosine kinase
SANT	SWI3, ADA2, N-CoR, and TFIIIB
SDS.	sodium dodecyl sulphate
SEP	sperm entry point
SH2	src homology 2
SH3	src homology 3
SSC	sodium chloride and sodium citrate
TBS-T	tris buffered saline-tween
TCA	trichloroacetic acid
TGFβ	transforming growth factor beta
UV	ultraviolet
V	vegetal
VV	ventrovegetal
Xbra	*Xenopus* brachyury
Xbra-En^R	Xbra construct with Engrailed repressor
Xcad3	*Xenopus* caudal
XFD	dominant negative FGF receptor
Xgsc	*Xenopus* goosecoid
Xsna	*Xenopus* snail

Chapter 1: Introduction

1.1 *Xenopus laevis* as a model system

Embryos from the amphibian *Xenopus laevis*, also known as the African Clawed Frog, have been used in the laboratory as a model system for decades. They were initially employed as a pregnancy test for women, although in recent years their primary use has been in the study of developmental mechanisms in vertebrates. There are a number of reasons why this species is preferred for such studies. One main advantage is the fact that the eggs develop outside of the female. This means that not only are they easily accessible to the researcher, but because development is external the presence of yolk in the egg is essential, causing the eggs themselves to be quite large in size (Jones & Smith, 1995). This makes them very easy to handle and manipulate. A second benefit is that the eggs are relatively simple to obtain at all times of the year, even in comparison with other amphibian species. This is accomplished by the injection of the hormone human chorionic gonadotrophin, or HCG. As well, the adult frogs are quite robust and often thrive in the laboratory setting.

The rapid development of the embryos into tadpoles is another advantage. Many researchers use this quality to investigate the function of a particular gene during development. This can be done by injecting a recently fertilized egg with a small amount of mRNA, letting the embryo develop, and then observing the tadpole for any effects the over-expressed gene may have had on its growth and development. As well, loss-of-function studies with this species are now becoming quite common in order to examine

the opposite scenario. This is accomplished through new techniques such as morpholino antisense oligonucleotides and RNA interference (RNAi). Studies such as these have revealed an increasingly intricate array of cellular and molecular interactions that are necessary for the proper development of eggs into tadpoles and ultimately viable adults. Therefore, the importance of *X. laevis* to the evolution of developmental biology has been tremendous.

1.2 Early development of *X. laevis*

During the development stages of *X. laevis*, the fertilized egg grows from a single cell into a complex organism (Figure 1.1) with many different tissue types and a defined body plan. The method by which this is achieved has been the focus of much investigation. It is now thought that this early development is characterized by three major steps: (1) the establishment of the dorsoventral axis; (2) the designation of the three prospective germ layers; and, (3) the various movements involved in gastrulation (Kuhl, 2002).

The first of these steps occurs soon after fertilization. When the eggs are initially laid, they are polarized along the animal-vegetal axis. The animal half or hemisphere is darkly pigmented, while the vegetal hemisphere is unpigmented. At this point the eggs possess a random orientation with respect to gravity and there is no indication of the dorsoventral axis. The sperm can enter the egg at any point in the animal hemisphere.

Once it does, the egg undergoes cortical granule release. Cortical granules are membrane-bound structures containing enzymes and proteins that are located in a layer

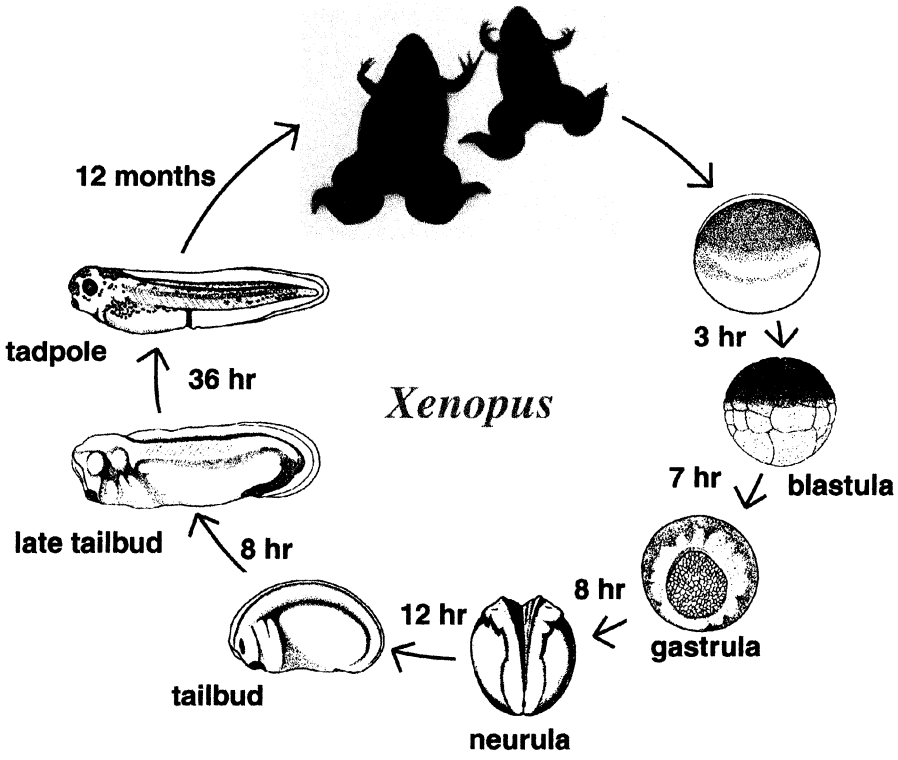

Figure 1.1 The lifecycle of *X. laevis*

The above diagram demonstrates the entire lifecycle of *X. laevis* from a single-celled egg all the way to a tadpole and then an adult. Reproduced from:

http://www.xenbase.org/intro.html.

directly beneath the plasma membrane. The cortical granule release enables the egg to rotate such that the denser vegetal hemisphere is down. During this process, the granules fuse with the plasma membrane and release their contents into the space between the egg and the vitelline membrane surrounding it. This is a protective membrane forming a fibrous mat around the egg that is essential for species-specific sperm binding and for the prevention of polyspermy.

Soon after this event, the cytoplasm undergoes a rearrangement as well based on the location of the sperm entry point, or SEP, as shown in Figure 1.2. The cortical or outer layer of cytoplasm shifts by approximately 30° toward the SEP (Manes & Elinson, 1980; Vincent *et al.*, 1986), driven by a parallel array of microtubules that lies between the cortical and inner cytoplasm in the vegetal hemisphere (Elinson & Rowning, 1988). These microtubules are thought to provide tracks that allow the cortex to move. This movement ultimately defines the future dorsoventral axis of the embryo, with the side opposite the SEP being dorsal. The newly established dorsal vegetal region encompasses a signalling centre named after the famous embryologist, Peter Nieuwkoop. It is therefore often referred to as the Nieuwkoop centre and provides a dorsalizing signal to be discussed in further detail later (reviewed in Harland & Gerhart, 1997; Jones & Smith, 1995).

During the early cleavage stages that follow fertilization, the embryo goes from a single cell to a multi-cellular organism in a remarkably short amount of time. Maternally derived stores of mRNA and protein regulate this process until stage 8 according to Nieuwkoop (1994). These maternal cytoplasmic determinants are asymmetrically

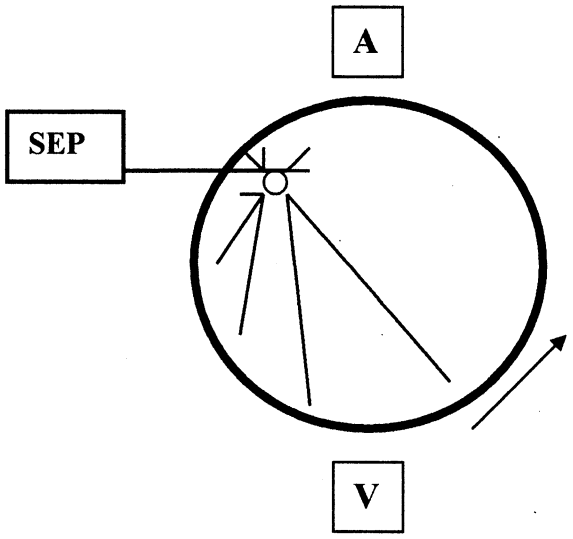

Figure 1.2 Cross section of the egg during cortical rotation

The two hemispheres of the egg are indicated as animal, A, and vegetal, V. The sperm entry point, or SEP, is highlighted in the animal hemisphere on the left. Once the egg is fertilized, microtubules align and the cortex located opposite the SEP rotates 30° in the direction of the arrow at the bottom right. Adapted from Harland & Gerhart (1997).

arranged throughout the embryo and this, together with cell-cell signalling, defines development throughout these early stages (McDowell & Gurdon, 1999).

The first cell cycle takes approximately 90 minutes, and the first cleavage, occurring at the end of this cycle, usually passes through the SEP and separates the prospective right and left sides of the embryo. Subsequent divisions generally require only 30 minutes to complete, with the second one also occurring along the animal-vegetal axis perpendicular to the first. This divides the future dorsal and ventral poles in the embryo and these can often be identified by the slightly smaller size of the dorsal cells or blastomeres. The third cleavage occurs in the equatorial region at a right angle to the first two divisions, and separates the animal and vegetal hemispheres. As these cleavages proceed, a small space forms inside the developing embryo that ultimately becomes the blastocoel, a large cavity significant during the blastula stages of development (Jones & Smith, 1995).

From stage 6.5 to 9 the embryo is referred to as a blastula. During this step, the embryo grows from a single to a double layer of cells. By cell cycle 13, corresponding to stage 8 of development according to Nieuwkoop (1994), an event known as the mid-blastula transition (MBT) occurs (Newport & Kirchner, 1982). At this time, the previously synchronous pattern of rapid divisions slows down and shifts to an asynchronous one. As well, it is at this point in development that zygotic transcription and cell motility begins (Newport & Kirschner, 1984).

The next phase is gastrulation, in which the hollow blastula becomes a three-layered structure. This phase encompasses the aforementioned steps 2 and 3 of early *X.*

laevis development. Gastrulation is characterized by a series of movements, as the prospective endoderm cells move inward at the dorsal side of the vegetal pole forming a visible structure known as the dorsal lip. This activity extends laterally, and, as more cells follow in this movement, the lip grows first into an arc and eventually into a full circle. Meanwhile, some of the prospective mesoderm cells that have recently been specified inside the embryo begin to migrate along the blastocoel roof at the dorsal region. The remaining mesodermal cells eventually join in with this movement by a process of convergent extension. That is, the cells intercalate causing the tissue to narrow and at the same time they move forward. As these movements continue, the outside of the embryo becomes completely surrounded by the cells of the animal hemisphere, which will eventually form the ectoderm. By the end of gastrulation, the three layers have reached their desired positions within the embryo. Underneath the outer ectoderm layer now lies the mesoderm, and beneath this is the endoderm. In this way, the three germ layers are established and organized, thus completing steps 2 and 3 of the development process.

With respect to the outcome of these germ layers, fate maps of the embryo at various stages of development provide a clear picture of the structures that develop from each tissue. Knowledge of the fates of these cells during normal development enables researchers to investigate abnormal development, especially when the abnormality is caused by the intentional over- or under-expression of a particular gene. These fate maps demonstrate that the ectoderm eventually becomes the epidermis and nervous system. The mesoderm forms the notochord, the somites, the urinary system, and the genital

ducts. Parts of it also develop into the heart, blood vessels and cells, as well as some tissue in the head. As well, the endoderm ultimately forms the lining of the digestive and respiratory tubes along with their respective organs.

Following gastrulation is the formation of the neural tube during neurulation, involving yet another set of intricate movements. The neural plate undergoes convergent extension in a manner similar to the mesoderm during the previous stage. Later on, the neural tube forms from the dorsal ectoderm. Also beginning in this phase and continuing after it, the mesoderm differentiates into various tissues along the dorsoventral axis. These events ultimately result in the formation of a complete tadpole. For a summary of the lifecycle of *X. laevis*, refer to Figure 1.1.

1.3 *X. laevis* patterning and mesoderm induction

Cells of the early embryo are considered to be pluripotent. That is, they can develop into different tissues depending on their environment. However, as development progresses, cells eventually lose the ability to differentiate into alternate cell types and in this way they become committed to one particular fate. This fate results largely from cellular interactions within the early embryo. It is these interactions, which occurs both between cells and between tissues, that ultimately pattern the organism (Chang & Hemmati-Brivanlou, 1998). With respect to the *X. laevis* embryo, the full range of processes involved in its patterning are not completely understood. Nevertheless, advances made in the past few years have clarified many uncertainties regarding this complex event.

When the egg is first laid, differences already exist along the animal-vegetal axis. Maternally derived proteins are thought to be precisely localized within the egg at this time. The patterning events that follow elaborate upon this initial arrangement. The first of these begins in the early embryo soon after fertilization. During cortical rotation, the cortex of the egg rotates 30° with respect to the inner cytoplasm. Also at this time, a set of organelles in the vegetal pole moves 60-90° to the prospective dorsal side of the embryo (Rowning *et al.*, 1997). These events are thought to distribute a dorsal determinant to the side of the egg opposite sperm entry (*i.e.*, the Nieuwkoop centre), ensuring that dorsal structures develop from this area. Evidence indicates that this determinant moves from the vegetal pole to the future dorsal side, and that its activity is transplantable (Moon & Kimelman, 1998). This is the first major patterning event that occurs in the embryo. Stemming directly from this organizational event is a second one that establishes the future mesoderm of the frog. This is known as mesoderm induction.

The process of mesoderm induction was first described by Pieter Nieuwkoop in 1969. In one of his most famous experiments, he joined parts of the animal cap together with explants from the vegetal pole and was able to induce the animal cap cells to form mesoderm instead of ectoderm, which is what would normally arise if these cells were left in isolation (Nieuwkoop, 1969). It is now well known that in *X. laevis* the mesoderm develops from the ring of cells located along the equatorial region of the blastula. The specification of the cells in this region occurs during the cleavage divisions such that by the mid-blastula transition, at approximately the 4000-cell stage, many of the mesoderm-specific genes in these cells are already turned on (Harland & Gerhart, 1997).

During the early stages of development, the embryo consists of only two cell types – the prospective ectoderm in the animal pole and the prospective endoderm in the vegetal pole. Mesoderm induction does not begin until the 64-cell stage (Smith, 1993) and involves signals originating from the cells in the vegetal pole of the embryo. In general, there are many differing views on how mesodermal patterning takes place, however three important trains of thought have developed over the years. In the first and earliest view that is derived from the aforementioned experiment by Nieuwkoop, the mesoderm and head endoderm are believed to be formed by the interaction between the cells of the animal hemisphere with those of the vegetal pole. This view holds that the signal produced by the vegetal cells forms a gradient from the dorsal to the ventral side thus enabling the induction of different types of mesoderm along the equatorial region (Harland & Gerhart, 1997).

The second view was the 'three-signal' model for mesoderm formation put forth by Smith and Slack (1983) (Figure 1.3). This model proposed that early cytoplasmic rearrangements cause two inductive centres to be established within the vegetal hemisphere of the *X. laevis* embryo – one located in the dorsal region and one in the ventral. Later on during the blastula stages, the dorso-vegetal cells induce the overlying cells in the marginal zone to form a region known as the organizer, while the ventro-vegetal cells induce the formation of ventral mesoderm also in the overlying marginal zone. It is the organizer that then produces the third signal referred to in this model. This does not occur until gastrulation (Harland & Gerhart, 1997) at which point it has a dorsalizing effect on the adjacent mesoderm and induces it to form intermediate

mesoderm (Smith & Slack, 1983; Dale *et al.*, 1985). The ability of these cells to 'organize' embryonic development was discovered through the early work of Spemann and Mangold (Harland & Gerhart, 1997). For this reason, the organizer is often referred to as the 'Spemann Organizer'.

In the current model, which has superseded the previous two, the body plan is thought to be organized by two maternal determinants present in the early embryo, one that controls mesoderm/endoderm development and a second that regulates dorsal development (Heasman, 1997). The latter event involves signalling through the Wnt/β-catenin pathway (Harland & Gerhart, 1997), while the former is regulated by the T-box transcription factor, VegT (Zhang *et al.*, 1998; Kofron *et al.*, 1999). This molecule has been found to be localized to the vegetal cortex of the oocyte and its presence leads to the expression of mesoderm inducers, which in turn signal the development of mesoderm in the marginal zone after MBT (reviewed in Kimelman & Griffin, 2000). The signalling events that power primary germ layer formation and dorsalization act through overlapping yet distinct signalling pathways (Lee *et al.*, 2001).

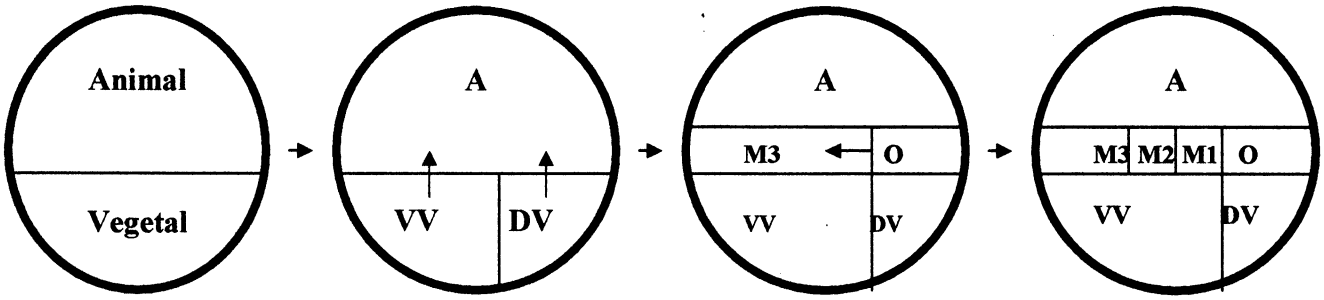

Figure 1.3 The three-signal model of mesoderm induction

In the early embryo, the vegetal hemisphere is divided into the ventro-vegetal (VV) and the dorso-vegetal (DV) regions. During mesoderm induction, the VV cells induce the overlying marginal zone cells to form ventral mesoderm (M3), and the DV cells induce the equatorial cells above to form the organizer (O). The organizer then signals the ventral mesoderm to differentiate into lateral mesoderm (M1 and M2). Adapted from Dale and Slack (1987).

1.4 Mesoderm inducing signals

By varying the signals produced by the vegetal blastomeres, or by changing the intensity of the signals or how cells respond to them, different types of mesoderm can be induced. Initially this induction event was thought to take place very early on in development, however it is now known that while these signals appear at low levels prior to zygotic gene transcription, they become much stronger after MBT (Zhang *et al.*, 1998). In general, the signals produced during mesoderm induction are active from the 64-cell stage until early gastrula. Many of these result from distinct but overlapping signal transduction pathways. They are the triggers thought to carry out the mesoderm induction models discussed previously, however the exact molecules involved have yet to be fully agreed upon.

There are two problems often encountered in trying to identify potential inducers (Christen & Slack, 1999). The first is that even if the gene expression of the inducer is confirmed at the mRNA level, there is no guarantee that it will be translated into protein, secreted, and processed in the correct manner. The second problem involves the idea of biological redundancy. If the factor under investigation does function as a true mesoderm inducer in the embryo there is still the possibility that other unidentified factors exist that can stimulate the same receptor or act in the same way. Nevertheless, by acknowledging these problems and by implementing the proper controls for them, it is still possible to pinpoint active inducing molecules.

With respect to the zygotic signals, much of the data in this area stems from 'animal cap' experiments in which an explant is taken from the prospective ectoderm of a

blastula stage embryo and incubated with potential inducers in an attempt to pinpoint the actual molecules responsible for mesoderm induction in the embryo. Although this method has made it relatively easy to discover proteins that can induce mesoderm from ectoderm *in vitro*, confirming the activities of these molecules in the whole embryo has been quite difficult. Nevertheless, through years of experimentation and debate, a few key signals have been identified.

In general, there appears to be a variety of molecules involved in the process of mesoderm induction (Harland & Gerhart, 1997). One of the earliest known signals is VegT, a maternally derived T-box transcription factor localized in the vegetal hemisphere. This factor is responsible for activating the zygotic signals that regulate mesoderm induction (Zhang *et al.*, 1998) and comprises the early low-level mesoderm induction signal mentioned earlier. VegT is known to activate several members of the transforming growth factor β (TGFβ) superfamily, including a number of nodal-related genes. These signals appear to be active during the cleavage and blastula stages of embryogenesis. Bone morphogenic proteins (BMPs), which are a subgroup of TGFβ-like molecules, function in the specification of ventral character in the mesoderm during gastrulation (Heasman, 1997). On the other hand, β-catenin has a dorsalizing effect during development and appears to be involved in regulating the expression of some mesodermal genes (Vonica & Gumbiner, 2002), while fibroblast growth factors (FGFs) are required for mesodermal maintenance (Isaacs *et al.*, 1994) and competence (Cornell *et al.*, 1995).

The involvement of the TGFβ pathway in mesoderm induction has been

confirmed by experiments involving a dominant negative TGFβ family receptor, as mesoderm formation is inhibited in embryos expressing this inactive receptor (Hemmati-Brivanlou & Melton, 1992). Members of this family that are thought to be involved in mesoderm induction include *Derrière*, and the *nodal related* genes *Xnr1*, *Xnr2*, and *Xnr4*, *-5*, and *–6* (Jones *et al.*, 1995; Joseph & Melton, 1997; Sun *et al.*, 1999; Takahashi *et al.*, 2000). These genes are expressed at the right time and place in the embryo to act as endogenous inducers (White *et al.*, 2002). While the *Xnrs* appear to be required throughout the body, *Derrière* may only be necessary for trunk and tail development (Kofron *et al.*, 1999; Sun *et al.*, 1999; Kimelman & Griffin, 2000).

Vg1 and activin, which are part of the TGFβ family as well, are also thought to play a role in mesoderm induction. Activins are known to possess potent mesoderm-inducing activity in animal cap experiments (Green & Smith, 1990). These inductions result in increasingly dorsal mesoderm as the concentration of activin is increased. Although its activity *in vivo* is somewhat controversial, activin has recently been found to be required for the induction of both mesoderm as well as endoderm (Lee *et al.*, 2001). Vg1 is a maternally expressed protein localized to the vegetal pole of cleavage stage embryos (Weeks & Melton, 1987). However, it should be noted that TGFβ-related molecules form disulfide-linked dimers that must be cleaved to release the mature, active protein. For Vg1, this cleaved form has yet to be found in the early embryo suggesting that its activity is tightly regulated throughout development (Kessler & Melton, 1994). Nevertheless, inhibition of this molecule using dominant negative mutants causes dorsal mesodermal defects (Joseph & Melton, 1998).

Also involved in mesoderm induction are the BMPs. Several maternally derived mRNAs have been identified in the early embryo, including BMP2, BMP4, and BMP7, although their respective functions are still unclear (Heasman, 1997). These molecules are thought to be involved in the specification of ventral mesoderm as activation of their signalling pathways in the mesoderm assigns a ventral character to this tissue (Dale *et al.*, 1992). In mesoderm induction assays, BMP4 has been found to induce ventral mesodermal tissues (Dale *et al.*, 1992; Kessler & Melton, 1994). Likewise, interference with the BMP signal inhibits the development of ventral mesoderm (Maeno *et al.*, 1994). While the *in vivo* involvement of BMPs in mesoderm induction has yet to be confirmed, the machinery for their pathway is well in place by the time this process begins, making them good candidates for mesoderm inducers (Eimon & Harland, 1999).

With respect to dorsal specification, β-catenin is a key determinant. It is the principle downstream target of the Wnt-1 signalling pathway and functions as a transcription factor once activated. Its levels are regulated by the upstream serine-threonine kinase known as glycogen synthase kinase, or GSK3 (Moon & Kimelman, 1998). β-catenin is known to be present in the early *X. laevis* embryo. Both over-expression and depletion studies have implicated this as a key endogenous molecule necessary for determining the dorsoventral axis. Interference with maternal β-catenin causes embryos to develop without dorsal structures (Heasman *et al.*, 1994). Overall, its levels are increased very early on in the embryo at the prospective dorsal side opposite the SEP. It continues to accumulate in all cells until the 16- to 32-cell stage, at which point its levels only rise higher in the dorsal blastomeres. Furthermore, β-catenin is

known to be involved in a complex with XTcf-3 (Molenaar *et al.*, 1996), and may function in the activation of organizer genes, such as *Siamois*, during mesoderm induction (Moon & Kimelman, 1998).

Of the FGFs, FGF-2 was the first to be implicated in mesoderm induction (Kimelman & Kirschner, 1987; Slack *et al.*, 1987). It was initially found to be a potent inducer of ventral mesoderm but later work demonstrated that FGF was involved in the formation of dorsal mesoderm as well (Harland & Gerhart, 1997). Much of this work was based upon dominant negative experiments with a mutant FGF receptor, XFD (discussed below), and on interference with downstream signals (Amaya *et al.*, 1991; Amaya *et al.*, 1993). It is now thought that the FGFs act in mesodermal maintenance rather than induction. The FGF family of proteins and their signalling pathways will be discussed in greater detail in the next section.

1.5 Fibroblast growth factors

Many members of the fibroblast growth factor family of proteins are involved in controlling cell growth, differentiation, and movement throughout the development of *X. laevis*. FGF activity has been implicated in both mesoderm formation as well as axial patterning. The proteins are expressed in the animal cap and marginal zone of the blastula stage embryo (Curran & Grainger, 2000). FGF signalling has also been shown to be required for mesoderm induction. In 1991, Amaya *et al.* found that embryos expressing a truncated and therefore inactive form of the FGF receptor known as XFD could completely abolish wild-type receptor function. Explants from these embryos

failed to respond to FGF to induce mesoderm and whole embryos had gastrulation defects and abnormal posterior development, thus implicating FGF signalling in early embryogenesis and in the development of posterior and lateral mesoderm (Amaya *et al.*, 1991). The role of FGF signalling was examined further when Amaya *et al.* found that the XFD protein inhibits the marginal zone expression of *Xenopus brachyury* (*Xbra*), a known immediate-early gene for FGF, yet it fails to affect the expression of *Xenopus goosecoid* (*Xgsc*), which is expressed dorsally in the first mesodermal cells that involute during gastrulation (1993). Later, Kroll and Amaya created transgenic frogs that only expressed the XFD construct after MBT when much of the mesoderm in the embryo is already induced and found that *Xbra* expression is lost in the mesoderm by mid-gastrulation and that the embryos lack a notochord and somites (1996). In this way, they demonstrated that FGF signalling is necessary for the maintenance of mesoderm.

The fibroblast growth factors belong to a large family of signalling molecules with a wide variety of biological functions. All members of the family are known to bind to heparin and heparan sulphate, and were therefore originally named as heparin-binding growth factors. However, the nomenclature has since changed due to the fact that many unrelated proteins are also known to bind heparin. This attribute nonetheless continues to play a big role in the behaviour of these proteins. Its purpose is thought to be twofold: (1) to protect FGFs from degradation; and, (2) to create a local pool of available growth factors (Powers *et al.*, 2000). The structural similarity between the members of the FGF family ranges from 40% to more than 70% amino acid sequence identity (Manetti *et al.*, 2000). In general, FGFs are defined by a central core of 140 amino acids that are highly

conserved between families (Powers *et al.*, 2000). Most act extracellularly through the activity of a high affinity receptor. Yet, three members lack the classical leader sequences targeting them for secretion. It is thought that these forms are transported to the extracellular space via an alternate mechanism (reviewed in Powers *et al.*, 2000).

Overall the FGF family consists of at least 20 different polypeptides. Of these, seven have been shown to be active in mesoderm induction assays using animal caps from *X. laevis* (reviewed in Isaacs, 1997). When investigating which proteins are active in the embryo during patterning, it is important to consider the presence of secretory signal peptides (Isaacs, 1997). FGFs both with and without these peptides are found in the early embryo. So far, there are a total of four FGFs that are known to be present in *X. laevis*. These include basic FGF (bFGF or FGF-2), int-2 (FGF-3), embryonic FGF (eFGF), and FGF-9, although int-2 mRNA does not appear until after MBT (Tannahill *et al.*, 1992; Isaacs, 1997; Kimelman & Kirschner, 1987). The remaining three are therefore good mesoderm inducing candidates, while all four are probably involved in mesoderm maintenance and post-MBT patterning as they are all expressed in the mesoderm after MBT (Isaacs, 1997).

Basic FGF, and the closely related acidic FGF (aFGF), were the first two FGFs to be identified and characterized (Gospodarowicz, 1974; Gospodarowicz *et al.*, 1975; Gospodarowicz *et al.*, 1986; Gospodarowicz, 1987). FGF-2 protein is present at low levels in the early embryo prior to the onset of zygotic transcription, indicating that it is maternally derived. These levels increase at mid-neurula stages when zygotic transcription of this gene is activated (Song & Slack, 1994). Localization during blastula

stages is predominantly in the animal hemisphere. This, together with the fact that it lacks a signal peptide and that antibodies against it fail to block mesoderm induction (Slack, 1991), suggest that this is not part of the mesoderm inducing signal originating from the vegetal pole (Isaacs, 1997).

As discussed earlier, FGF-3 is also an unlikely candidate for the vegetal inducing signal as it is only expressed zygotically. FGF-9 is maternally derived, but is found in the animal hemisphere of the early embryo and later throughout the developing axis. It too lacks a secretory signal sequence, but may still be secreted.

With eFGF, the localization also appears to be in the animal hemisphere of the blastula stage embryo however this FGF does indeed possess a signal sequence. Despite this fact, none of the four FGFs found in *X. laevis* appear to be at the right place at the right time to be one of the vegetally localized mesoderm inducing signals. That is, none of them are vegetally localized. Yet, they still appear to be required for mesoderm formation, as demonstrated by the work of Amaya and his colleagues (Amaya *et al.*, 1991; Amaya *et al.*, 1993). A new role therefore has emerged for FGFs. Rather than acting as the signals themselves, they appear to be present in the animal hemisphere as competence factors for the cells in the marginal zone receiving the mesoderm induction signal (Isaacs, 1997). Their activity in the region then continues in the maintenance of this tissue after induction is complete.

Supporting this theory is the finding that eFGF expression is activated in animal caps treated with mesoderm inducing factors (Isaacs *et al.*, 1994). It is therefore likely that the same occurs in the presumptive mesoderm of the developing embryo. But levels

of eFGF are highest in the mesoderm during gastrulation (Isaacs *et al.*, 1994) after this tissue has already been induced, reinforcing the role of FGFs in mesodermal tissue maintenance. Nevertheless, the role of FGFs during mesoderm induction is still integral to the development of a normal embryo. In fact, the establishment and preservation of mesoderm in *X. laevis* has been shown to depend upon FGF signalling within this tissue by way of a regulatory loop involving *Xbra* (Isaacs *et al.*, 1994). The FGF pathway must be intact downstream of *Xbra* to allow it to in turn activate the expression of eFGF which then regulates *Xbra* expression (Schulte-Merker & Smith, 1995).

1.6 FGF signal transduction

FGF signal transduction begins at the cell surface with a ligand and a transmembrane receptor. In the FGF signal transduction pathway, the receptor is a high affinity receptor that is a member of the tyrosine kinase receptor family. There are four known FGF receptor genes, named FGFR-1 through FGFR-4, that share 55% to 72% sequence homology at the protein level (reviewed in Powers *et al.*, 2000). These receptors are transmembrane proteins possessing three extracellular immunoglobulin (Ig)-like domains (IgI, IgII, and IgIII), an acidic region situated between IgI and II, a transmembrane domain, and an intracellular tyrosine kinase domain (Figure 1.4). Diversity of the four FGFRs can be enhanced through the expression of splice variants of the FGFR genes. This enables the same FGFR gene to code for a number of different receptor protein isoforms. It is thought that the expression of different isoforms allows for the great diversity seen in FGF function.

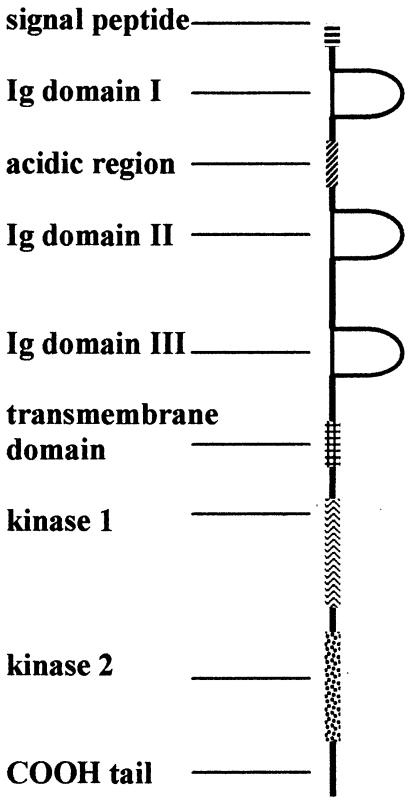

Figure 1.4 Schematic of the FGF receptor

FGF receptors are transmembrane proteins possessing three extracellular immunoglobulin (Ig)-like domains (designated IgI, IgII, and IgIII above), an acidic region situated between IgI and II, a transmembrane domain, and intracellular tyrosine kinase domains responsible for phosphate transfers to the tyrosine residues of other proteins. Adapted from Powers *et al.* (2000).

FGF receptors are similar to other receptor tyrosine kinases in that they transmit extracellular signals through the cell membrane to various signal transduction pathways in the cytoplasm by tyrosine phosphorylation. FGF ligands are thought to first bind to low affinity receptors in the extracellular matrix (ECM). This promotes binding of the ligand to the high affinity tyrosine kinase receptors (RTK) (Powers *et al.*, 2000). Once a ligand binds to one of these receptors, the receptor dimerizes giving it the ability to phosphorylate specific tyrosine residues on its own as well as on its partner's cytoplasmic tail. This dimerization and phosphorylation can occur between both homodimers as well as heterodimers of different FGFRs and enhances the diversity of FGF signalling (Powers *et al.*, 2000). After a receptor has been activated in this manner, it can recruit additional signalling molecules to propagate the signal through many possible pathways.

Within *X. laevis*, three FGFR members have been identified: FGFR1, -2, and -4. Of these, the FGFR1 appears to be important in early development, as it has been shown to be present in the embryo at this time (Musci & Kirschner, 1990). Localization of its mRNA and protein is predominantly in the animal hemisphere, which is similar to the FGF protein ligands. As well, this receptor is activated during mesoderm induction in *X. laevis* (Ryan & Gillespie, 1994).

Triggering of the FGFR in *X. laevis* by FGF binding leads to the recruitment of signalling molecules, including several SH2-containing proteins that play specific roles within the FGF signalling pathway (Mohammadi *et al.*, 1991; Ryan & Gillespie, 1994; Zhan *et al.*, 1994; Larsson *et al.*, 1999). These target proteins interact with the cytoplasmic tail of the receptor, which in turn modifies them by phosphorylation. They

can then act as substrates for receptor-mediated phosphorylation or may function as adaptor proteins to recruit other targets (Powers *et al.*, 2000). While not all of these molecules affect the induction of mesoderm in animal cap explants, there appears to be two active FGF pathways triggered in this manner that are required for mesoderm development: the *ras/raf*/MAPK pathway and the phosphoinositide 3 kinase (PI3K) pathway. A third pathway, the PLCγ pathway, may also be involved in this process.

MAP kinase, or Mitogen Activated Protein kinase, is a serine-threonine kinase that is activated in response to a variety of stimuli (Hartley *et al.*, 1994). The kinase that is responsible for the activation is known as MEK, or MAP kinase kinase (MAPKK), which itself gets phosphorylated by MEK kinases (MEKK). One type of MEKK is RAF, which is activated in a complex together with RAS. Both are proto-oncogenes known to lie downstream of tyrosine kinase receptors. When the FGF receptor is activated, it gets bound by docking molecules such as FRS2. These recruit a protein complex known as GRB2-SOS. SOS then causes the dissociation of GDP from the membrane-bound RAS, enabling it to associate with GTP and become activated. RAS can then recruit RAF-1, which can in turn activate MAPKK. This latter molecule activates MAPK, enabling it to phosphorylate transcription factors and other substrates.

With respect to the second pathway, PI3Ks are lipid kinases that phosphorylate the 3'-OH position of the inositol ring to give rise to a variety of activated membrane phospholipids. These phospholipids have the ability to act as second messengers and are known to regulate numerous processes within the organism. Similar to the MAPK signalling cascade described above, the PI3K pathway was recently shown to be turned

on by RAS as well (Carballada *et al.*, 2001). It was also demonstrated that these signals act in parallel to the MAPK pathway and are required for the formation of trunk mesoderm in *X. laevis* during blastula stages.

In the phospholipase C gamma (PLCγ) pathway, PLCγ gets activated resulting in the hydrolysis of phosphatidylinositol 4,5-biphosphate to both diacylglycerol and IP_3. The former activates protein kinase C (PKC) while the latter causes the release of Ca^{2+} from intracellular stores. Both of these second messengers activate other molecules that ultimately bring about the transcription of target genes. While this pathway is activated during FGF-induced mesoderm induction in animal cap explants, it is not sufficient to induce mesoderm in explants, although it may be part of a negative feedback mechanism on FGF signalling (Gillespie *et al.*, 1992).

The greatest evidence for the role of FGF signalling in mesoderm formation comes from investigating the consequences of its inhibition. One of the most visible effects seen with these experiments is on the expression of mesodermal markers at the beginning of gastrulation (Isaacs, 1997). The inhibition of FGF signalling causes a decrease in the levels of *Xcad3* (*Xenopus caudal*) and *Xbra*, which are normally expressed in the entire marginal zone at this point in development (Amaya *et al.*, 1993; Northrop & Kimelman, 1994). *Noggin* expression is also down regulated but not as much as the first two. *XmyoD* does not appear to be affected initially but is greatly reduced at the end of gastrulation and the beginning of the neurula stages (Fisher *et al.*, 2002). Also, the expression of *Xgsc*, *Xwnt-8*, and *Xsna* (*Xenopus snail*) in the prospective mesoderm at the start of gastrulation is not affected by FGF inhibition (Amaya *et al.*,

1993; Christian & Moon, 1993). Thus, the proper functioning of the FGF signalling pathway is required in the early embryo in order to promote or maintain the expression of some but not all of the genes throughout the developing mesoderm (Isaacs, 1997).

1.7 Immediate-early genes

In a signal transduction cascade such as that induced by FGF, the pathway transmits a signal from the extracellular environment to the nucleus resulting in the rapid transcription of specific genes in the cell. These first genes to become transcribed in response to a signalling pathway are known as immediate-early or early-response genes. Immediate-early genes are frequently transcription factors, and for this reason they are often targeted to the nucleus. Their expression can therefore lead to the transcription of even more genes that ultimately carry out the requirements or functions relayed by the original signal. Immediate-early genes are identified by their ability to be transcribed in a manner independent of *de novo* protein synthesis, along with the rapidity of their expression, thus reinforcing their role as the very first genes to be transcribed in a signalling pathway.

1.8 MI-ER1

In an effort to further elucidate the FGF signal transduction pathway, an attempt was made in the Terry Fox Cancer Research Lab to identify the particular immediate-early genes that are active in this signalling cascade. Resulting from this search was the discovery of a novel, developmentally regulated gene encoding a nuclear protein that was

activated by FGF-2 in *X. laevis* (Paterno *et al.*, 1997). This gene was eventually named mesoderm induction early response 1, or *mi-er1*. *Xmi-er1*, the *X. laevis* form, was isolated using polymerase chain reaction-based differential display (Paterno *et al.*, 1997) and demonstrated increased expression levels in animal cap explants in response to treatment by FGF-2. The PCR product that was obtained through this method was then cloned and found to represent a 2.3-kilobase pair cDNA encoding a protein of 493 amino acids (aa). By analyzing its expression in FGF-2-treated animal caps in the presence of cycloheximide, a protein synthesis inhibitor, it was found that transcription of *Xmi-er1* was not dependent upon *de novo* protein synthesis. This suggested that *Xmi-er1* was a true immediate-early gene. Further support for this concept came from the fact that the gene was targeted exclusively to the nucleus during immunocytochemical analysis, and an acidic domain at the N terminus was found to function as a potent transcriptional activator when tested in mammalian cells (Paterno *et al.*, 1997). Thus, all of the evidence supported a role for *Xmi-er1* as an early-response gene within the FGF signalling cascade, suggesting that this molecule played a part in FGF-regulated cellular activities.

Subsequent studies on this gene led to the discovery of a closely related human homologue, *hmi-er1* (Paterno *et al.*, 1998). The two proteins showed 91% sequence similarity. Analysis of *hmi-er1* expression in numerous human tissues revealed that mRNA levels were negligible in all 50 normal human tissues tested. However, upon examination of various breast carcinoma-derived cell lines and breast tumour tissue samples, it was indicated that *hmi-er1* was expressed at significant levels in all samples but remained undetectable in normal breast-derived cell lines and tissue. Two of the

major isoforms, hMI-ER1α and hMI-ER1β, were recently found to function as transcriptional repressors by the recruitment of histone deacetylase 1 (HDAC1) through the highly conserved ELM2 domain (Ding *et al.*, 2003).

Within both XMI-ER1 and hMI-ER1, there appears to be a number of conserved functional domains, the ELM2 being one of them, to be discussed in full detail below (Figure 1.5). At the N-terminus there are four highly conserved acidic regions. Towards the centre of the molecule is the aforementioned ELM2 domain (aa 168-272) and along the C-terminal side of this is a second large domain known as the SANT domain (aa 276-321). This is followed by a putative MEK phosphorylation site (TDY), a proline-rich (PXXP) motif, as well as the only functional nuclear localization signal (NLS) (Post *et al.*, 2001). Between XMI-ER1 and hMI-ER1, there is 100% identity within the SANT domain, the NLS, and the proline-rich region.

During *X. laevis* embryonic development, the XMI-ER1 protein is present in the early embryo (Paterno *et al.*, 1997). It is a maternally derived protein that is found at constant levels during early developmental stages and only becomes localized in the nucleus at MBT (Luchman *et al.*, 1999). Using an anti-MI-ER1 antibody on whole mounts and sections, this movement into the nucleus can be first seen in the cells of the future mesoderm at stage 8. Following this, XMI-ER1 becomes localized to the nucleus in the cells of the presumptive ectoderm, and by late blastula all of the nuclei in the animal hemisphere are stained. Nuclear localization occurs last in the endodermal cells. At early gastrula stages, the nuclear localization of XMI-ER1 is ubiquitous in the embryo. At later stages following this, the protein gradually disappears from the nuclei

such that by tadpole stages it is gone from all nuclei with the exception of a few cells in the endoderm. Some mesodermal tissues at this point also show cytoplasmic staining.

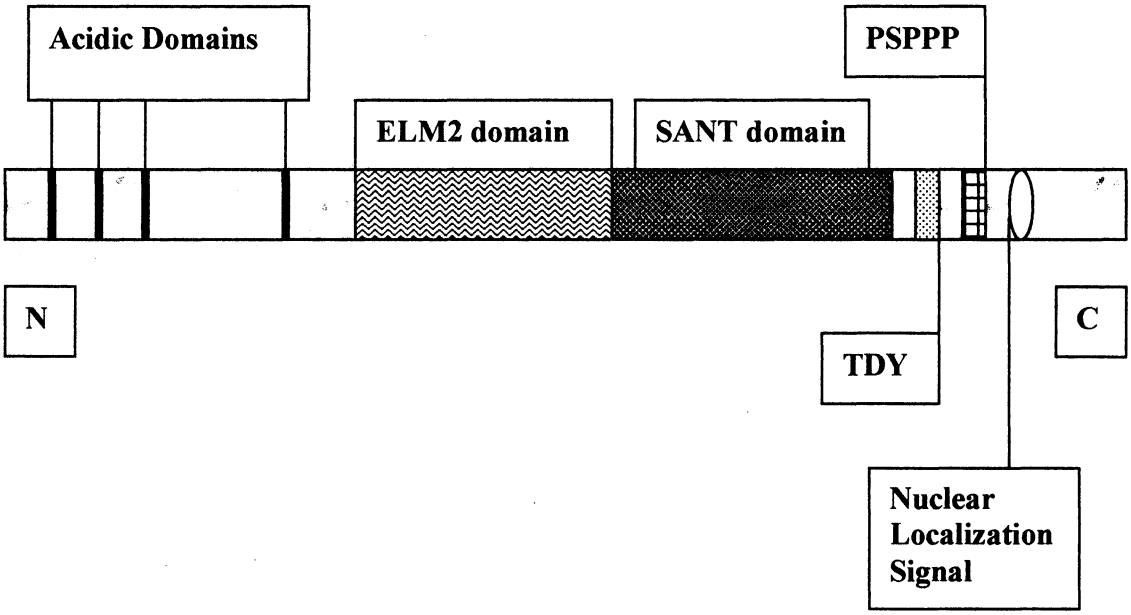

Figure 1.5 Illustration of the putative functional domains in XMI-ER1

The N-terminal domain consists of four regions of acidic amino acids. Located in the centre of the protein is the ELM2 domain. Towards the C-terminus, the SANT domain can be found, followed by a putative MEK phosphorylation site (TDY), a PXXP motif, and a *bona fide* NLS.

1.8.1 The ELM2 domain

The ELM2 domain, which stands for EGL-27 and MTA1 homology domain 2, was initially identified in EGL-27 (Solari *et al.*, 1999). EGL-27 is a *C. elegans* protein that is involved in embryonic patterning and plays a key role in Wnt signalling possibly by regulating HOX gene expression (Herman *et al.*, 1999; Solari *et al.*, 1999). It is thought to act in the regulation of transcription factors that function during embryonic patterning by way of a protein complex that may alter the acetylation status of the target chromatin. Recent data suggests that the transcriptional activity of a gene can be controlled by modifications of its chromatin structure (Wade *et al.*, 1999; Sterner & Berger, 2000). That is, when the chromatin is acetylated, the gene is active, and when the chromatin has been deacetylated, the gene is inactive or repressed. The second gene for which the ELM2 domain is named is *mta*1. This encodes a protein that is known to be part of a protein complex possessing ATP-dependent nucleosome remodelling and histone deacetylating activities (Xue *et al.*, 1998). Thus, it is thought to be involved in gene repression by hypoacetylating chromatin. The ELM2 domain is a highly conserved sequence that is also found in many SANT domain-containing proteins. It has recently been shown to recruit HDAC1 and to be required for transcriptional repression (Ding *et al.*, 2003).

1.8.2 The SANT domain

The SANT domain was named for the four transcription factors in which it was first discovered: SWI3, ADA2, N-CoR, and TFIIIB (Aasland *et al.*, 1996). The motif

consists of approximately 50 amino acid residues and is often found more than once within a protein. In general, there tend to be a number of highly conserved residues throughout the domain including two or three regularly spaced aromatic amino acids thought to be important in the maintenance of its hydrophobic core. Within the XMI-ER1 SANT domain, there are two tryptophans at amino acids 6 and 48, and a phenylalanine at amino acid number 25.

Although the function of the SANT domain has yet to be fully understood, it is thought to act in transcriptional regulation either through DNA binding or protein-protein interactions (Aasland *et al.*, 1996). In fact, it is highly related to the DNA-binding domains of myb-related proteins and may therefore function in a similar manner. Like these domains, the SANT domain has two or three repeated subdomains each resembling the helix-loop-helix design in secondary structure. These are thought to assist with DNA binding. However, studies suggest that only those proteins that have two or more SANT domains are involved in DNA binding (Aasland *et al.*, 1996). Proteins with only one SANT domain are more likely to function in protein-protein interactions. Recent data has demonstrated that CoREST, a corepressor to the REST transcription factor, interacts with HDAC through its single SANT domain (You *et al.*, 2001). It is therefore probable that XMI-ER1, which has only one SANT domain, is involved in transcriptional regulation via protein-protein interactions rather than DNA binding.

1.8.3 The proline-rich region

At the C terminus of XMI-ER1 there is a proline-rich motif that conforms to the

consensus PXXP for binding Src homology 3 (SH3)-containing proteins (Ren *et al.*, 1993; Cohen *et al.*, 1995). SH3 is a small domain that is present in many proteins, especially those involved in signalling. These domains are thought to operate as modules that mediate protein-protein interactions and control signalling within the cell (Cohen *et al.*, 1995). Binding domains that are designated as being "modular" are often constructed with two related features: a common core able to recognize other proteins; and, a second more specific means of control. Using this system of both general and precise regulation, these modulators are able to arbitrate the interaction of one protein with another and in this way they aid and perhaps direct many signal transduction pathways. The presence of a region concentrated in prolines that can potentially interact with SH3-containing signalling molecules therefore supports the idea of XMI-ER1 functioning in transcriptional regulation via protein-protein interactions.

1.9 Project Goals

The purpose of this study was twofold: (1) to investigate the function of XMI-ER1 during *X. laevis* development and mesoderm induction; and, (2) to identify functional domains that are integral to XMI-ER1 activity during development.

Part 1) Investigation of XMI-ER1 function during *X. laevis* development and mesoderm induction.

At the time this project was undertaken, not much was known about the activity of XMI-ER1 in development. It was found to be present in the early embryo, and its

expression pattern had recently been elucidated (Luchman *et al.*, 1999), but little was known about its role during this time. In an attempt to contribute to the general understanding of XMI-ER1, I began my research with a series of in depth over-expression experiments in the early *X. laevis* embryo. Following these studies, its role was further analyzed during FGF- and activin-induced mesoderm induction in animal caps. This was achieved by culturing stage 8 animal caps in a series of concentrations of these two potent mesoderm inducers.

Part 2) Analysis of functional domains critical to XMI-ER1 activity.

This was accomplished through an examination of the domains present in the full-length protein. The analytical techniques used involved the mutagenesis of potentially key amino acids within these domains. Residues were deemed to be "key" based on comparisons with other proteins containing the same domains. The activity of these mutated forms of XMI-ER1 was then investigated within both the developing embryo and animal caps and compared to the activity of the wild-type XMI-ER1 form.

Chapter 2: Materials and Methods

2.1 *In vitro* fertilization of *X. laevis* eggs

Adult female *X. laevis* frogs (Nasco) were injected subcutaneously in the upper hind leg on the dorsal side with 550 I.U. of Human Chorionic Gonadotrophin (Sigma) 14 to 16 hours before embryos were needed. The frogs were then left at room temperature overnight to ovulate. The following morning, eggs were collected from the induced females in a petri dish (Fisher) by gentle massaging. The eggs were fertilized with a small piece of testes obtained from a previously sacrificed adult male frog. Whole testes were stored in 1X Normal Amphibian Medium (NAM; Table 2.1) (Slack & Forman, 1980) at 4°C and had a shelf life of approximately a week and a half. A small portion of the testes was macerated and diluted with 2-3ml of distilled water (dH_2O) and then added to the isolated eggs. In order to mix the eggs and sperm together, the petri dish was rocked for a few seconds and then left at room temperature to allow the fertilization to take place. After ten minutes, the eggs were flooded with enough dH_2O so that they were completely submerged. A waiting period of 5-15 minutes was then required to let the eggs rotate so that the animal pole was facing up, indicating a successful fertilization.

Once this cortical rotation occurred, the embryos were de-jellied in order to facilitate manipulation during injections. In this step, the embryos were swirled in 50ml of 2% L-cysteine (Sigma) in dH_2O, pH 7.8-8.1, until all the jelly had dissolved and the embryos were packed closely together. They were then rinsed with 1L of dH_2O and

transferred to a petri dish containing NAM/20 where they were left to develop at room temperature until required.

Table 2.1 **Components of Normal Amphibian Medium (NAM) used for *X. laevis* experiments**

Composition and concentration of 10X stock and 1X solution

	10X stock (g/L)	**1X solution (mM)**
NaCl (Fisher)	65	110
KCl (Fisher)	1.5	2
$Ca(NO_3)_2 \bullet 4H_2O$ (Fisher)	2.4	1
$MgSO_4 \bullet 7H_2O$ (Fisher)	2.5	1
EDTA (0.5M, pH 8) (Fisher)	2ml	0.1
Hepes (1M, pH 7.5) (Fisher)	100ml	10

Composition of NAM Solutions (in 100 ml)

	1X NAM (ml)	**NAM/2 (ml)**	**NAM/20 (ml)**
10X NAM	10	5	0.5
Gentamycin (Sigma)	0.25	0.25	0.25
$NaHCO_3$ (Fisher)	1.0	1.0	0
dH_2O	88.75	93.75	99.25

2.2 Microinjection of *X. laevis* embryos

When the embryos had reached the two-cell stage approximately 1.5 hours after fertilization, the required number of embryos (usually 30-50) was transferred to a grid-lined petri dish containing NAM/2 + 4% ficoll (Amersham). A glass needle made from a $3^1/_2$" Drummond glass capillary tube that had been pulled using a Narishige PB-7 micropipette puller and ground using a Narishige EG-40 grinder was then filled with 1µl DEPC- (Sigma) treated dH_2O. Each embryo was injected with 4.6nl of liquid in the marginal zone beside the cleavage furrow. Once the injections were complete, the group was transferred to another petri dish also filled with NAM/2 + 4% ficoll and left to develop at room temperature. This procedure was repeated for each RNA concentration injected. Injected embryos were scored for phenotypic abnormalities using the Normal Table of Xenopus laevis (Nieuwkoop, 1994) 24 and 72 hours post-injection. The dorso-anterior index (DAI)(Kao & Elinson, 1988) was also utilized at the latter stage. Once these scores were collected, the embryos were fixed in a solution of MEMFA (Table 2.2) and stored in glass scintillation vials (Fisher) at 4°C for further study. The MEMFA was eventually replaced with 1X PBSA + 0.02% azide (Fisher; Table 2.3).

Injections for the FGF- and activin-induced mesoderm induction experiments were carried out at the four-cell stage. These embryos were injected in the animal pole of each cell with 2.3nl of liquid so that a total of 9.2nl was injected per embryo. Approximately 40 embryos were injected for each set with 0.375ng/2.3nl dilutions of RNA. The total RNA injected into each embryo under these conditions was therefore 1.5ng. They were then left at room temperature until stage 8 at which point they were

used for mesoderm induction assays (see 'Micro-dissection and Induction Assays'). The purpose of injecting them in the animal cap of four cells rather than into one or two cells at an earlier stage was to ensure that when the explants were excised, the cut included the part of the animal cap that had been injected.

Table 2.2 Components of MEMFA

	For 1L Solution (mL)	**Final Concentration (mM)**
MOPS (1M, pH 7.4) (Fisher)	100	100
EGTA (0.5M, pH 8.0) (Fisher)	4	2
$MgSO_4$ (1M) (Fisher)	1	1
Formaldehyde (37%) (Fisher)	100	3.7%
dH_2O	795	N/A

Table 2.3 Components of 10X Phosphate Buffered Saline Amphibian (PBSA)

	For 1L Solution (g/L)	**Final Concentration (mM)**
NaCl (Fisher)	56.0	100
KCl (Fisher)	1.4	2
KH_2PO_4 (Fisher)	1.7	5
$Na_2HPO_4 \bullet 7H_2O$ (Fisher)	15.1	1.5
dH_2O	Up to 1L; pH 7.4	N/A

2.3 Micro-dissection and induction assays

Approximately 4.5 hours after fertilization when the embryos had reached stage 7.5, a solution of NAM/2 + 1mg/ml Bovine Serum Albumin (BSA, RIA grade; Sigma) was prepared fresh. This was used to make a set of serial dilutions of the FGF or activin to be used for culturing animal caps. The FGF used in this study was recombinant *Xenopus* FGF-2. It was expressed and purified according to Kimmelman *et al.* (1988). The stock concentration was 18.5μg/ml and was stored in aliquots at –20°C.

At stage 8 the embryos were transferred to a petri dish lined on the bottom with 1.5% agar (Fisher) in NAM/2 and filled with 1X NAM solution. Animal cap explants were dissected manually according to Godsave *et al.* (1988). The vitelline membranes were removed using forceps and the top 1/4 of each embryo was cut in a square shape also with forceps and removed from the animal cap. The explants were transferred to a multi-well plate and cultured in 20μl of liquid, whose constitution and concentration varied according to the experiment being performed, as described below.

There were three different induction experiments that were conducted in this project. For the FGF-induced mesoderm induction of *Xmi-er1*- or water-injected embryos, four culturing conditions were prepared. NAM/2 + 1mg/ml BSA was used as a negative control for induction in addition to four concentrations of FGF-2: 0.5ng/ml, 1.0ng/ml, 2.0ng/ml and 5.0ng/ml. Five explants from each injection set were cultured in the control condition, while ten from each set were cultured in each dilution of FGF. Thus, a total of 45 explants were cut from each set of injected embryos and a total of 90 explants were cut and cultured per experiment.

For the FGF-induced mesoderm induction of the XMI-ER1 constructs, explants were cut from embryos injected with a total of 1.5ng of *Xmi-er1*, ^{365}PS→AA, ^{365}P→A, or ^{366}S→A, or with DEPC-treated dH_2O. They were cultured in 20µl of 1ng/ml FGF, or in NAM/2 + 1mg/ml BSA as a negative control. Again, five explants from each injection set were cultured in the control condition, while ten from each set were cultured in FGF.

In the activin induction experiment, explants were cut from embryos injected with a total of 1.5ng of *Xmi-er1* or with DEPC-treated dH_2O. They were cultured in one of five concentrations of recombinant human activin (rhActivin; R&D Systems) that included 0.01ng/ml, 0.025ng/ml, 0.05ng/ml, 0.1ng/ml, and 0.15ng/ml, or NAM/2 + BSA as a negative control. For this experiment, five explants per injection set were cultured in each condition such that a total of 30 explants were cut from each set and 60 were cut for the whole experiment.

Approximately 24 hours after fertilization, 7µl of dH_2O was added to each well in order to accommodate for evaporation of liquid and to increase survival. Explants were left in the multi-well trays for 3 days and scored for mesoderm formation on the third day following injection (after 72 hours). Mesoderm induction by FGF and activin were scored as first described by Slack *et al.* (1987); *i.e.*, an explant was positive for induction if it both elongated from its initial ball-like shape and expanded to resemble a bubble. Once these scores were recorded, the explants were fixed in MEMFA and stored in 1X PBSA + 0.02% azide at 4°C for further investigation.

2.4 Mutagenesis

In order to create the desired mutations in the *Xmi-er1* DNA sequence two different methods were employed. For $\Delta^{175\text{-}236}$*ELM2*, two endogenous *Bam*H1 sites were used to delete the specified sequence from wild-type *xmi-er1*. With respect to the remaining constructs, the QuikChange™ Site-Directed Mutagenesis Kit (Stratagene) was utilized. This is an *in vitro* mutagenesis technique that is able to introduce mutations into any double-stranded plasmid using the polymerase chain reaction (PCR). The reaction was made up of the provided 10X reaction buffer, dNTP mix, and *PfuTurbo*™ DNA polymerase; the two primers containing the desired mutation (one primer for each strand of DNA; Table 2.4); dH_2O; and the plasmid DNA. The cycling parameters were as described in the PCR section.

Once the PCR was finished, the products were run on a 1% agarose gel to check for sufficient amplification. The samples were then digested with the provided *Dpn1* restriction enzyme. 1µl was added to each reaction and mixed gently by pipetting up and down several times. This was incubated at 37°C for 1 hour in order to digest the parental strand and to ensure that only the mutated DNA remained. The endonuclease used in this step is specific for methylated and hemi-methylated DNA only and is therefore able to target the non-mutated parental DNA template. Following the digestion, the products were transformed into the provided Epicurian coli® XL1-Blue Supercompetent Cells. 1µl of product was combined with 50µl of cells and incubated on ice for 30 minutes. The cells were then heat-shocked at 42°C for 45 seconds and placed on ice again for 2 minutes. A mixture of preheated NZY+ broth (Table 2.5) was added to this. The sample

was shaken at 37°C for 1 hour at 225 rpm. The entire reaction was then plated on a 50μg/ml ampicillin (Sigma) + LB agar plate (Table 2.6) and grown overnight at 37°C. The resulting colonies were subsequently used for plasmid preparations and RNA production.

Table 2.4 List of primers used to make mutations

Mutation	Primers
$^{277}W \rightarrow A$	5'CTTCTTCAGTCGCAACGGAAAGTTCTTCTCTGGCGG3'
	5'CCGCCAGAGAAGAACTTTCCGTTGCGACTGAAGAAG3'
$^{277}W \rightarrow G$	5'GCCAGAGAAGAACTTTCCGTTGGGACTGAAGAAGAATGTAG3'
	5'CTACATTCTTCTTCAGTCCCAACGGAAAGTTCTTCTCTGGC3'
$\Delta^{292}YGKDF$	5'GAGCAAGGTCTAAAAGCTCACTTGATTCAGGC3'
	5'GCCTGAATCAAGTGAGCTTTTAGACCTTGCTC3'
$^{319}W \rightarrow A$	5'GTGTGGCATTCTACTACATGGCGAAAAAATCAGAACGTTATGAC3'
	5'GTCATAACGTTCTGATTTTTTCGCCATGTAGTAGAATGCCACAC3'
$^{346}TDY \rightarrow ADF$	5'CTACATCCTGGTGTAGCGGATTTCATGGATCGTCTTTTGG3'
	5'CCAAAAGACGATCCAGGAAATCCGCTACACCAGGATGTAG3'
$^{365}PS \rightarrow AA$	5'CCTCCAGCAGGGCGGCAGCTCCTCCACCAACTACCTCC3'
	5'GGAGGTAGTTGGTGGAGGAGCTGCCGCCCTGCTGGAGG3'
$^{365}P \rightarrow A$	5'CCAGCAGGGCGGCATCTCCTCCACCAACTACCTCC3'
	5'GGAGGTAGTTGGTGGAGGAGATGCCGCCCTGCTGG3'
$^{366}S \rightarrow A$	5'CCAGCAGGGCGCCAGCTCCTCCACCAACTACCTCC3'
	5'GGAGGTAGTTGGTGGAGGAGCTGGCGCCCTGCTGG3'

Table 2.5 Components of NZY+ broth

	g/L
NZ amine (or casein hydrolysate) (Difco)	10
yeast extract (BDH)	5
NaCl (Fisher)	5
dH_2O	up to 1L; pH 7.5
Prior to use add:	
$MgCl_2$ (Fisher)	12.5ml
$MgSO_4$ (Fisher)	12.5ml
2M glucose (Sigma)	10ml

Table 2.6 Composition of Luria-Bertani (LB) Medium agar plates

	g/L
peptone (BDH)	10
yeast powder (BDH)	5
NaCl (Fisher)	10
agar (BDH)	15
dH_2O	up to 1L; pH 7.0

2.5 Polymerase Chain Reaction

The polymerase chain reaction (PCR) was used to amplify DNA sequences during the formation of the XMI-ER1 constructs. This *in vitro* technique uses two oligonucleotide primers that hybridize to opposite strands of DNA to carry out the synthesis of a specific DNA sequence with the help of an added enzyme (Erlich, 1989). The three steps to this reaction are denaturation of the template strand, annealing of the primers, and extension of the DNA sequence from the primers. When put together, these steps make up one cycle in the reaction. It is the repetition of these cycles that allows for the exponential accumulation of the target sequence.

The general PCR protocol used was as follows. Prior to each reaction, a master mix was prepared by combining the enzyme buffer (Promega) with dNTPs (Gibco), $MgCl_2$ (Promega), and deionized water. The Taq DNA Polymerase was added next, followed finally by the appropriate primers (Table 2.4). The reaction was carried out in a thermal cycler using three steps. The cycling parameters used for making $^{292}\Delta$YGKDF and ^{277}W→G involved the following program:

1 cycle: 95°C for 30 seconds

X cycles: 95°C, 30 seconds for denaturation

55°C, 1 minute for primer annealing

68°C, 9 minutes and 36 second for primer extension

X represented 18 cycles for the former construct and 12 cycles for the latter.

For the ΔELM2 deletion, a slightly different program was used:

1 cycle: 94°C, 5 minutes

35 cycles: 94°C, 55 seconds for denaturation

55°C, 1 minute for primer annealing

72°C, 1 minute for primer extension

1 cycle: 72°C, 6 minutes

Once completed, the PCR products were examined on a 1% agarose gel.

2.6 Agarose gel electrophoresis

This technique was used in order to separate nucleic acids according to size by taking advantage of the fact that these molecules are highly charged. All gels were made up of 1% agarose (Gibco) in 1X tris borate / EDTA electrophoresis buffer (TBE; Table 2.7) and were stained with ethidium bromide (Bio-Rad). This binds to the nucleic acids and enables them to be visualized under ultraviolet light.

Table 2.7 Components of TBE

	10X stock	**1X solution**
Tris base (Fisher)	108g	10.8g
Boric Acid (Fisher)	55g	5.5g
EDTA (0.5M, pH 8.0) (Fisher)	40ml	4ml
dH_2O	up to 1L	up to 1L

2.7 Plasmid preparation and purification

Two different methods were used for the preparation of plasmids. The XMI-ER1 constructs were made by the first method of transformation, inoculation, and isolation using a plasmid preparation kit (Qiagen), while XMI-ER1 itself was prepared using the cesium chloride method because attempts to use the first method with this sequence were unsuccessful.

Method 1:

In order to amplify plasmid DNA, it was transformed into Epicurian coli® XL1-Blue Supercompetent Cells (Stratagene) and cultured overnight. The transformation reaction involved adding approximately 10ng of DNA to the cells. This was gently swirled and incubated on ice for 30 minutes. The cells were then heat-shocked at 42°C for 45 seconds and placed on ice for 2 minutes. A mixture of preheated NZY+ broth (Table 2.5) was added to this and the sample was shaken at 37°C for 1 hour at 225 rpm. The entire reaction was then plated on an LB + ampicillin agar plate and grown overnight at 37°C.

The next morning, the plates were checked for bacterial colony growth. If growth was successful, the plates were wrapped in parafilm (American National Can) and stored at 4°C. If not, the previous step was repeated until growth was observed. Once this occurred, two colonies were chosen from each plate and used for an inoculation. This technique enables the growth of individual bacterial colonies from which plasmid DNA will be isolated. The colonies were grown in large flasks of LB medium and ampicillin. These were incubated overnight at 37°C with vigorous shaking (~225 rpm).

To isolate plasmid DNA from the cultured bacterial cells, the HiSpeed Plasmid Midi Kit (Qiagen) was used. The protocol was carried out as per the manufacturer's directions. The plasmid DNA was checked by agarose gel electrophoresis and stored at 4°C.

Method 2:

This method involved a number of steps carried out over three consecutive days. On the first day, a previously prepared *Xmi-erl* glycerol stock was grown in LB + ampicillin overnight at 37°C while shaking at ~230rpm. The following day, 1.5ml of culture was combined with 300µl glycerol and stored as a stock at –80°C. The remaining culture was transferred to 250ml bottles, cooled on ice for 20 minutes, and then centrifuged at 4000rpm for 5 minutes. The supernatant was drained off and the pellet was re-suspended in 6.5ml of solution #1 (see Table 2.8 for composition of solutions). This was transferred to a 50ml Oakridge tube and left at room temperature for 5 minutes. 13ml of solution #2 was then added to lyse the cells and the sample was placed on ice for 5 minutes. 6.5ml of solution #3 (pre-chilled on ice) was added next in order to precipitate the chromosomal DNA and protein, and placed on ice for 10 minutes. The sample was then centrifuged at 12000rpm for 30 minutes. The resulting supernatant was carefully poured into a fresh Oakridge tube and precipitated with 2-propanol (Fisher). This was left at room temperature for 15 minutes, and the sample was once again centrifuged at 8000rpm for 30 minutes. Following this, the supernatant was drained and discarded, and the pellet was re-suspended in 3ml of solution #4. The sample was then topped off with this solution so that the total volume was 4.2ml. This was transferred to a 15ml Corex

tube. 42µl of RNase A (Boehringer Mannheim) was then added followed by 4.7g of CsCl. The tube was placed at 37°C to dissolve fully. 0.5ml of 10mg/ml ethidium bromide was added next and the sample was centrifuged at 8000rpm for 10 minutes. The clear supernatant was injected into a quick seal tube using a syringe. The tube was then balanced, heat-sealed, and centrifuged at 45000rpm overnight at 20°C.

The next day, the tube was removed carefully from the rotor, and the plasmid DNA was taken out under UV light using a 16-gauge needle. The ethidium bromide was extracted using an equal volume of water-saturated butanol (BDH). This was repeated six times, followed by two extractions with phenol: chloroform: isoamylalcohol 25:24:1 (P:C:I; Invitrogen) and one chloroform extraction. The DNA was then precipitated with 1/10 the volume of 3M sodium acetate, pH 5.2, and 2 times the volume of 100% ethanol (Fisher) and incubated at –20°C for 1 hour. The precipitate was centrifuged at 8000rpm for 30 minutes. Next, the supernatant was drained off and the pellet was washed with 70% ethanol and dried under vacuum. It was then re-suspended in solution #4 and tested on a 1% agarose gel. RNA contamination was removed using 20µl RNase A (10mg/ml) and incubating at 37°C for 20 minutes. The sample was once again extracted using P:C:I, sodium acetate, and ethanol, and the final product was stored at 4°C.

Table 2.8 Components of the four plasmid preparation solutions

Solution	Components	Final Concentration
1	Glucose 1M Tris, pH 8.0 0.5M EDTA	50mM 25mM 10mM
2	10% SDS 10N NaOH	 2mM
3	5M CH_3COOK Glacial Acetic Acid	3M 11.5%
4	Tris, pH 8.0 EDTA, pH 8.0	50mM 1mM

2.8 Sequencing plasmid DNA

This procedure was used in order to confirm the nucleotide sequences of all RNA constructs used for injections. It was carried out using the USB Sequencing Kit. The method involved three major steps: denaturing, annealing, and labelling. In the first step, a solution of 0.2N NaOH (Fisher) and 0.2M EDTA was added to 5μg of plasmid DNA. This was incubated at 37°C for 20 minutes. Next, it was precipitated using 3M sodium acetate, pH 5.2, and 95% ethanol. The sample was then mixed, briefly centrifuged, and placed at –70°C for 15 minutes. Following this was a 20-minute centrifugation at 4°C. The resulting DNA pellet was washed using 70% ethanol, spun again, dried, and re-suspended in 7 μl of dH_2O.

In the annealing step, the provided sequencing reaction buffer was added to the DNA, along with 10ng of primer. This was mixed and heated at 65°C for 2 minutes. Following this was a slow cool down, which took approximately 20 to 30 minutes. Once cool, the samples could be placed on ice.

In the final step, the annealed primer-DNA was combined with 0.1M dithiothreitol (DTT), diluted labelling mix, [α^{35}S]-dATP (NEN Technologies), and the sequenase enzyme. After 5 minutes, 3.5μl of this mixture was added to each of the four nucleoside phosphates at 37°C. After another 5 minutes, the reaction was stopped using 5μl of the provided stop solution. The samples were either checked immediately using gel electrophoresis or stored at –20°C until required.

2.9 Polyacrylamide sequencing gel electrophoresis

In order to analyze the samples obtained from the sequencing reaction (described previously), a 6% polyacrylamide/urea sequencing gel was used. Prior to pouring the gel, the plates and chambers (Bio-Rad) were cleaned thoroughly with detergent, dH_2O, and ethanol to prevent the formation of bubbles. The apparatus was then assembled as described in the manufacturer's instructions. The gel was prepared with 80ml Sequencing Mix (40ml water, 10ml 10X TBE, 48g Urea (Fisher), 15ml 40% acrylamide), 440µl 10% ammonium persulfate (BRL), and 45µl TEMED (Bio-Rad). The solution was poured immediately and left to polymerize for at least 1.5 hours.

Once the gel was set, it was pre-run in 1X TBE at 60V for 30 minutes. The sequencing samples were denatured at ~85°C for 3 minutes and 3-6µl was loaded into each well. The gel was run at 60V usually until the dye reached the bottom of the gel. Following this, the gel was uncovered and fixed with 10% glacial acetic acid/10% methanol (Fisher). It was then dried under vacuum, packed with film, exposed overnight, and developed.

2.10 RNA production

To begin this procedure the plasmid DNA was first linearized with an appropriate restriction enzyme. Full-length *Xmi-er1* SP6 plasmid DNA was cut using SmaI (Invitrogen). The Ribomax RNA Production Kit (Promega) was then utilized to make RNA from the linearized DNA.

In this protocol, the four ribonucleotide phosphates were added to the DNA along with a customized buffer, cap analogue (New England Biolabs), and SP6 RNA polymerase. The components were mixed and incubated at 37°C for approximately 3 hours. RQ1 RNase-free DNase (Promega) was then added to the reaction to digest the template DNA. This was followed by a second incubation time of 15 minutes and a subsequent P:C:I 25:24:1 extraction in order to remove the enzyme. The RNA was precipitated overnight with 1/10 the volume of 3M sodium acetate, pH 5.2, and 2X the volume of 95% ethanol, and washed repeatedly the next day using 75% ethanol. The final RNA product was then re-suspended in 50µl DEPC-treated dH_2O and stored at –70°C until required.

2.11 Ultraviolet spectrophotometry

This method was used to determine the concentration of RNA and required the use of an ultraviolet (UV) spectrophotometer. The UV light (260nm) was turned on 30 minutes prior to use in order to properly warm up the apparatus. Quartz cuvettes were rinsed and filled with dH_2O to calibrate the machine. 1µl of sample was then combined with 300µl of dH_2O and placed inside the spectrophotometer (1 in 300 dilution). The reading was recorded once any fluctuations stopped (after ~5 seconds). Another 300µl of dH_2O was added to this and a second reading was taken and recorded (1 in 600 dilution). This process was then repeated for all samples.

2.12 Spectrofluorophotometry

This method was used in conjunction with the Ribogreen RNA Quantitation Reagent and Kit (Molecular Probes) to determine the concentration of RNA. The Ribogreen reagent is an ultra-sensitive fluorescent nucleic acid stain that can be used for quantitating *in vitro* transcribed RNA in solution. The RNA concentrations that were obtained from this method were compared with those obtained by UV absorbance (above) to ensure the accuracy of the results. The reasoning behind this is that the presence of free nucleotides in a solution (often resulting from the nucleic acid preparations) has the ability to skew the UV absorbance readings, causing the concentrations calculated to be incorrect. The use of a more sensitive nucleic acid stain (such as Ribogreen) overcomes this problem. When a discrepancy between the two systems existed, the concentrations calculated from the Ribogreen method were considered to be the more accurate result.

The Ribogreen RNA Quantitation Kit provides the user with the fluorescent nucleic acid stain, as well as a ribosomal RNA standard. The first step involves the creation of a standard curve using the provided RNA in order to relate the spectrophotometer readings of the unknown samples with the actual concentration of RNA (known). In the second step, the spectrophotometer readings are recorded for the unknown RNA samples. The concentration of the unknown samples can then be determined from the standard curve created in step one.

Using the RNA sample stock, five different dilutions were made for generating the standard curve. Unknown sample RNA was diluted 10 000 fold. Dilutions were

done in a combination of TE Buffer and Ribogreen reagent. Spectrofluorophotometer (Shimadzu; model RF-1501) readings were then taken and recorded according to the following procedure. Cuvettes were first rinsed thoroughly with dH_2O. Next, excitation and emission values were set to 480nm and 520nm, respectively. The entire sample (2ml) was then transferred to the cuvette, which was placed inside the machine. Once the cover was closed, a timer was started. After 45 seconds, the shutter was opened in order to obtain the reading, and 15 seconds after that the reading was recorded to allow for any fluctuations in the initial value to settle. The shutter was once again closed and the sample was removed. This was then repeated for the remaining samples.

2.13 RNA translation

In order to ensure that the RNA used for injection could be translated into protein efficiently, an *in vitro* translation was performed using the TnT® Couple Reticulocyte Lysate System (Promega) prior to conducting any injection experiments. Before beginning, all components of the kit were thawed at room temperature and stored on ice. Once thawed, they were used to prepare a master mix that would be equally distributed to all samples. The reaction components were as follows (the first four were provided in the kit): Rabbit Reticulocyte Lysate, Reaction Buffer, Amino Acid Mixture minus methionine, RNAguard, [^{35}S]-methionine, 1μg RNA template, and DEPC-treated dH_2O. This was gently mixed by pipetting up and down, and then added to each sample. The remaining quantity of master mix was used as a negative control for translation. Next, the reaction was incubated for 90 minutes at 30°C. After this, the translation was

complete and the results could be analyzed. If analysis was done immediately, samples were stored on ice. If not, they were stored at –70°C until required.

In order to perform the protein analysis, two different methods were employed and used in conjunction with one another. In the first, a portion of the sample was submitted for radioactive counts. This provided a numerical value for the amount of protein made by each sample based on the amount of [^{35}S]-methionine incorporated into the protein. In the second method, the translated RNA was run on a 10% protein gel in order to visualize the results.

Prior to doing the radioactive counts, 2µl of the TnT® sample was bleached with 1M sodium hydroxide and 2% hydrogen peroxide (Fisher) at 37°C for 10 minutes or until the colour disappeared. The samples were then put directly on ice and combined with 25% trichloroacetic acid (TCA; Fisher) / 2% casein amino acids (Merck). This was left to precipitate on ice for 20 minutes. 1ml of each sample was run through a filter using a vacuum flask and washed with 5% TCA and 95% ethanol, both of which were kept ice cold throughout the procedure. Next, 5ml of Biodegradable Counting Scintillant (Amersham) was added to each filter, and the vials were immediately placed in the scintillation counter to be read. Results were recorded and analyzed.

For the second method, an additional 2µl of the TnT® sample was combined with 28µl of 1.5X SSB and run on a 10% SDS-PAGE gel at 30mA for approximately 1.5 hours. The gel was then fixed and destained (Table 2.9) for 15 minutes each, and placed in Amplify (Amersham) for 30 minutes. Following this the gel was dried and exposed to Kodak XAR Scientific Imaging Film (Amersham) for visualization.

Table 2.9 Composition of Fix and Destain solutions

	Fix (ml)	**Destain (ml)**
Methanol (Fisher)	45	20
Glacial Acetic Acid (Fisher)	10	6
dH_2O	45	74

2.14 Protein extraction

In order to ensure that the various RNA constructs injected into embryos were being made into equivalent amounts of protein, total protein was extracted from the embryos and analyzed for the presence of XMI-ER1. For each RNA set, 35 embryos were injected in the marginal zone at the 2-cell stage beside the cleavage furrow with 1ng of RNA and left to develop at room temperature. At stage 8.5, once the embryos had passed the mid-blastula transition, five embryos from each group were placed in a petri dish. Using forceps, the vegetal pole was removed and discarded and the animal poles were placed in a 1.7ml tube with 175µl 1.5X SSB (without bromophenol blue) and immediately homogenized. After 20 minutes on ice, the samples were centrifuged at 10000g for five minutes at 4°C. The middle layer containing the proteins was then removed using a 1ml syringe and frozen at –80°C until required. If the middle layer was cloudy upon removal, the layer was spun again and the middle layer removed a second time. This procedure was followed by Western Blotting to allow for protein visualization.

2.15 Western blotting

The Western Blot technique uses antibodies to bind to a desired protein, which enables the visualization of the protein. It was used here in order to confirm that the XMI-ER1 constructs injected into embryos were being made into equal amounts of protein thus allowing the resulting embryos from each injection set to be compared. Prior to loading the extracted protein on a gel, the amount of total protein was measured to

ensure equal loading of protein. These measurements were completed using the Bio-Rad Protein Assay (Bio-Rad).

The Bio-Rad assay is a procedure for determining the concentration of protein in a sample by adding an acidic dye to the sample, measuring it with a spectrophotometer, and comparing the readings with a standard curve. To create the standard curve, a set of serial dilutions was made from a 1mg/ml stock of BSA. The absorbance of these samples at 595nm was then measured and graphed. Following this, 1µl of the unknown protein samples was diluted in 799µl of dH_2O and 200µl of dye. Using the spectrophotometer results and the standard curve, the concentrations of the isolated samples were determined.

Based on these calculated concentrations, the samples were diluted using 1.5X SSB with bromophenol blue dye (BDH) and a total of 40µg protein was loaded onto an 8% polyacrylamide gel. The gel was run for 1.5 hours at 30mA in order to separate all the components. Once complete, the protein was transferred to a Hybond-ECL nitrocellulose membrane (Amersham) using the Bio-Rad Western Apparatus. The transfer was carried out over 1.5 hours at 60V from the negative to the positive electrode.

After the procedure was complete, the nitrocellulose membrane was placed in a blocking solution of 5% powdered milk (Carnation) in 1X TBS-T (Table 2.10) for 1 hour with slight agitation in order to block all of the non-specific binding sites on the nitrocellulose membrane. Following this, the membrane was transferred to a solution of 1X TBS-T and stored overnight at 4°C.

The next day, the liquid was poured off and the membrane was placed directly in a 1 in 5000 dilution of the primary antibody (anti-MI-ER1) (Paterno *et al.*, 1997). It was incubated there for 1 hour, and washed every 10 minutes for the next hour with 1X TBS-T. After this, the secondary antibody (HRP-labelled donkey anti-rabbit; Amersham) was applied, again in a 1 in 5000 dilution. It was incubated for 1 hour, followed by another hour of 10-minute washes in 1X TBS-T. At this point, the proteins were ready to be detected using the reagents supplied by the ECL (Amersham) detection kit. This step involved incubation for 1 minute in equal volumes of the two supplied reagents. The liquid was then poured off and the membrane was wrapped in plastic and immediately exposed to ECL Hyperfilm. Exposure times ranged from 10 seconds to 1 minute. The membrane was stored at 4°C in 1X TBS-T + 0.02% azide for further analysis.

Table 2.10 Composition of TBS-T

	1X (in 4L) (ml)	Final Concentration
Tris pH 7.6 (Fisher)	80	20mM
NaCl (Fisher)	109.6	137mM
Tween-20 (Bio-Rad)	4	0.1%
dH_2O	3806.4	N/A

2.16 Non-denaturing protein gel

This technique was used to compare the behaviour of the constructs analyzed in an attempt to identify whether the differences observed with the embryo injections could be explained by varying protein confirmations (Berrada *et al.*, 2002; Zhang *et al.*, 2003). Despite the fact that it is unclear whether XMI-ER1 itself dimerizes or not, any differences in this ability would nonetheless have been evident on a non-denaturing protein gel. To carry out this procedure, proteins that had been *in vitro* translated using the TnT® Kit (Promega) were run on a 5% acrylamide gel that had been pre-run at 100V for 30 minutes prior to loading. Total running time was one hour and ten minutes, again at 100V. Once completed, the gel was fixed and destained (Table 2.9) for ten minutes each using methanol, glacial acetic acid, and dH_2O. It was then placed in Amplify (Amersham) for 15 minutes and dried. The following day the proteins were visualized by autoradiography.

2.17 Whole mount staining of *X. laevis* embryos

Whole mount antibody staining experiments were performed as described by Harland (1991), with some modifications. Embryos that had been previously stored at 4°C in 1X PBSA + 0.02% azide were transferred to 12-well culturing plates (Fisher) and washed in a solution of Maleic Acid Buffer (MAB; Table 2.11) for 10 minutes. This solution was then removed using suction and replaced with 0.1M $K_2Cr_2O_7$ (Fisher) in 5% Acetic Acid (Fisher) for 30 minutes. Following this, the embryos underwent three 10-minute washes with MAB. Next, they were placed in 5% hydrogen peroxide (Fisher) in

MAB and were stored directly under a lamp for approximately 90 minutes until all structures including the eyes became bleached. Once this occurred, the embryos were washed once more with MAB and transferred to 2% Boehringer Mannheim Blocking Buffer (BMB) for 1 hour. The primary antibody was then added as a 1/1000 dilution in 2% BMB/MAB for the 12/101 antibody and a 1/5 dilution for 2G9. The plates were stored at 4°C overnight.

The next day, the embryos were washed every half hour for five hours with MAB. At the end of this second day, the secondary antibody, an alkaline phosphatase goat-anti-mouse antibody (AP-GAM; Amersham), was applied as a 1/1000 dilution. The plates were once again stored at 4°C overnight. On the third day, the embryos were washed every hour for at least five hours using MAB and stored overnight at 4°C. On day four, the BCIP/NBT (Roche) visualization reaction was used. First the embryos were washed twice with AP buffer (Table 2.12) for ten minutes each. Following this, 90µl NBT and 70µl BCIP were diluted in 10ml AP buffer and added to each set of embryos. The colour reaction was left to develop in the dark at room temperature. After 40 minutes, or when the staining was strong enough, the buffer was removed and replaced with MEMFA in order to stop the reaction. The plates were then stored at 4°C until required for photographs. The MEMFA solution was replaced with MAB after approximately 24 hours.

In order to obtain good photographs of the stained embryos, they were cleared by placing them for five minutes in each of the following solutions: 100% methanol, 100% ethanol, and 50% ethanol:50% BA:BB 1:2 (benzyl alcohol {Kodak}: benzyl benzoate

{Sigma}; Murray's Clearing Reagent). They were then moved to a 100% BA:BB solution and photographed for approximately one hour. After this, the embryos were put through the same clearing procedure except in reverse so that they ended up in a solution of methanol and were then transferred to 1X PBSA + 0.02 % azide for further storage at 4°C.

Table 2.11 Components of Maleic Acid Buffer (MAB)

	In 1L
Maleic Acid (Fisher)	11.6g
NaCl (Fisher)	8.8g
dH_2O	up to 1L; pH to 7.5

Table 2.12 Components of Alkaline Phosphatase (AP) Buffer

	In 100ml	Final Concentration (mM)
1M Tris pH 9.5 (Fisher)	10ml	100
1M $MgCl_2$ (Fisher)	5ml	50
1M NaCl (Fisher)	10ml	100
Tween-20 (Bio-Rad)	500µl	0.1%
Levamisole (Sigma)	0.024g	5
dH_2O	~74.5ml	N/A

2.18 Whole mount *in situ* hybridization

This procedure was carried out as described by Harland (1991), with minor modifications. Stage 10.5 albino embryos that had been previously fixed in MEMFA for 45 minutes and stored in 1X PBSA were washed three times in 0.1% Tween-20/1X PBSA (PBSAT) for 20 minutes each. The solution was then replaced with 2.5µl proteinase K in 10ml PBSAT and left at room temperature for 8 minutes. Following this were three 5-minute washes carried out while rocking first with 5ml 0.1M triethanolamine (TEA; Sigma) pH 7.8, then with 5ml 0.1M TEA + 12.5µl acetic anhydride, and finally with an additional 12.5µl acetic anhydride added. The embryos were rinsed twice for 5 minutes with PBSAT and fixed for 20 minutes in 4% paraformaldehyde in PBSAT. The fixative was removed with five PBSAT washes over a 15-minute period. The embryos were then incubated in 1ml PBSAT and 200µl Hybridization Buffer (Table 2.13), followed by 10 minutes in 1ml of Hybridization Buffer at 60°C, and 6 hours at 60°C in 1ml of fresh Hybridization Buffer with shaking. After the incubation, the embryos were placed in 1ml of a digoxigenin-labelled *Xbra* RNA probe and kept overnight at 60°C while shaking.

The probe was made previously by mixing approximately 2.5µg of linearized DNA template with 0.1M DTT (Sigma), NTP mix including digoxigenin-labelled UTP (Boehringer Mannheim), RNA Guard (Pharmacia), Transcription Buffer (Promega), polymerase (Promega), and DEPC-treated dH_2O. The reaction mixture was incubated at 37°C for 2 hours and then 1µl of 1mg/ml RNAse-free DNAse I (Promega) was added. The mixture was incubated an additional 15 minutes at 37°C. Following this, 0.2M

EDTA (Fisher), 4.0M LiCl (Fisher), and 100% ethanol was added for overnight precipitation at –20°C. The next day, the probe was centrifuged at 4°C for 5 minutes, washed with 70% ethanol, and dried. It was precipitated again at –20°C overnight with 4.0M LiCl and 100% ethanol, and once again centrifuged, washed, and dried as before. It was then re-suspended in Hybridization Buffer and stored at –70°C.

On the second day of the hybridization experiment, the probe was removed from the embryos and stored again at –70°C and the embryos were incubated in fresh Hybridization Buffer for one hour at 60°C with shaking. There were then three washes in 2X SSC (0.3M sodium chloride and 0.03M sodium citrate) and 0.1% Tween-20 for 20 minutes at 60°C. This was followed by RNase A and RNase T1 treatment in 2X SSC at 37°C for 30 minutes. The embryos were washed with 2X SSC and 0.1% Tween-20 for 10 minutes at room temperature, and then placed at 60°C in 0.2X SSC and 0.1% Tween-20 twice for 30 minutes each. Next, they were rinsed with MAB (Table 2.11) and blocked with 2% BMB for 1 hour. They were stored overnight at 4°C in 4ml BMB and 2.67µl anti-digoxigenin AP Fab fragments.

The next day the embryos were washed every half hour for at least 4 hours with MAB. They were then rinsed four times with AP Buffer (Table 2.12) over a period of 20 minutes and placed in a solution of NBT and BCIP in AP Buffer to stain in the dark for approximately 2 hours. Once the stain was intense enough, the reaction was fixed in MEMFA (Table 2.2) and the embryos were stored at 4°C until required.

Table 2.13 Components of Hybridization Buffer and Denhart's Solution

Hybridization Buffer:

	In 100ml
Formamide (Fisher)	50ml
20X SSC (3M NaCl, 0.3M Na citrate (Fisher))	25ml
100mg/ml *Torula* RNA (Boehringer Mannheim)	1ml
50X Denhart's Solution	2ml
0.5M EDTA (Fisher)	1ml
Heparin (Sigma)	10mg
Tween-20 (Bio-Rad)	100µl
CHAPS (Sigma)	100mg
DEPC-treated dH_2O	up to 100ml

100X Denhart's Solution:

	In 100ml
BSA (Sigma)	2%
Ficoll (Amersham)	2%
Polyvinylpyrrolidone (BDH)	2%
3X SSPE (NaCl, $NaH_2PO_4(H_2O)$, EDTA) (Fisher)	up to 100ml

Chapter 3: Results

3.1 Over-expression of *Xmi-er1* affects embryonic development

Xmi-er1 cRNA was injected into the marginal zone of embryos at the two-cell stage beside the cleavage furrow. The embryos were left to develop for three days and subsequently scored alongside four different sets of controls that included two RNA controls, one water-injected set, and an uninjected group. The two control RNAs were *β-galactosidase* (*β-gal*) and *Green Florescent Protein* (*GFP*). They were used to measure the background levels of abnormalities and non-specific effects caused by the injection of RNA into developing embryos. These were injected at a concentration of 2ng each, which was the maximum RNA concentration used for the *Xmi-er1* injections. As well, the water control, which consisted of DEPC-treated dH_2O, served as a control for the injection itself, ensuring that abnormalities were not simply due to penetration by the needle nor to the increase in total volume of the embryo.

Four different concentrations of *Xmi-er1* were injected (2ng, 1.5ng, 1ng, and 0.5ng) over a series of at least 5 independent experiments. Approximately 30-50 embryos were injected per condition in each experiment. Embryos were then scored for phenotypic abnormalities at stage 40 of development, which is about three days after fertilization. A large percentage of abnormal embryos were observed in the *Xmi-er1*-injected groups when compared with the four controls. It was also found that as the injected concentration of *Xmi-er1* was increased, there was a dose-dependent increase in the percentage of abnormal embryos that formed. As displayed in Figure 3.1, the

background levels of abnormality observed in the control embryos were 21% for both *GFP* and *β-gal*, 9% for the water injections, and 11% for the uninjected embryos. Although injection of the control RNAs resulted in percentages that were slightly higher than the remaining controls, these values were still significantly lower than those obtained with equal amounts of *Xmi-er1* (87%). The dose-dependant increase in abnormalities observed with *Xmi-er1* was not seen with the controls, which resulted in low levels of abnormality even at such a high concentration. The percentages of abnormality measured for the remaining *Xmi-er1* injections were 74%, 49%, and 33% for 1.5ng, 1ng, and 0.5ng RNA, respectively.

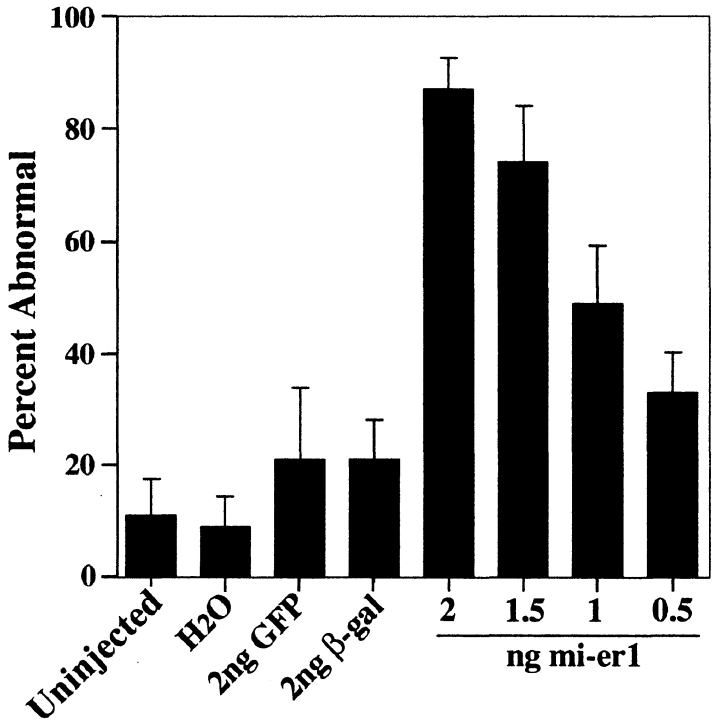

Figure 3.1 Over-expression of *Xmi-er1* RNA causes abnormalities in embryos

Embryos were injected with one of four concentrations of *Xmi-er1* RNA and compared with the following four controls: *GFP* RNA, *β-gal* RNA, DEPC-treated dH_20, and uninjected embryos. Injections were carried out at the two-cell stage in the marginal zone beside the cleavage furrow, as described in "Materials and Methods". The embryos were then left to develop at room temperature for three days until they reached stage 40, at which point they were scored for any abnormalities regardless of severity. From this the percent abnormality was calculated based on the total number of surviving embryos, approximately 400-600 per sample. For the *Xmi-er1* injections, 95% of the embryos injected survived, compared to 98% of the controls. Shown are the results from 5 experiments for the two RNA controls, 21 experiments for the water-injected set, 18 for the uninjected embryos, and 15, 13, 13, and 14 for the 2ng, 1.5ng, 1ng, and 0.5ng sets, respectively. Adapted from Teplitsky *et al.* (2003).

3.2 *Xmi-er1* phenotype includes both anterior and posterior abnormalities

To investigate its biological activity, *Xmi-er1* was over-expressed in *X. laevis* embryos using microinjection techniques. Most abnormalities that resulted from these injections were situated along the anteroposterior axis and could therefore be graded according to the dorso-anterior index (DAI) (Kao & Elinson, 1988). They involved various truncations along the length of the tadpole with a wide range of severity, including strictly anterior abnormalities (DAI 3-4), strictly posterior abnormalities (DAI 7-8), and abnormalities or truncations at both ends (DAI 2+7 combined). A representative photograph of each of these phenotypes is illustrated in Figure 3.2. As demonstrated, the 'abnormal anterior' phenotype appears to be the least severe and only causes a reduction or slight truncation at the head. Embryos exhibiting the other two phenotypes show significant shortening of the anteroposterior axis. It must be noted that a certain amount of variation was observed within each phenotype category. As well, each concentration of *Xmi-er1* resulted in the full range of phenotypes. Nevertheless, the proportion of only the 'abnormal anterior & posterior' phenotype, which was by far the most severe, varied with the concentration injected, while the proportion of the other two remained relatively consistent regardless of the amount of RNA injected (Figure 3.3). The 'abnormal anterior' phenotype varied from 8% to18% and the 'abnormal posterior' phenotype only varied from 11% to 16% throughout the *Xmi-er1* injections. Figure 3.3 displays the percentages of each phenotype present per concentration of *Xmi-er1* injected. It demonstrates that as the concentration of *Xmi-er1* was increased, the percentage of embryos with anterior and posterior abnormalities also increased from 10% for the 0.5ng

injections to 61% for 2ng *Xmi-er1*.

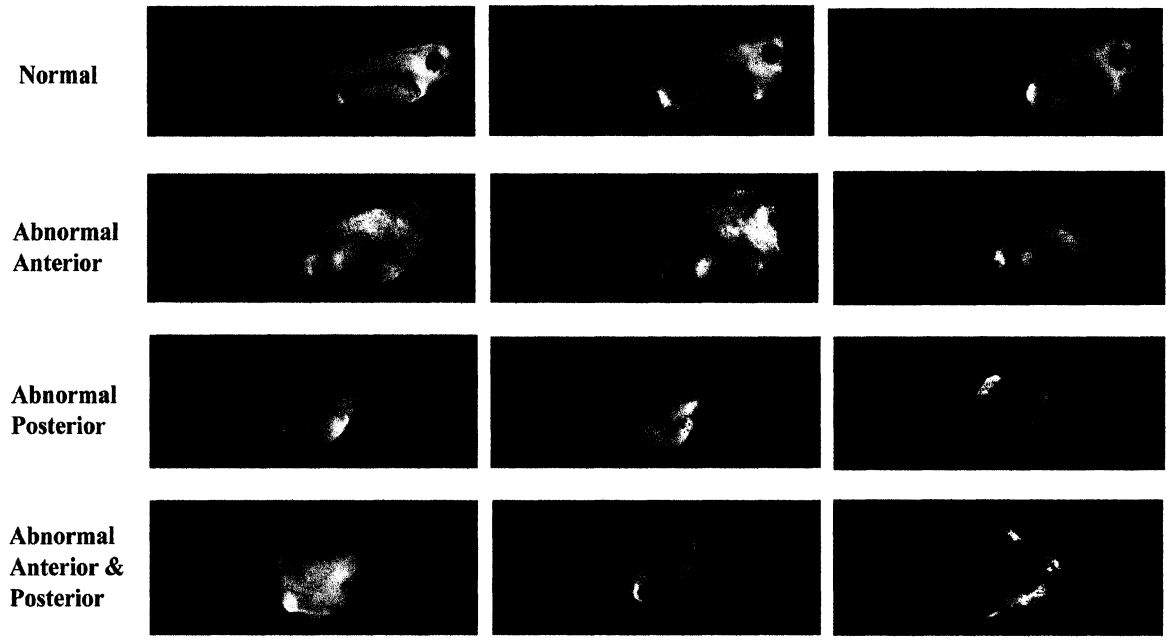

Figure 3.2 Phenotypic effects of *Xmi-er1* over-expression

Embryos were injected at the two-cell stage with 1.5ng *Xmi-er1* RNA and left at room temperature to develop until control stage 40. At this point they were fixed in MEMFA and photographed. The above photographs show the range of tadpole phenotypes observed upon *Xmi-er1* injection. These include (from top to bottom) normal embryos, embryos with anterior truncations, those with posterior truncations, and embryos with truncations at both the anterior and posterior end. Adapted from Teplitsky *et al.* (2003).

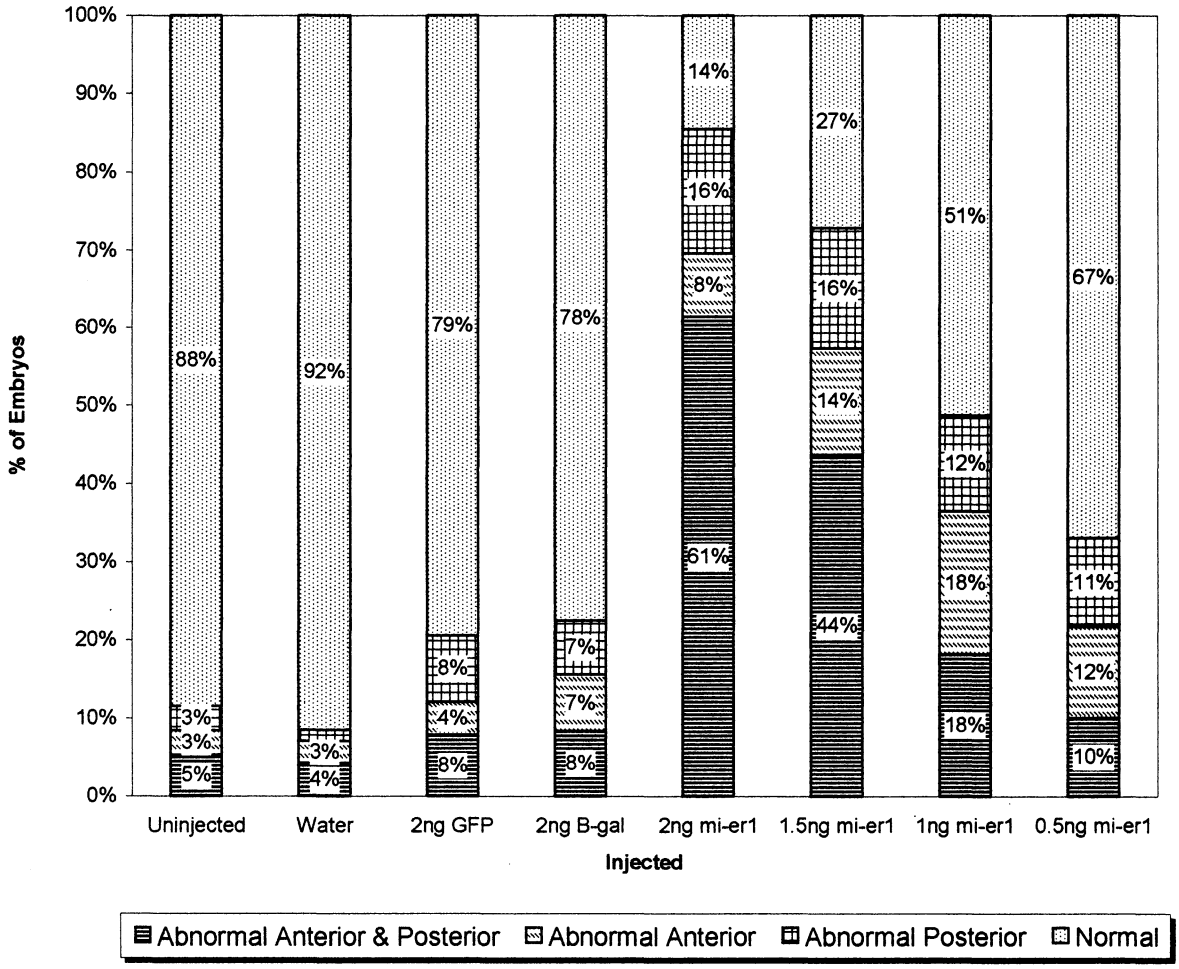

Figure 3.3 Percentages of abnormalities observed with *Xmi-er1* injections

Embryos were injected with different concentrations of *Xmi-er1* as indicated and allowed to develop at room temperature until stage 40 alongside the four sets of controls. At this point they were fixed in MEMFA and scored according to the level of abnormality observed. Three categories were used for scoring these abnormalities, all of which were along the anterior-posterior axis: abnormal anterior; abnormal posterior; and abnormal anterior and posterior.

3.3 Over-expression of XMI-ER1 adversely affects gastrulation

Throughout the early cleavage stages, the injected embryos developed normally. However, by the time they became tadpoles the situation was quite different. In order to determine whether this change occurred early or late in development, the injected embryos were also scored on the day after fertilization (at or before stage 20 in the control sets). In doing so, it was observed that gastrulation in a large number of these embryos was abnormal. In many cases, the blastopore remained open, often with a large number of loose cells protruding through it and surrounding parts of the already-gastrulated embryo such that the embryos appeared white rather than the normal brownish colour.

The graph in Figure 3.4 demonstrates that by the end of gastrulation almost all of the abnormal tadpoles that resulted from injection of *Xmi-er1* RNA had already begun their irregular development. The abnormality data collected at this stage includes all observed deformities, from the most severe to the least. The specific % abnormalities observed on day one were 91%, 75%, 42%, and 28% for 2ng, 1.5ng, 1ng, and 0.5ng of *Xmi-er1* RNA, respectively. In comparison, the percentage of abnormally gastrulated control embryos were 9%, 11%, 8% and 20% for the water-injected, uninjected, *β-gal*, and *GFP* groups, respectively. For the 2ng and 1.5ng values, the percentage of abnormal embryos was actually higher on day one than at tadpole stage for *Xmi-er1* injections. This suggests that perhaps a certain number of embryos recover. One explanation for this is the fact that the percentage abnormality calculated on day one included all abnormally gastrulated embryos, from the most severe to the least. Thus, it is possible that a few

with only slight gastrulation defects did in fact recover over the three days.

From these results it is evident that the phenotypes seen upon injection of *Xmi-er1* are the result of events affecting normal gastrulation processes and are not initiated by problems in subsequent development. Perhaps the over-expression of *Xmi-er1*, a transcriptional regulator, interferes with key signalling events in developing embryos and impairs morphogenic movements involved in gastrulation.

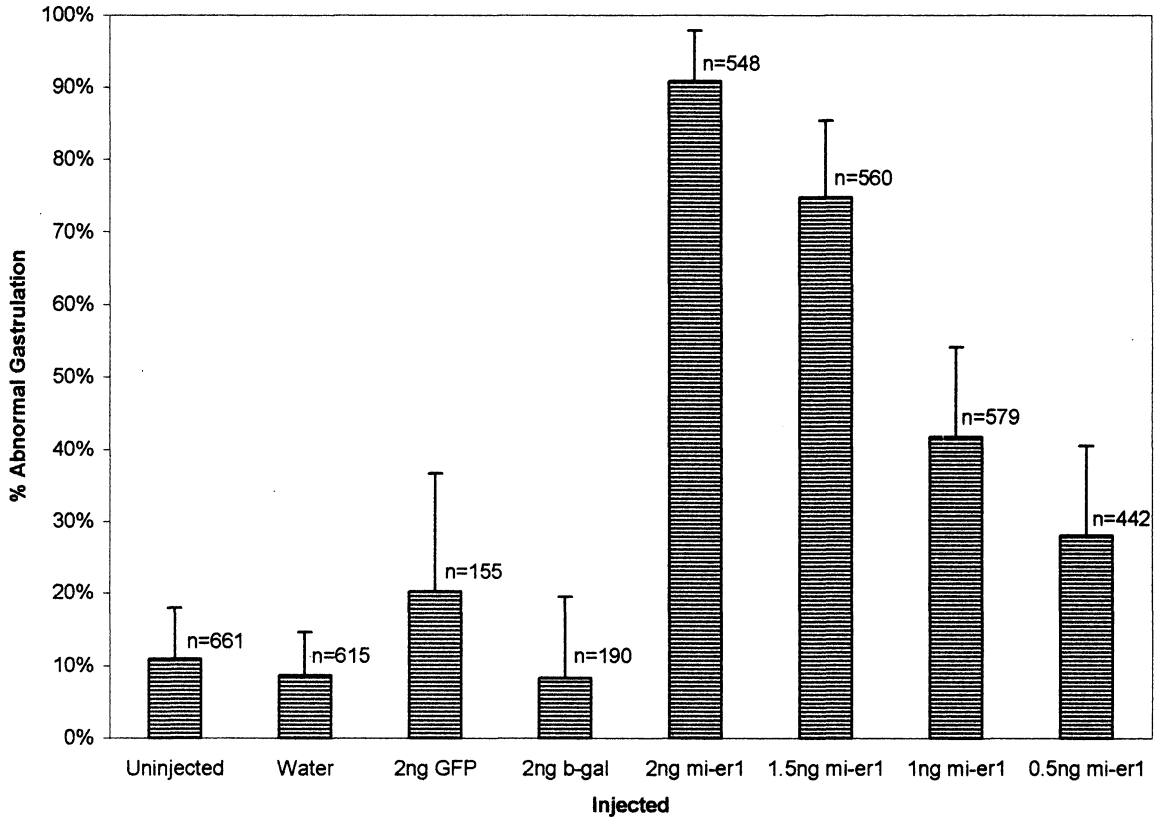

Figure 3.4 Over-expression of *Xmi-er1* causes embryos to gastrulate abnormally

Embryos were injected with one of four concentrations of *Xmi-er1* RNA and compared with the following four controls: *GFP* RNA, *β-gal* RNA, DEPC-treated dH_20, and uninjected embryos. Injections were carried out at the two-cell stage and were located at the marginal zone beside the cleavage furrow, as described in "Materials and Methods". The embryos were then left at room temperature and scored for any gastrulation defects, from the most severe to the least, by control stage 20. These are reported above as the % of abnormally gastrulated embryos out of the total number of surviving embryos (n). Data was collected from 17 experiments for the 2ng and 1.5ng data, 16 for the 1ng set, and 14 for 0.5ng. With respect to the controls, the dH_2O data is from 24 experiments; the uninjected value is from 19; and, each of the RNA controls are based on 6 experiments.

3.4 Whole mount antibody staining demonstrates that mesodermal and neural tissues still differentiate in truncated embryos

To further analyze the defects caused by *Xmi-er1* over-expression, whole mount antibody staining of neural and mesodermal gene markers was performed. This enabled the investigation of *Xmi-er1* to focus specifically on tissue development in the whole organism. Thus, embryos injected with *Xmi-er1* were fixed at the tadpole stage and subsequently stained with two different antibodies. In this way, two distinct tissue types derived from separate germ layers were examined. As FGF is known to play a critical role in the development and maintenance of mesoderm (Amaya *et al.*, 1991; Isaacs, 1997), and *Xmi-er1* was initially isolated as an early-response gene to FGF, mesoderm was one of the tissues analyzed. To accomplish this, the 12/101 monoclonal antibody was used. This antibody recognizes somitic mesoderm and would therefore clearly indicate the extent of mesoderm inhibition brought about by the over-expression of XMI-ER1 (Kintner & Brockes, 1984). By comparing the *Xmi-er1*-injected embryos with water-injected and uninjected controls, it was observed that muscle tissue development was reduced and disorganized but not altogether absent, even in the most severe *Xmi-er1* phenotypes (Figure 3.5).

In addition to its function in mesoderm development, FGF is also thought to play a role in the formation of the nervous system in *X. laevis* (Kroll & Amaya, 1996). It is known to regulate the expression of caudal genes (Northrop & Kimelman, 1994), and in doing so it has a posteriorizing effect on the neural ectoderm during gastrula and early neurula stages (Cox & Hemmati-Brivanlou, 1995). For this reason, neural tissues were

also analyzed by this method. This was carried out using the second monoclonal antibody, 2G9. 2G9 is a pan-neural antibody and therefore assesses ectodermally-derived tissues and particularly neural differentiation (Jones & Woodland, 1989). A similar result was obtained for this antibody. Again, even in the most severely abnormal tadpoles, the neural tissue was reduced and disorganized but still present (Figure 3.6).

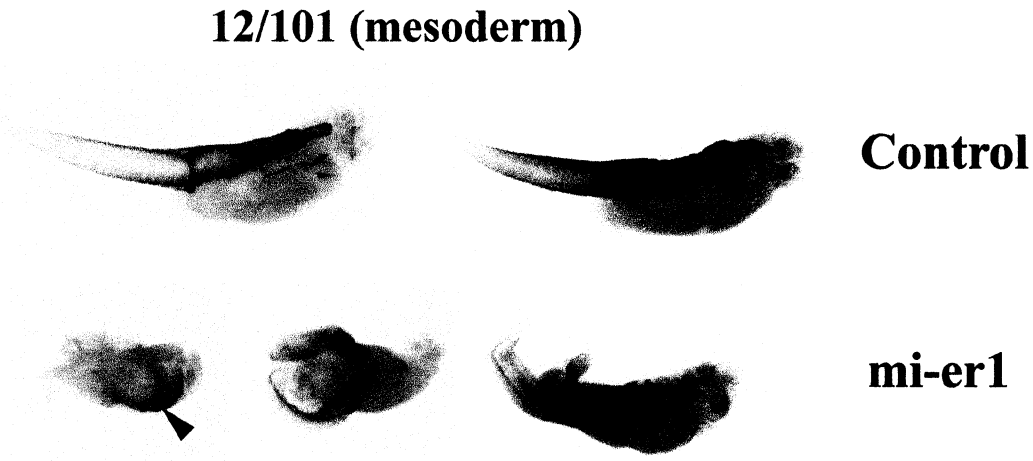

Figure 3.5 Whole mount staining with the anti-muscle antibody 12/101

Stage 40 embryos that had been previously injected with *Xmi-er1* or DEPC-treated dH_2O were fixed in MEMFA and stored in 1X PBSA + azide. The tadpoles were subject to whole mount antibody staining with the 12/101 monoclonal antibody, as described in "Materials and Methods". The above photographs are of cleared embryos and are representative of the results obtained from five separate experiments. Positive 12/101 staining appears dark purple and can be seen in all embryos, even those with the most severe abnormalities (arrow). Each embryo is oriented with the anterior to the right and the posterior to the left. Adapted from Teplitsky *et al.* (2003).

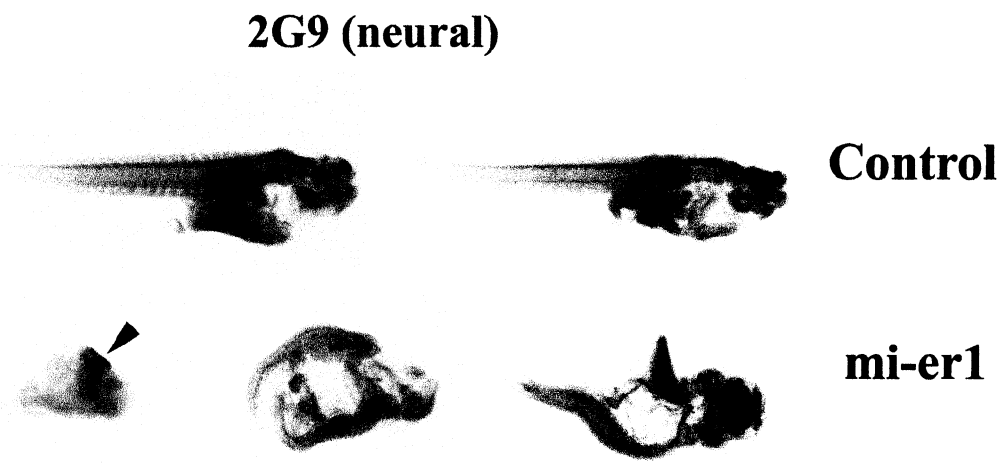

Figure 3.6 Whole mount staining with the pan-neural antibody 2G9

Embryos that had been previously injected with *Xmi-er1* and DEPC-treated dH_2O were fixed in MEMFA at control stage 40 and stored in 1X PBSA + azide until required. The tadpoles were subject to whole mount antibody staining with the monoclonal antibody 2G9, as described in "Materials and Methods". The above photographs are of cleared embryos and are representative of the results obtained from 3 individual experiments. Positive 2G9 staining of neural tissue appears dark purple and was observed in all embryos, even the most severe (arrow). Embryos are oriented with the anterior to the right and posterior to the left. Adapted from Teplitsky *et al.* (2003).

3.5 *Xmi-er1* injections cause abnormal *brachyury* expression

In an attempt to clarify the effects of *Xmi-er1* on gastrulation, an *in situ* hybridization experiment was performed using a digoxigenin-labelled *brachyury* (*Xbra*) RNA probe. *Xbra* is a transcriptional activator known to be essential for gastrulation (Conlon *et al.*, 1996). During early gastrula stages, *Xbra* is normally expressed throughout the marginal zone, forming a ring around the embryo (Smith *et al.*, 1991). As suggested by its expression pattern, this gene plays a critical role in mesoderm formation and therefore serves as a general mesodermal marker (Smith *et al.*, 2000). Isaacs *et al.* found that *Xbra* expression in *X. laevis* is regulated by eFGF (1994). As *Xmi-er1* was initially isolated as a response gene to FGF, using *Xbra* was a logical choice not only to enhance our understanding of the gastrulation defects, but of XMI-ER1 as a whole.

In order to determine whether the gastrulation defects observed upon injection of *Xmi-er1* were due to the abnormal expression of *Xbra*, albino embryos were injected with 1.5ng of *Xmi-er1* at the two-cell stage so that a percentage abnormality greater than 50% would be observed. They were then left to develop overnight at 13°C. As a control, a second set of embryos was injected with DEPC-treated dH_2O. The following day, the embryos were once again brought to room temperature and subsequently fixed in MEMFA at stage 10.5. They were then subject to whole mount *in situ* hybridization (Figure 3.7). It was found that 59% of the embryos injected with *Xmi-er1* had incomplete expression rings of *Xbra*, while only 3% of those injected with dH_2O had incomplete rings (standard deviation values are 20% and 8%, respectively). The embryos with this incomplete staining showed large gaps in the *Xbra* ring, or in some cases the staining was

almost entirely absent.

These results may serve as an explanation for the incomplete gastrulation movements observed upon *Xmi-er1* injection, as embryos with inhibited *Xbra* expression are known to have gastrulation defects (Conlon *et al.*, 1996). Furthermore, they may also explain the absence of posterior structures seen at the tadpole stage for some of these embryos, as *Xbra* is required for the formation of posterior mesoderm and axial development (Conlon *et al.*, 1996). The results could shed some light on the anterior defects as well, because defects in gastrulation could impair the migration of the already reduced mesoderm cells towards the anterior pole thus causing truncations at the head too.

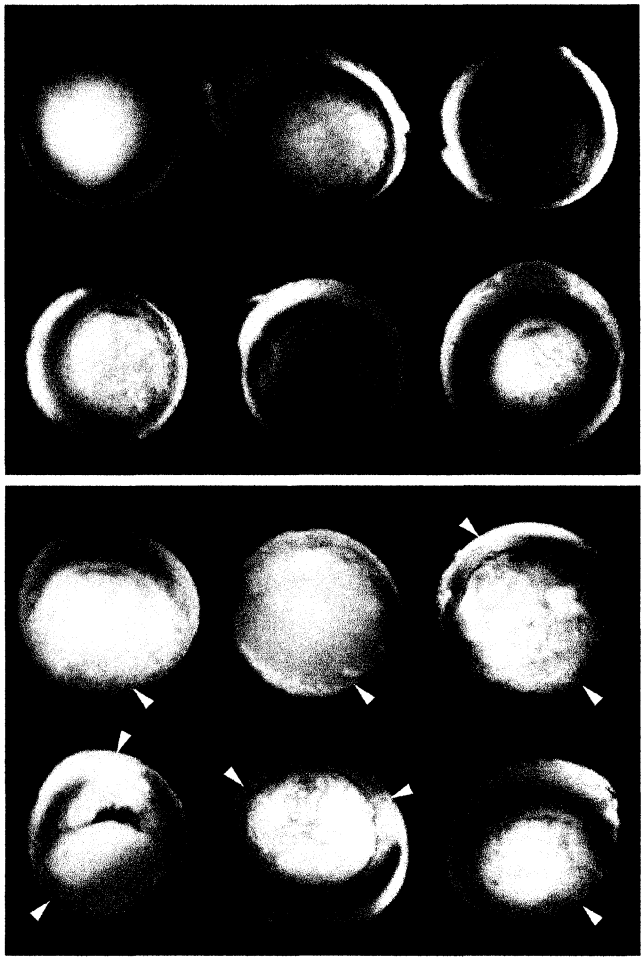

Figure 3.7 Embryos injected with *Xmi-er1* show abnormal expression of *Xbra*

Albino *X. laevis* embryos were injected with 1.5ng of *Xmi-er1* or DEPC-treated dH_2O and fixed in MEMFA at stage 10.5. Whole mount *in situ* hybridization was carried out using a probe for *Xbra*. Digital photographs representative of the *Xbra* expression patterns observed are shown above for both injected sets. White arrows in the bottom photographs highlight gaps in *Xbra* expression pattern observed in 59% (n=20) of *Xmi-er1*-injected embryos. These results are based on five independent experiments. Adapted from Teplitsky *et al.* (2003).

3.6 Over-expression of *Xmi-er1* inhibits *in vitro* mesoderm induction by FGF

Due to the fact that *Xmi-er1* was initially discovered in response to FGF-induced mesoderm induction, this phenomenon was revisited once a phenotype had been assigned to the gene upon up-regulation. Thus, in an attempt to define the activities of XMI-ER1, its effect on mesoderm induction was next analyzed.

Embryos were injected with *Xmi-er1* in the animal cap of each cell at the four-cell stage such that a total of 1.5ng was injected. This was done in order to increase the probability that the majority of the injection site was excised when caps were cut at stage 8. As a control for induction, a second set of embryos was injected with DEPC-treated dH_2O. They were then left to develop at room temperature until stage 8. At this point, the animal cap was removed and placed in *Xenopus* FGF-2, a known mesoderm inducer. Four different concentrations of FGF-2 were used for this experiment: 0.5ng/ml, 1ng/ml, 2ng/ml, and 5ng/ml. A number of embryos in each experiment were also placed in NAM/2 + BSA as a negative control for mesoderm induction. The explants were left at room temperature for three days and then scored for mesoderm induction. Scores were marked as positive if the explant elongated from its original ball-like shape and expanded to form a bubble.

Preliminary experiments using only one concentration of FGF-2 suggested that mesoderm induction was reduced in those embryos that had been injected with *Xmi-er1* when compared with water-injected controls. It was therefore expected that if *Xmi-er1* was a true inhibitor of mesoderm induction, then its inhibitory activity should be demonstrated at near-threshold levels of FGF-induced mesoderm induction (1ng/ml and

2ng/ml) but could be rescued at higher FGF concentrations. In fact, this is precisely what was found in six separate experiments, as summarized in Figure 3.8. Over-expression of *Xmi-er1* resulted in a lower percentage of induced explants when compared with the water-injected controls, and this induction level was dependent on FGF-2 concentration. The greatest differential occurred at 0.5ng/ml FGF-2, where only 19% of *Xmi-er1*-injected explants were induced compared to a 50% induction in the controls. When the FGF-2 concentration was raised to 1ng/ml, 37.5% of those injected with *Xmi-er1* formed mesoderm, whereas 64% of the water-injected controls were induced. Likewise, at 2ng/ml FGF-2, the difference between the two sets was 57% versus 87%, respectively. Yet, at the highest concentration of FGF-2, no such difference was observed, as 92% of the *Xmi-er1*-injected explants were induced, and a corresponding 90% of the water-injected explants were also induced. Thus, the high FGF concentration alone was able to entirely rescue the effects of *Xmi-er1* over-expression, indicating that XMI-ER1 in *X. laevis* specifically inhibits mesoderm induction.

As a whole, these results, which demonstrate a partial inhibition of mesoderm induction, are consistent with the observations made with the whole mount antibody staining showing a reduction of tissues rather than a complete lack of them. They also agree with the *Xbra in situ* hybridization data, which establishes that XMI-ER1 interferes with *Xbra* expression but does not completely abolish it. Similarly, *Xmi-er1* over-expression also appears to reduce FGF-induced mesoderm induction, but again it does not appear to inhibit this event altogether.

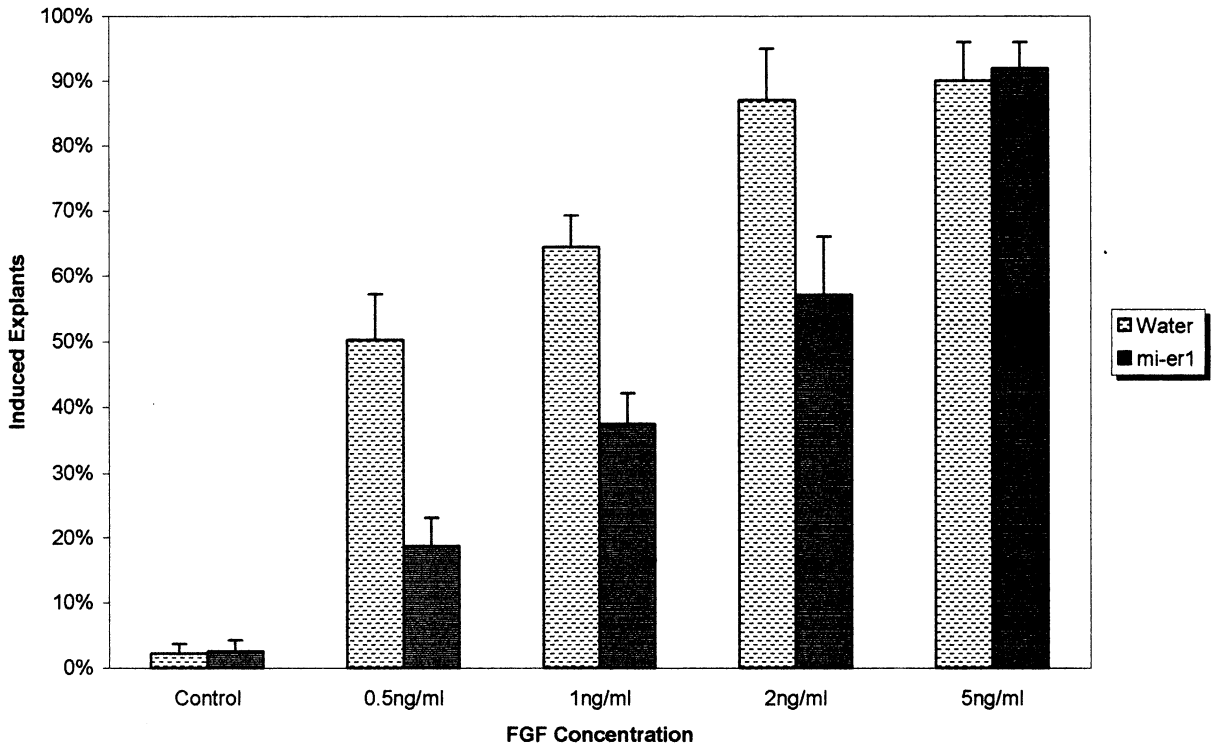

Figure 3.8 Over-expression of *Xmi-er1* inhibits mesoderm formation at near-threshold levels of induction by FGF

Embryos were injected at the four-cell stage in the animal cap of each cell with a total of 1.5ng *Xmi-er1* RNA or with DEPC-treated dH_2O. At stage 8, explants were cut and cultured in one of four different concentrations of FGF or in the control medium which was NAM/2 + 1mg/ml BSA. The explants were left to grow for three days and scored on the third day for mesoderm induction. The graph is based on six individual experiments and the percentage induction was calculated from the total number of explants induced to form mesoderm out of the total number of explants cultured (75 per sample).

3.7 Activin-induced mesoderm induction is not inhibited by XMI-ER1

In order to examine whether XMI-ER1 acts as a general inhibitor of mesoderm formation or is specific to the FGF pathway, its activity was tested in conjunction with a second mesoderm inducer, activin. Embryos were injected in the animal pole of each cell at the four-cell stage with 1.5ng *Xmi-er1* or DEPC-treated dH_2O. These embryos were left to develop until stage 8 at which point explants were removed and cultured in one of five concentrations of activin for three days (0.01ng/ml, 0.025ng/ml, 0.05ng/ml, 0.1ng/ml, and 0.15ng/ml). The induction results are demonstrated in Figure 3.9. It was found that below the induction threshold for the controls, at 0.01ng/ml activin, only 3% and 4% of water-injected and *Xmi-er1*-injected explants were induced, respectively. However, at the next highest concentration of activin, the 0.025ng/ml threshold, 96% of the control explants were induced compared to 86% of the *Xmi-er1*-injected explants. At 0.05ng/ml activin, the values were 77% for the controls and 61% for *Xmi-er1*. For the two upper concentrations, both sets had equivalent induction levels. Statistical analysis of the induction values observed at 0.025ng/ml and 0.05ng/ml activin demonstrated that there is no significant difference between the *Xmi-er1*-injected sets and the controls. These results suggest that XMI-ER1 does not play a role in the activin pathway.

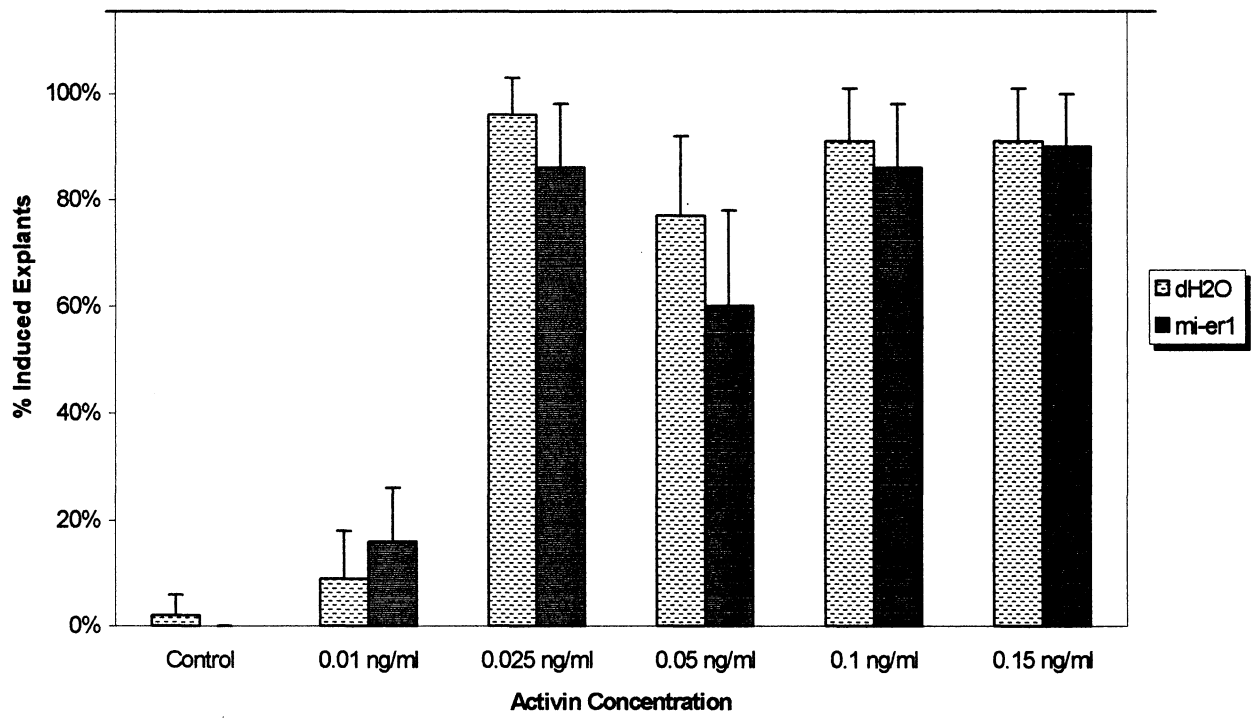

Figure 3.9 Over-expression of *Xmi-er1* does not inhibit mesoderm formation during activin-induced mesoderm induction

Embryos were injected at the four-cell stage with 1.5ng *Xmi-er1* or with DEPC-treated dH_2O. At stage 8, explants were cut and cultured in one of five concentrations of activin (listed above), or in NAM/2 + 1mg/ml BSA as a negative control. Explants were scored three days later for mesoderm induction. The above results are based on seven separate experiments and the percentage induction was calculated from the number of explants induced to form mesoderm out of the total number cultured (approximately 35-45 per sample).

3.8 The proline-rich domain is critical to the development of the XMI-ER1 abnormalities, while the SANT domain, ELM2 domain, and putative MEK phosphorylation site are not

There are numerous functional domains present in the XMI-ER1 protein. In order to investigate which of these are required for inducing the abnormalities seen upon injection of *Xmi-er1* into embryos, a number of constructs were created that had mutations at key amino acids within these domains (Figure 3.10). The purpose of creating these constructs was twofold: first, to identify which domains were essential for XMI-ER1 protein function during early *X. laevis* development; and second, to pinpoint the activity of these domains to specific amino acid residues within them.

The domains investigated included the ELM2 domain, the SANT domain, a proline-rich motif, and a putative MEK phosphorylation site. The mutated amino acids were selected based on comparisons with the same domains in other proteins using the National Center for Biotechnology Information BLAST Network Service. The chosen residues were those that appeared to be the most highly conserved throughout evolution (*i.e.*, in all types of organisms), which is suggestive of their significance to the activity of the domain in their respective protein. Generally, in a mutational analysis, one of two approaches can be taken: 1) the amino acids can be mutated to other amino acids; or, 2) they can be deleted entirely. In the first method, these new residues can be similar to the original in terms of acidity/basicity, size, polarity, and charge, or they may be completely different. No one approach is better than another. For this reason, both methods were applied in this study, and a variety of tactics were employed for the mutations.

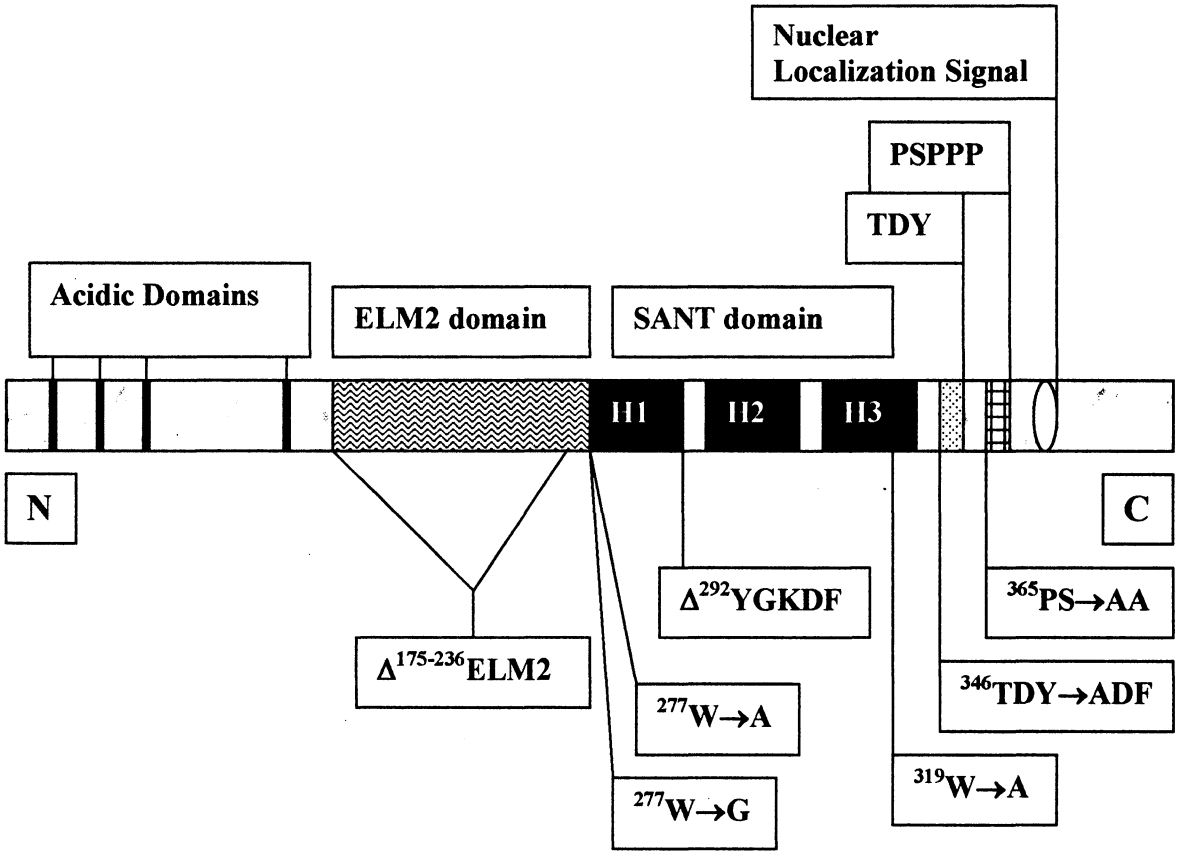

Figure 3.10 Schematic demonstrating the putative functional domains in XMI-ER1 and the mutations made in each domain

The above illustration summarizes the functional domains found in XMI-ER1 (labelled on top), as well as the general location of the mutation-containing constructs made in four of the domains (labelled below the diagram). The N-terminal domain consists of four regions of acidic amino acids. Located in the centre of the protein are the ELM2 domain and the corresponding $\Delta^{175\text{-}236}$ELM2 construct. Towards the C-terminus is the SANT domain composed of three helices, labelled H1, H2, and H3. The four constructs made in this region include ^{277}W→A, ^{277}W→G, ^{319}W→A, and Δ^{292}YGKDF. Following this is a putative MEK phosphorylation site (TDY), and the ^{346}TDY→ADF construct. Next is the proline-rich motif (designated PSPPP) thought to bind SH3 domains of other proteins. The construct in this domain is ^{365}PS→AA. At the C terminus is a *bona fide* NLS (Post *et al.*, 2001).

The mutation in the ELM2 domain, named $\Delta^{175\text{-}236}elm2$, involved a deletion of the majority of this domain to see whether this region was required for XMI-ER1 function. Those in the SANT domain, $^{319}W\rightarrow A$, $^{277}W\rightarrow A$, $\Delta^{292}YGKDF$, and $^{277}W\rightarrow G$, encompassed a variety of approaches to mutational analysis. The former two were considered to be moderate mutations in that a large, bulky, non-polar residue (tryptophan) was replaced with a small, also non-polar one (alanine). One the other hand, the latter mutation was more disruptive because the non-polar tryptophan was replaced with a polar glycine, which is a suspected helix-breaker. With respect to $\Delta^{292}YGKDF$, this construct involved a deletion of five highly conserved amino acids. Rather than deleting the whole SANT domain, it was hoped that this smaller deletion would accomplish the same goal of interfering with the SANT domain function without affecting the whole protein. The mutation in the proline-rich motif, $^{365}PS\rightarrow AA$, was made in these two residues to disrupt the activity of this region. The proline is a critical residue for the consensus SH3 binding motif and the serine in this sequence has the potential to be phosphorylated. Therefore both were mutated. As well, the mutation in the putative phosphorylation site was $^{346}TDY\rightarrow ADF$ in an attempt to disrupt possible phosphorylation at the threonine and tyrosine by MEK.

All of the mutations were made by site-directed mutagenesis of *Xmi-er1* cDNA. After they were sequenced to confirm the presence of the desired mutations, the constructs were transcribed into RNA and then injected into *X. laevis* embryos alongside wild-type *Xmi-er1*. Due to the fact that wild-type *Xmi-er1* injections led to abnormal embryos, it was predicted that a successful mutation (*i.e.*, one that obstructed the activity

of a required functional domain in XMI-ER1) would result in normal embryos. Thus, by interfering with the function of a particular domain, the activity of the protein itself would also be affected, which would in turn influence the abnormalities seen with the wild-type injections. This would indicate that the specific domain plays a role in that activity and that the mutated amino acids are integral to this role.

All of the mutants caused abnormalities that were similar to those obtained for *Xmi-er1* injections except for the ^{365}PS→AA mutant. For this latter construct, the percent abnormality was comparable to that of the control RNAs. The overall percentages of abnormal embryos observed with these injections are shown in Figure 3.11.

The specific percentages from 1ng to 2ng ranged from approximately 15% to 100% for $^{277}W\rightarrow A$, $^{277}W\rightarrow G$, and $^{319}W\rightarrow A$. While these constructs were only analyzed in two experiments at most due to their failure to alter the *Xmi-er1* injection phenotype, all of the remaining constructs were injected over four or more separate experiments. The corresponding range of the percentage abnormality from 1ng to 2ng was about 36% to 94% for $\Delta^{175\text{-}236}elm2$, $^{346}TDY\rightarrow ADF$, and $\Delta^{292}YGKDF$. As was the case for *Xmi-er1*, the injection of increasing concentrations of each of these constructs resulted in a dose-dependent increase in the percentage of abnormal embryos. As each of these mutants gave phenotype results similar to *Xmi-er1* when injected, they did not appear to interfere with an active domain in the XMI-ER1 protein. From this it can be inferred that the amino acids affected by these various mutations are not involved in mediating the effects seen in the *Xmi-er1* phenotype.

This was not the case for the PXXP motif construct, pictured in Figure 3.12. The

percentage abnormalities observed for $^{365}PS\rightarrow AA$ were 17%, 24%, and 15% at 2ng, 1.5ng, and 1ng, respectively, compared to the RNA controls at 21%. Thus, the majority of embryos injected with $^{365}PS\rightarrow AA$ consistently developed normally, as observed in 2 experiments for the 2ng injections and 6 or more experiments for the other sets. The abnormalities did not increase in a dose-dependent manner like those for *Xmi-er1* but stayed relatively constant and low, regardless of the amount of RNA injected.

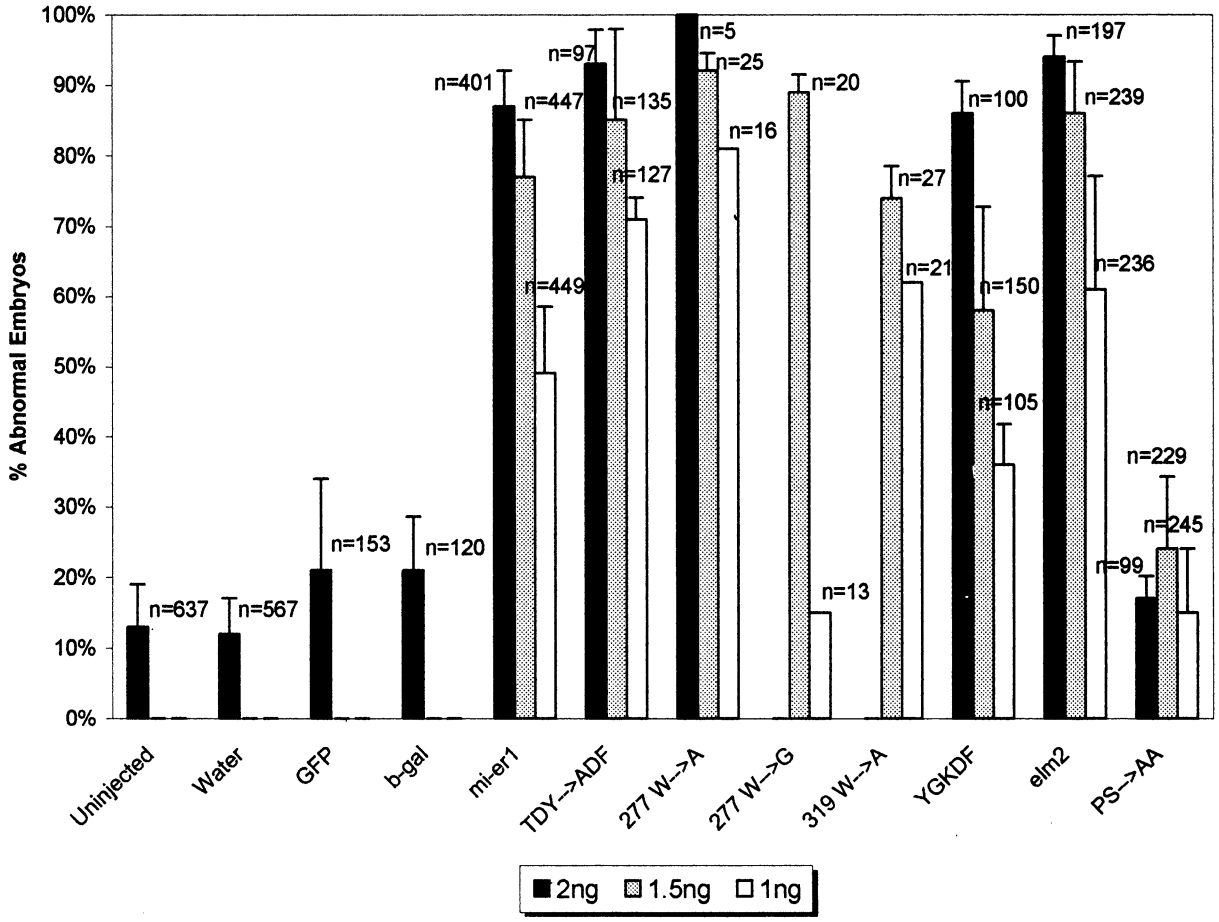

Figure 3.11 **$^{365}PS\rightarrow AA$ mutant highlights amino acids that are required for the development of XMI-ER1 abnormalities**

Embryos were injected with one of three concentrations of $^{346}TDY\rightarrow ADF$, $^{277}W\rightarrow A$, $^{277}W\rightarrow G$, $^{319}W\rightarrow A$, $\Delta^{292}YGKDF$, $\Delta^{175\text{-}236}elm2$, $^{365}PS\rightarrow AA$ at the two-cell stage in the marginal zone alongside *Xmi-er1*. After three days at room temperature, the stage 40 tadpoles were scored for abnormalities. The above graph shows the percentage of abnormal embryos out of the total number of surviving embryos (n, indicated above each bar). The results for $^{277}W\rightarrow A$, $^{277}W\rightarrow G$, and $^{319}W\rightarrow A$ are based on one experiment only with the exception of the 1.5ng data, which is based on two experiments. For $^{346}TDY\rightarrow ADF$ and $\Delta^{292}YGKDF$, the data is based on 5 experiments for the 1.5ng set and 4 experiments for the other two concentrations. For $\Delta^{175\text{-}236}elm2$, the results are from 9 experiments. The $^{365}PS\rightarrow AA$ values are from 2, 6, and 8 experiments for the 2ng, 1.5ng, and 1ng sets, respectively. There is no data available for $^{277}W\rightarrow G$ and $^{319}W\rightarrow A$ at 2ng.

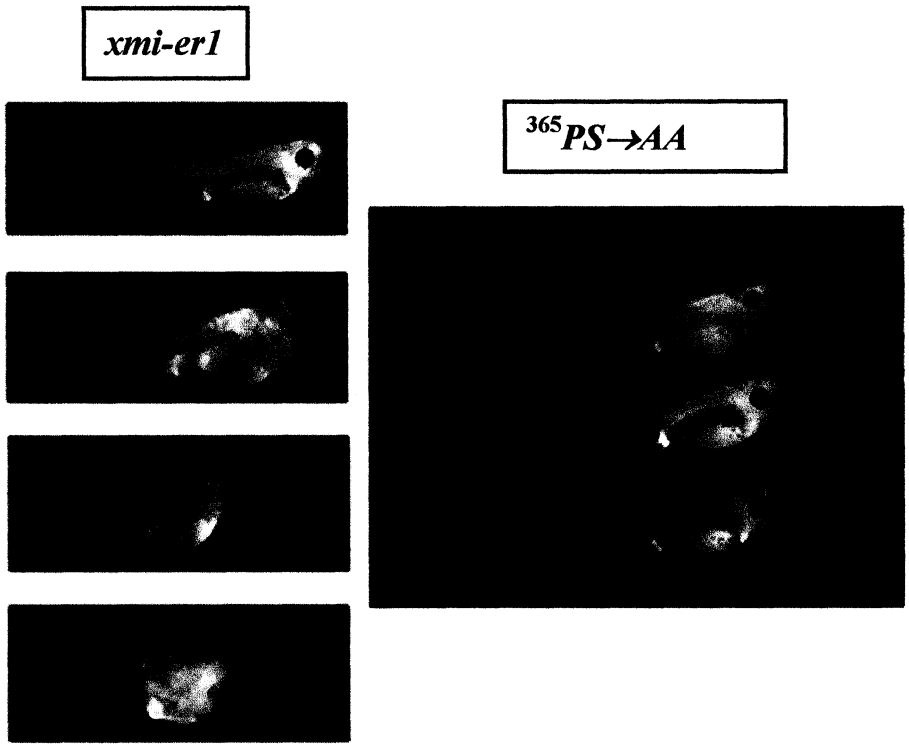

Figure 3.12 Embryos injected with $^{365}PS\rightarrow AA$ develop normally compared to *Xmi-er1*-injected embryos

Embryos were injected at the 2-cell stage with 1ng of $^{365}PS\rightarrow AA$ RNA and left at room temperature to develop until control stage 40. They were then fixed in MEMFA and photographed. The above photographs demonstrate the phenotypes expressed by the majority of embryos over-expressing $^{365}PS\rightarrow AA$ compared to embryos injected with *Xmi-er1*.

3.9 ^{365}P is critical for XMI-ER1 effects on development, while ^{366}S is not

After discovering that the $^{365}PS \rightarrow AA$ mutation was able to knock-out the *Xmi-er1* effect when injected into developing embryos, this construct was analyzed further to determine whether this was due to the proline residue, the serine residue, or to both. To do this, the following two additional mutants were made: $^{365}P \rightarrow A$ and $^{366}S \rightarrow A$. These were then injected into embryos and compared with both $^{365}PS \rightarrow AA$ as well as *Xmi-er1*. The percentage abnormality results observed in these experiments are displayed in Figure 3.13, and photographs of the embryos are shown in Figure 3.14.

The $^{365}P \rightarrow A$ construct led to results that were similar to $^{365}PS \rightarrow AA$ in that the percentage abnormality was low and remained constant regardless of the RNA concentration. Again, no dose-dependent increase was observed for these injections. The specific results for this construct were 20%, 21%, 19%, and 19% for 2ng, 1.5ng, 1ng, and 0.5ng, respectively. On the other hand, the $^{366}S \rightarrow A$ results were 77%, 57%, 46%, and 35%, for 2ng, 1.5ng, 1ng, and 0.5ng, respectively, compared to 87%, 77%, 49%, and 44% for the *Xmi-er1* injections. Thus, it appears as though the $^{366}S \rightarrow A$ mutation causes no deviation from the *Xmi-er1* results.

The fact that the injection of both $^{365}PS \rightarrow AA$ and $^{365}P \rightarrow A$ caused the development of embryos with a phenotype different from those injected with *Xmi-er1* suggests that the domain in which these mutations are located is important for the proper functioning of XMI-ER1. Moreover, the results show that the presence of one specific proline in the region (^{365}P) is integral to this activity while the adjacent serine is not (^{366}S). It is therefore evident that the mutation in this first proline and not the serine is responsible for

the difference observed upon $^{365}PS \rightarrow AA$ injection when compared with *Xmi-erl*.

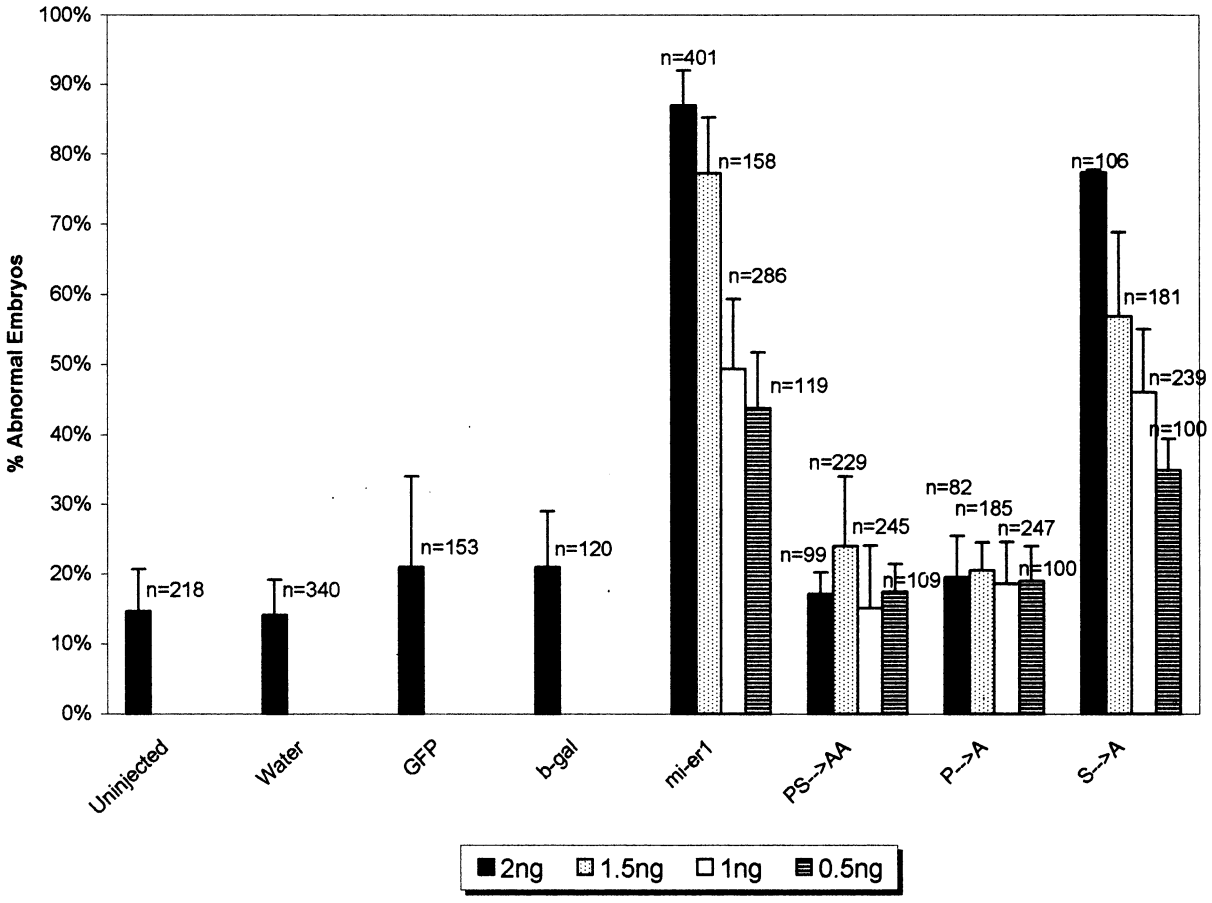

Figure 3.13 Over-expression of $^{365}PS\rightarrow AA$ and $^{365}P\rightarrow A$ has no effect when injected into embryos but $^{366}S\rightarrow A$ results in phenotype similar to that of wild-type *Xmi-er1*

Embryos were injected with one of four concentrations of $^{365}PS\rightarrow AA$, $^{365}P\rightarrow A$, or $^{366}S\rightarrow A$ at the two-cell stage in the marginal zone alongside *Xmi-er1* injections. After three days at room temperature, the stage 40 tadpoles were scored for abnormalities. The above graph shows the percentage of abnormal embryos out of the total number of surviving embryos for each set of injections (n, indicated above each bar). The number of experiments upon which this data is based is 2 for the 2ng injections, 6 for the 1.5ng set, 9 for the 1ng set, and 3 for the 0.5ng injections. The data for $^{365}PS\rightarrow AA$ at 1ng is based on 8 experiments rather than 9.

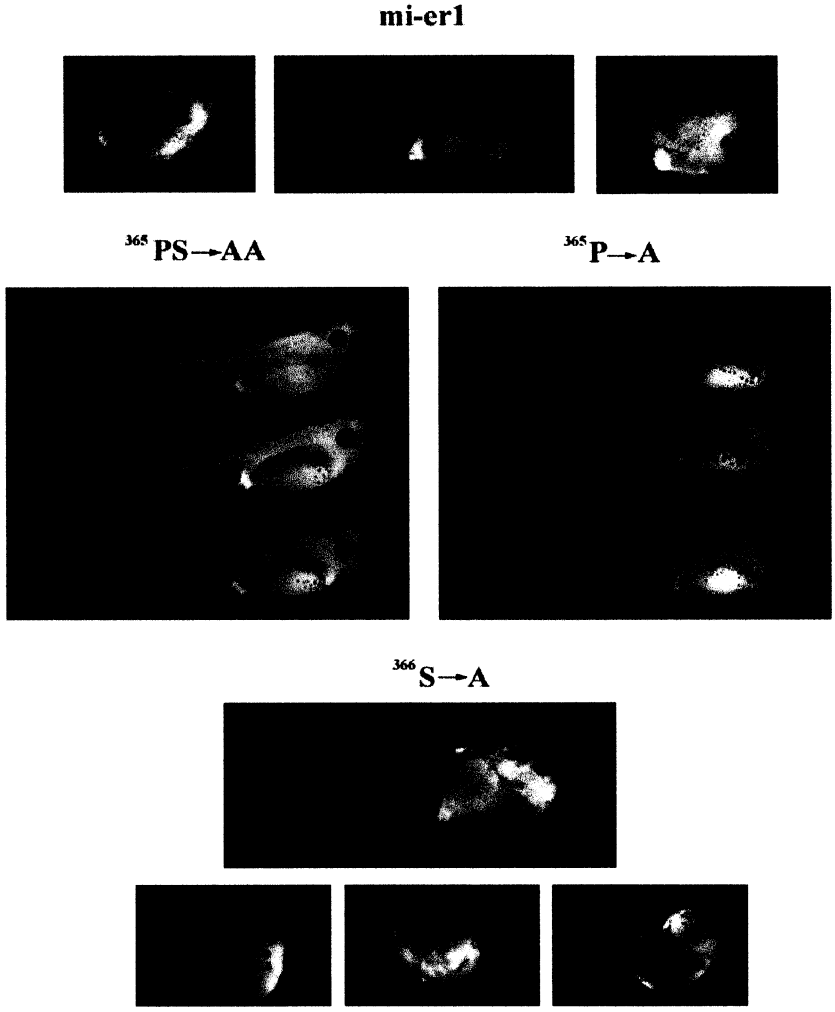

Figure 3.14 Phenotypic effects of over-expressing ^{365}PS→AA, ^{365}P→A, & ^{366}S→A

Embryos were injected at the 2-cell stage with one of *^{365}PS→AA*, *^{365}P→A*, or *^{366}S→A* and left at room temperature to develop until control stage 40. They were then fixed in MEMFA and photographed. The embryos pictured were injected with 1.5ng *^{365}PS→AA*, *^{365}P→A*, *^{366}S→A*, or *Xmi-er1*. The above photographs demonstrate the phenotypes expressed by the majority of embryos in each group. Thus, *^{365}PS→AA* and *^{365}P→A* gave mainly normal embryos while *^{366}S→A* resulted in primarily abnormal embryos upon injection.

3.10 Injected embryos show similar levels of XMI-ER1 protein expression

In order to ensure that the observed phenotypic differences described above were not due to variations in the amount of protein being translated from each RNA, the total protein per embryo was extracted. Using Western Blot analysis with an anti-MI-ER1 antibody, the expression levels of XMI-ER1 (and its mutants) were determined. It was found that the protein levels were equivalent for all constructs, as is demonstrated by the bands in Figures 3.15a and 3.15b.

The data in (a) represents *Xmi-er1*, $^{346}TDY \rightarrow ADF$, $^{319}W \rightarrow A$, $^{277}W \rightarrow A$, $\Delta^{292}YGKDF$, $^{277}W \rightarrow G$, and $\Delta^{175\text{-}236}elm2$. The comparable protein levels confirm that the abnormal effects of injecting these RNAs were not caused by irregular protein expression, and were due to the constructs themselves. As a negative control for this data set, water-injected embryos were analyzed as well. Despite its known presence in the embryo at this time, endogenous XMI-ER1 expression was not visible because its levels were too low to detect.

Figure 3.15(b) shows the expression levels of *Xmi-er1*, $^{365}PS \rightarrow AA$, $^{365}P \rightarrow A$, and $^{366}S \rightarrow A$. Again, the protein levels for these constructs were similar. This implies that the development of normal tadpoles upon the injection of $^{365}PS \rightarrow AA$ and $^{365}P \rightarrow A$ into embryos was not due to a lack of protein expression or to abnormal protein expression. Rather, these results demonstrate that normal tadpoles were able to develop despite the presence of excess ^{365}PS→AA and ^{365}P→A protein but could not do so with over-expression of ^{366}S→A or XMI-ER1.

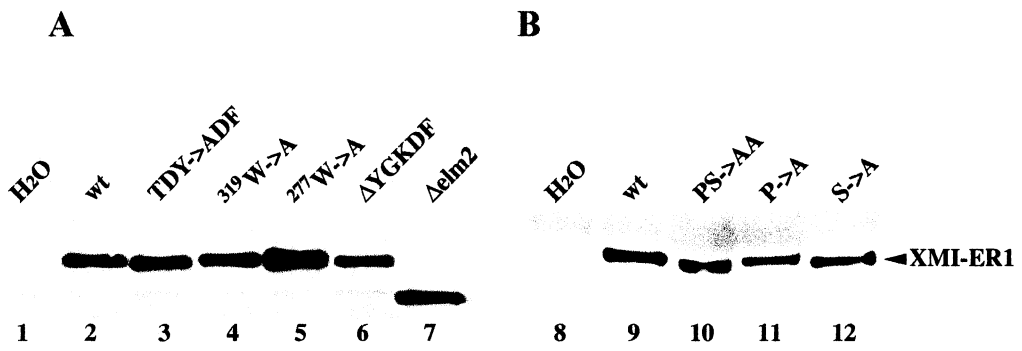

Figure 3.15 Protein expression levels in injected embryos

Embryos were injected in the marginal zone at the 2-cell stage with RNA, as specified below. Protein was extracted at stage 8.5 and subjected to SDS-PAGE and Western Blot analysis, as detailed in "Materials and Methods". Isolated protein was loaded onto a 10% protein gel. The western blots were stained using a 1/5000 dilution of the anti-MI-ER1 antibody and a 1/5000 dilution of the secondary antibody. a) Embryos were injected with H_2O, *Xmi-er1 (wt)*, $^{346}TDY \rightarrow ADF$, $^{319}W \rightarrow A$, $^{277}W \rightarrow A$, $\Delta^{292}YGKDF$, $^{277}W \rightarrow G$, or $\Delta^{175\text{-}236}elm2$, as indicated. H_2O was used as a negative control. b) Embryos were injected with H_2O, $^{365}PS \rightarrow AA$, $^{365}P \rightarrow A$, $^{366}S \rightarrow A$, or *Xmi-er1*, as indicated. Adapted from Teplitsky *et al.* (2003).

3.11 The lack of effects seen with $^{365}PS \rightarrow AA$ and $^{365}P \rightarrow A$ injections are not due to differences in protein behaviour

In order to further investigate the role of the first proline in the proline-rich domain of XMI-ER1, a gel shift assay was performed. This was done to determine whether the absence of this residue or the presence of an alanine in $^{365}PS \rightarrow AA$ and $^{365}P \rightarrow A$ caused any changes in the conformation of the protein (Berrada *et al.*, 2002; Zhang *et al.*, 2003). To resolve this, the constructs were first translated *in vitro* and the resulting proteins were run on a 5% non-denaturing acrylamide gel (Figure 3.16). This technique was employed to reveal any major physical differences in the proteins that could affect how they run on a gel. Discrepancies would have been evident by a band shift on the gel. Nonetheless, as demonstrated in the figure, there were no differences observed in the proteins. Therefore, a conformational change for ^{365}PS→AA and ^{365}P→A cannot explain the variations in the injection results obtained for these constructs when compared with *Xmi-er1*.

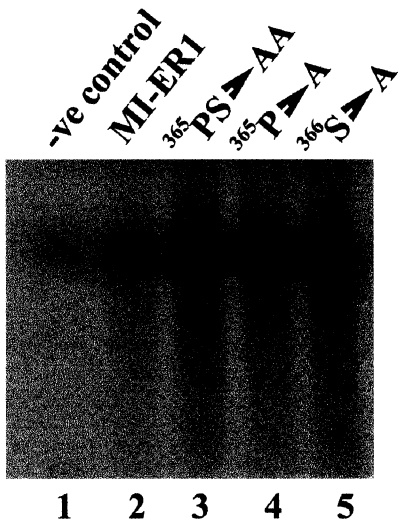

Figure 3.16 Migration of mutant and wild-type XMI-ER1 on a non-denaturing protein gel

Mutant and wild-type *Xmi-er1* RNA were translated into protein *in vitro* and loaded onto a 5% non-denaturing protein gel for analysis. All bands migrated the same distance indicating no changes in the overall structure of the constructs when compared with XMI-ER1. The negative control used was translation mix with no RNA added. The protein shown in each lane is indicated above.

3.12 FGF-induced mesoderm induction is inhibited by $^{366}S\rightarrow A$ but not by $^{365}PS\rightarrow AA$ or $^{365}P\rightarrow A$

As demonstrated, the *Xmi-er1* constructs involving the residues of the proline-rich motif did not affect the development of embryos into tadpoles when the first proline was mutated to an alanine. Thus, two of the constructs, $^{365}PS\rightarrow AA$ and $^{365}P\rightarrow A$, had no effect on tadpole development, while the third one, $^{366}S\rightarrow A$, caused abnormalities similar to those resulting from *Xmi-er1* injections. The next step was therefore to determine what effects these constructs would have on mesoderm induction *in vitro*. These could then be compared to the effects of wild-type *Xmi-er1* in this assay.

Embryos were injected in the animal pole of each cell at the four-cell stage either with *Xmi-er1*, $^{365}PS\rightarrow AA$, $^{365}P\rightarrow A$, or $^{366}S\rightarrow A$ such that the total concentration injected per embryo was 1.5ng. As a control, dH_2O was also injected. These embryos were allowed to develop at room temperature until stage 8, at which point explants were removed from the animal poles and cultured in 1ng/ml FGF or in NAM/2 + BSA as a negative control. The results for this experiment are shown in Figure 3.17. The graph demonstrates that $^{365}PS\rightarrow AA$ and $^{365}P\rightarrow A$ resulted in induction levels of 76% and 75%, respectively, compared to 76% for the water-injected controls. Furthermore, the induction level recorded for $^{366}S\rightarrow A$ was 38%. This is similar to the percent induction observed for *Xmi-er1* (32%) reinforcing the observation that this construct fails to eliminate the effects of XMI-ER1 over-expression. Conversely, $^{365}PS\rightarrow AA$ and $^{365}P\rightarrow A$ do appear to knock out the inhibitory effect of XMI-ER1 on FGF-induced mesoderm induction, confirming the fact that the mutated proline common to both mutants is integral for this function.

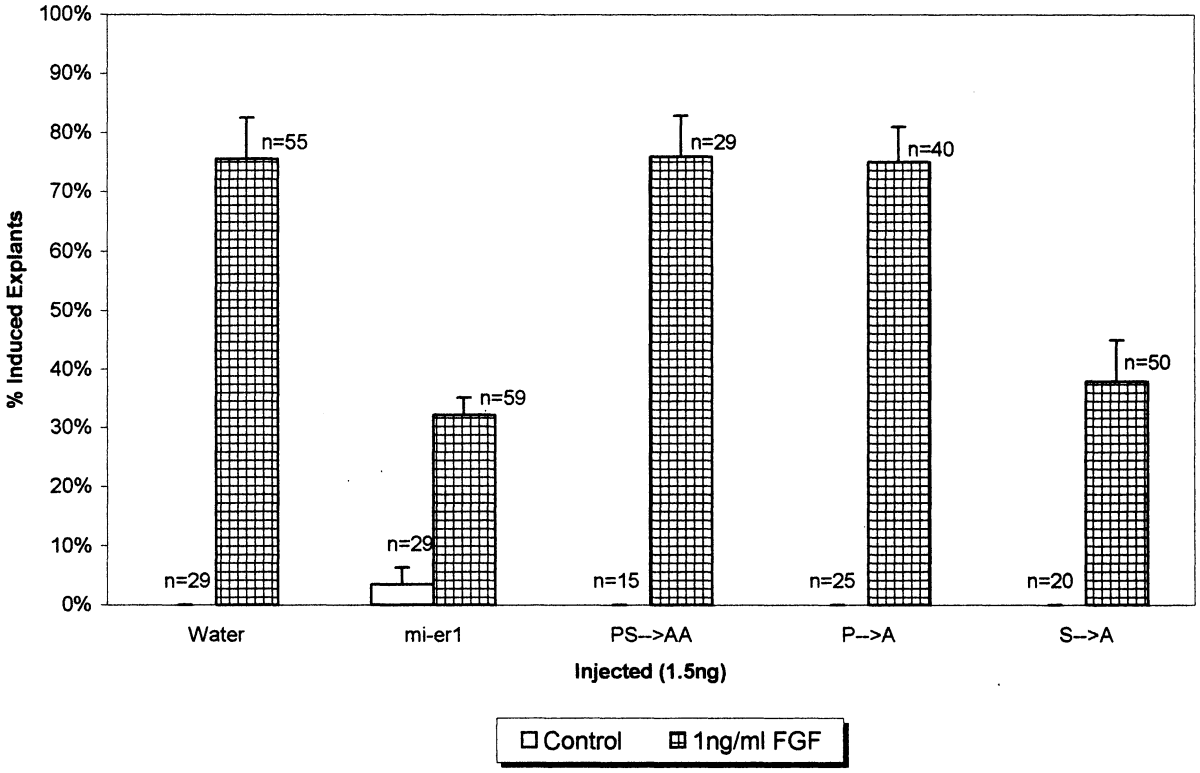

Figure 3.17 **$^{366}S\rightarrow A$ shows inhibition similar to that of *Xmi-er1* during mesoderm induction by FGF, while $^{365}PS\rightarrow AA$ and $^{365}P\rightarrow A$ do not**

Embryos were injected at the four-cell stage in the animal pole of each cell with a total of 1.5ng *Xmi-er1*, $^{365}PS\rightarrow AA$, $^{365}P\rightarrow A$, $^{366}S\rightarrow A$, or with DEPC-treated dH_2O. They were left to develop until stage 8, at which point explants were cut and cultured in 1ng/ml FGF or in NAM/2 + 1mg/ml BSA as a control. Explants were left to grow for three days and scored on the third day for mesoderm induction. The graph is based on 3 different experiments for the $^{365}PS\rightarrow AA$ and $^{366}S\rightarrow A$ data, 4 experiments for $^{365}P\rightarrow A$, and 6 for the *Xmi-er1* and water sets. The percentage induction was calculated from the number of explants induced to form mesoderm out of the total number of explants cultured (indicated as n above each bar).

Chapter 4: Discussion

It is now well established that FGF signal transduction plays a critical role in the proper development and maintenance of mesoderm in the developing *X. laevis* embryo (Amaya *et al.*, 1991; Amaya *et al.*, 1993; Isaacs, 1997). The recent discovery of MI-ER1, an immediate-early gene in the FGF signalling pathway, has revealed a possible key player in this event, although its exact function is still being uncovered. An understanding of its role during embryogenesis can therefore shed some light not only on the protein itself but also on the intricacies and carefully controlled details of FGF signalling. In an attempt to enhance the understanding of the *X. laevis* orthologue of *mi-er1*, this study of XMI-ER1 was carried out using *X. laevis* as a model system.

Based on the work presented here, and on other studies performed in the laboratory, it is now clear that the over-expression of *Xmi-er1* in *X. laevis* embryos causes them to develop abnormally. Results indicate that as the injected RNA concentration is increased, the percentage of abnormal embryos also increases. These abnormalities are manifested along the length of the anterior-posterior axis of the embryo and vary quite dramatically in their severity. They result in tadpoles with a truncated anteroposterior axis that appears to be shortened from either the anterior end, or the posterior end, or both.

There is a possibility that the variations observed may be due at least in part to the techniques used. The injection of RNA may over time lead to partitioning throughout the embryo causing protein expression to be quite mosaic in nature, as has been demonstrated

by Amaya *et al.* (1991; 1993). The authors found that when embryos were injected at the two-cell stage with XFD, the dominant-negative FGF receptor, a wide range of phenotypes resulted. These included the most severe phenotypes possessing normal heads yet extreme trunk deficiencies, but less extreme and normal embryos were found in each experimental group as well (Amaya *et al.*, 1991). This variability was attributed to the injection technique, which can lead to a non-uniform distribution of RNA and may account for the small percentage of normal embryos that were often obtained in each experimental group for *Xmi-er1* injections. Nevertheless, by acknowledging this limitation, it is still possible to view the overall effects of RNA over-expression on embryonic development. One method that could be employed in future studies of *Xmi-er1* to overcome this limitation is the use of a co-injected RNA, such as β-galactosidase, that can be visualized to determine the expression pattern.

To account for the possibility that the observed effects of *Xmi-er1* over-expression were merely due to the presence of added RNA or to the resulting increase in cell volume, two RNA controls were used in the injection experiments, as well as a DEPC-treated dH_2O control. In addition to this, for each experiment a group of embryos that had not been injected were set aside and scored at the same time as the injected ones. This was to ensure that the effects seen were due to the expressed RNA and not the result of batch variation. By comparing the effects of the *Xmi-er1* injections with the controls, it was clear that the *Xmi-er1* abnormalities were specific. The percentage of abnormal embryos obtained for all concentrations of *Xmi-er1* was significantly higher than those of each control, including the two RNA controls which were injected at 2ng each, the

highest concentration used for *Xmi-er1*. This indicated that it was specifically the expression of XMI-ER1 that caused the abnormal development. Nevertheless, it should be noted that the embryos injected with 2ng of the RNA controls had a slightly higher percentage abnormality than the water-injected or uninjected controls. However, this difference was not shown to be significant by statistical analysis. As well, the values for the RNA controls were still significantly lower than the percentage of abnormal embryos resulting from the lowest *Xmi-er1* concentration.

Two additional RNA controls were actually created in this project through the production of various XMI-ER1 mutant constructs. These were located in the proline-rich motif at the C-terminus and were named $^{365}PS\rightarrow AA$ and $^{365}P\rightarrow A$. Injection of these RNAs consistently resulted in the development of normal embryos despite the fact that they were identical to XMI-ER1 with the exception of one or two amino acids. This confirms that the effects of XMI-ER1 over-expression were specific. Subsequent investigations into the *in vivo* activity of *Xmi-er1* will benefit from the existence of these constructs.

The in-depth analysis of the phenotypic effects of *Xmi-er1* over-expression demonstrates the importance of this gene in the development of both anterior as well as posterior structures. Yet, FGF signalling is known to function in the development of only posterior structures, as seen by the results of expressing XFD (Amaya *et al.*, 1991). One possible explanation for this is that *Xmi-er1* acts in other signalling cascades aside from those triggered by FGF. Although many possible pathways exist, the only additional pathway tested in this study was activin. It was observed that the induction of mesoderm

in animal caps injected with *Xmi-er1* was not reduced when compared with controls. Thus, XMI-ER1 does not appear to act in this pathway. Further analysis of its role in other pathways would have to be done to determine whether the activities of XMI-ER1 does in fact extend beyond the realm of FGF signalling.

Although many other genes have been described that affect either anterior or posterior development when over-expressed, there are few genes known to result in truncations at both ends. *Xcad3*, which is one of these rare examples, belongs to the *caudal* family of genes, well known for their prominent role in posterior development. These genes lie downstream of FGF signalling and upstream of the Hox genes (Isaacs *et al*, 1998), which function in the regulation of anteroposterior specification. The injection of *Xcad3* mRNA into developing embryos produces tadpoles that look quite similar to the *Xmi-er1* phenotype displaying both anterior and posterior truncations (Pownall *et al.*, 1996; Isaacs *et al.*, 1998). It would be interesting to see whether the expression of *Xcad3* and the Hox genes are affected in *Xmi-er1*-injected embryos using RT-PCR. Preliminary results have already demonstrated that at least one gene from the Hox family, the posterior marker *HoxB9*, is down regulated in embryos over-expressing *Xmi-er1* (Luchman, unpublished results).

Although the effects observed for the *Xmi-er1* phenotype varied significantly in different embryos, as a whole this gene appears to be essential for a wide range of tissue types. As muscle, bone, cartilage, and blood vessels make up a large portion of the anterior and posterior structures, some tissues of mesodermal origin are likely to be dependent on XMI-ER1 for proper development. Since the central nervous system also

makes up a significant part of the head, it is possible that some tissue of ectodermal origin may too be controlled by XMI-ER1 activity during development. The association of both of these tissue types with *Xmi-er1* activity was confirmed by whole-mount antibody staining, which showed that muscle, as well as neural tissue, was reduced and disorganized in embryos injected with *Xmi-er1*. Yet, even embryos with the most severe deformities, involving truncations of both the head and the tail, showed positive staining for both tissues analyzed. Thus, tissue differentiation was still possible in *Xmi-er1*-injected embryos. This observation was supported by the FGF mesoderm induction experiments, which demonstrated that *Xmi-er1*-injected embryos exhibited reduced mesoderm induction *in vitro* but that this process was not altogether inhibited.

The fact that these tissues were not entirely absent from any of the embryos stained indicated that while XMI-ER1 may play a role in their formation, it is not wholly responsible for it. Whether additional structures are also influenced by this protein has yet to be discovered and could be the focus of future studies. Additional antibodies could be used to focus in on other tissues using the same technique. As well, histological analysis could indicate the specific structures that are absent in the abnormal embryos and could connect XMI-ER1 activity with these features rather than with the anterior or posterior ends as a whole. Further analysis of the dorsoventral pattern of the neural tube and notochord using histology could determine whether XMI-ER1-associated truncations arise from an interference with patterning along the anteroposterior axis, as problems with the establishment of dorsoventral polarity could cause similar anterior truncations (Wallingford *et al.*, 1997; Isaacs *et al.*, 1998). Knowledge of the particular tissues

affected by *Xmi-er1* over-expression is key to understanding the role of endogenous XMI-ER1 and FGF during normal *X. laevis* development.

The investigation into precisely when *Xmi-er1*-associated abnormalities begin revealed that embryonic development appears normal until soon after gastrulation. The percentages of abnormal embryos at this stage and at tadpole stages were almost identical for each RNA concentration injected. This suggests that the abnormalities observed in the tadpoles were the direct result of difficulties in development that occurred at or near gastrulation, though the exact timing of this disruption is unclear. One possibility that arises with abnormalities at this stage is that they are caused by interference with the convergent-extension movements that occur during gastrulation. Sokol found that overexpression of a dominant negative *Dishevelled* mutant in *X. laevis* embryos caused severe posterior truncations in tadpoles and blocked convergent-extension in ectodermal explants (1996). With respect to XMI-ER1 overexpression, the fact that these movements are still observed in the presence of activin rules out the possibility of abnormal convergent-extension as the cause of the observed gastrulation defects. In order to confirm the precise start of injected XMI-ER1 activity and further insight into what this activity entails, more studies would have to be done perhaps using its cellular localization and molecular markers as an indication of its effects.

With respect to endogenous XMI-ER1, it is known that while the protein is present throughout early development, it does not go to the nucleus until MBT (Luchman *et al.*, 1999), suggesting that this is when it becomes active as a transcriptional regulator. Based on this, it is therefore likely that the effects of *Xmi-er1* over-expression begin

when the protein undergoes nuclear localization and when its endogenous activity also begins, although it is still possible that XMI-ER1 acts earlier in the cytoplasm. As FGF signalling is required for primary mesoderm induction (Amaya *et al.*, 1993), and XMI-ER1 is thought to play a part in this event, an active role for this protein at MBT makes sense. Perhaps the results of this influence are not evident at the gross morphological level until gastrulation movements are well under way, suggesting that cellular motility may in some way be compromised.

Moreover, in addition to the known role of FGF during mesoderm induction, it has also been shown that FGF signalling during gastrulation is required for mesoderm maintenance (Kroll & Amaya, 1996). Experiments with transgenic frogs expressing XFD at this stage demonstrate that embryos develop abnormally due to the de-regulation of mesodermal markers despite the fact that mesoderm induction had occurred normally earlier on. Thus, it is also a possibility that XMI-ER1 acts during this period of FGF-regulated cellular activities. Numerous FGFs are expressed at this stage of development, including eFGF, FGF-2, FGF-3, and FGF-9 (reviewed in Isaacs, 1997), implying that signalling through the FGF receptor, and therefore a potential requirement for XMI-ER1, is a natural occurrence at this time.

One of the mesodermal markers that is affected by the aforementioned experiment involving the de-regulation of FGF signalling during gastrulation, is *Xbra*. Analysis reveals that its expression is completely lost by mid-gastrulation, and as a result embryos develop without a notochord or somites (Kroll & Amaya, 1996). Whole mount *in situ* hybridization experiments with embryos over-expressing *Xmi-er1* demonstrate that while

Xbra expression is not completely knocked out during gastrulation it is partially inhibited. Specifically, examination of its expression pattern at stage 10.5 in these embryos shows that there are gaps in its normally ring-like expression. By this stage in development, endogenous XMI-ER1 has been shown to be localized to the nucleus of all cells in the *X. laevis* gastrula (Luchman *et al.*, 1999), indicating that the injected XMI-ERI should be active in the region of *Xbra* expression at this time. Thus, the activity of XMI-ER1 appears to have an effect on the expression of *Xbra*.

Due to the fact that *Xbra* expression is not completely inhibited, this suggests that there must be additional regulators present in the embryo. The existence of a gap in *Xbra* expression within gastrulating embryos indicates that XMI-ER1 may be acting in a particular subset of mesodermal tissues regulated by FGF. Further investigation of the precise location of the *Xbra* gap would be required to make this conclusion. Pinpointing the exact site of the gap may also link this effect with the original *Xmi-er1* injection site, which was beside the cleavage furrow at the marginal zone and therefore either dorsal or ventral. Analysis of *Xbra* expression following injections that are ventral or dorsal only could provide further insight into the mechanisms involved in this suppression. Identifying the gap in *Xbra* expression as specifically dorsal could also determine the region of the *Xbra* promotor that is used by XMI-ER1 in regulating its expression. Using point mutations and deletion analysis, Lerchner *et al.* discovered two repressor modules within the *Xbra* promotor that regulate Xbra expression differently both spatially and temporally (2000). One was found to control expression in the marginal zone during early gastrulation, while the second was responsible for dorsal mesoderm and ectoderm

expression at mid-gastrula stages. If XMI-ER1 repression of *Xbra* expression in solely dorsal in nature, then it is likely that it acts through this latter module of the promotor. This dorsal effect of XMI-ER1 would explain many of the abnormalities observed both during gastrulation and subsequent development.

A recent study by Hayata *et al.* (2002) analyzed the effect of over-expressing *Mig30*, an organizer-secreted protein, on *Xbra* expression. As with *Xmi-er1*, they too observed a gap in the expression pattern. This was localized at the dorsal marginal zone in 86% of the embryos analyzed (n=14) at stage 10.5. They also found an inhibition of elongation upon treatment of animal caps with activin. The authors hypothesize that the down-regulation of *Xbra* impairs gastrulation movements such as those seen in activin-treated animal caps. It is therefore possible that the same applies to *Xmi-er1*. The problems observed during gastrulation may very well be related to the reduction of *Xbra*. This explanation could easily be extended to the FGF mesoderm induction results as well, as *Xbra* is a known immediate-early gene in this pathway. It could also explain other abnormalities caused by *Xmi-er1*, such as the tissue reductions found with 12/101, and ultimately the *Xmi-er1* tadpole phenotype as a whole. The elongation of the anterior-posterior axis is dependent upon a series of coordinated cell movements (Park *et al.*, 2002) beginning at gastrulation. One possibility is that XMI-ER1 impedes these movements by interfering with signalling and repressing important genes, such as *Xbra*, that are required for proper gastrulation. Perhaps the anterior abnormalities observed in the *Xmi-er1*-injected embryos result from interference with *Xbra* signalling, which in turn affects gastrulation movements and prevents cells from migrating anteriorly. This,

together with the reduction in induced mesoderm seen with the animal cap assays can in fact explain the range of anterior-posterior abnormalities present in the *Xmi-er1* phenotype. While the posterior development is inhibited due to a general reduction of mesoderm induction and patterning, as explained by the induction assays as well as the whole-mount antibody staining, the anterior formation is affected not only by this reduction but also by the impaired gastrulation movements. This latter hypothesis could be tested using migration assays of individual mesodermal cells on a fibronectin substrate (Kwan & Kirschner, 2003). As well, the additional analysis of *Xbra* expression at stage 12.5 could confirm whether gastrulation movements are in fact slowed (Hayata *et al.*, 2002).

With respect to the aforementioned mesoderm induction experiments, the *Xmi-er1*-associated reduction of induced mesoderm was observed at near-threshold levels of FGF only. By increasing the concentration of FGF, the inhibiting effects of XMI-ER1 over-expression were rescued. This ultimately demonstrated that the inhibition of mesoderm induction seen with *Xmi-er1* injections was reversible and therefore specific. While it was already known that XMI-ER1 acts in the FGF-signalling pathway, as it was initially isolated in response to FGF treatment in animal caps, these results further support a regulatory role for endogenous XMI-ER1 in this pathway during mesoderm induction in the embryo.

Besides its role in mesoderm development, FGF is also thought to be involved in the formation of the nervous system (Kroll & Amaya, 1996), by regulating caudal gene expression (Northrop & Kimelman, 1994). This is thought to have a posteriorizing effect

on the neural ectoderm during gastrula and early neurula stages (Cox & Hemmati-Brivanlou, 1995). To determine the full range of effects caused by *Xmi-er1* over-expression, neural tissue was analyzed using the pan-neural antibody, 2G9. Results from these immunostainings indicated that while neural tissue was reduced and disorganized it was not absent. This lends itself to two possibilities: that *Xmi-er1* has a role in the neuralizing effects of FGF, in addition to its part in mesoderm development; and/or that its effect on neural differentiation occurs through other signalling pathways aside from FGF. As *Xmi-er1* appears to regulate anterior as well as posterior development, while the effects of FGF seem to be limited to the posterior nervous system, the latter is a good possibility. To confirm the function of XMI-ER1 in neural development and to isolate the signalling pathway(s) in which it acts, further experiments should be conducted, beginning with an analysis of neuronal markers in *Xmi-er1*-injected embryos compared to controls.

In order to identify the mechanisms by which XMI-ER1 fulfills its functions during embryonic development, a number of the domains located within the protein were investigated by mutational analysis. Initially, the amino acid sequences of these domains were compared with similar sequences in other proteins that were found using BLAST searches. These were analyzed in order to detect specific amino acids that appeared to be highly conserved throughout evolution. However, due to the vast number of conserved residues that were highlighted through this process, and the time limitations associated with this project, not all of these sequences could be investigated. Thus, to a certain extent, the conserved regions of each domain had to be chosen somewhat arbitrarily.

Once these were selected, mutations were made at some of these key residues, and the developmental effects of injecting these constructs were compared with those from the wild-type *Xmi-er1* injections.

The domains that were analyzed using this method included the SANT domain, the ELM2 domain, a putative MEK phosphorylation site, and a proline-rich region. It was expected that if these domains were involved in the activity of the injected protein during development, then the mutation of a critical amino acid within the domain would suppress or interfere with this activity. The subsequent injection of an *Xmi-er1* construct whose function had been compromised was then expected to have no effect on embryonic development.

Results from these injections yielded a number of interesting observations whose validity was confirmed by Western Blot analysis showing similar levels of XMI-ER1 protein expression for all constructs. The deletion of the majority of the ELM2 domain in $\Delta^{175\text{-}236}$*elm2*, did not lead to the development of normal embryos. The tadpoles that developed when injected looked much like those resulting from wild-type *Xmi-er1* injections. It can therefore be concluded that the deletion did not encompass amino acids that were essential to the activity of this domain; or, that this domain was not involved in the events leading to the abnormal effects observed with wild-type *Xmi-er1* over-expression. With respect to the former conclusion, it should be pointed out that at the time this deletion construct was made, the amino acids removed (aa 175-236) were thought to comprise the majority of this domain. It was not until after the experiments were completed that it was discovered in our lab that the ELM2 domain in XMI-ER1

actually includes more amino acids than initially thought and that this additional sequence C terminal to the domain is required for ELM2 and XMI-ER1 activity (Ding *et al.*, 2003). For this reason, it would be interesting to see the effects of injecting an *Xmi-er1* construct that had the whole of the ELM2 domain deleted to see if the results would be any different from those found here. Perhaps the additional residues are key to the function of this particular domain in XMI-ER1 so that by deleting them as well or even on their own, the over-expression effects on embryos would be abolished.

With respect to the second conclusion, it was recently found that within hMI-ER1, the human homologue of XMI-ER1, the ELM2 domain is essential for the recruitment of HDAC1, which is required to enable hMI-ER1 to act as a transcriptional repressor (Ding *et al.*, 2003). It therefore seems unlikely that two proteins that are so similar differ in this function that appears to be so essential. Nevertheless, it is a possibility. XMI-ER1 is known to possess potent transcription transactivational activity (Paterno *et al.*, 1997) and is not known to function as a repressor (unpublished results). Perhaps this difference in transcriptional regulation accounts for the unexpected results observed upon injecting $\Delta^{175\text{-}236}$*elm2* into embryos. Obviously to fully understand these results, more work needs to be done at this level. What can be taken from this, however, is the fact that the amino acids that were deleted in this region were not critical to the development of the abnormalities seen with the wild-type *Xmi-er1* injections.

The second major domain that was tested was the SANT domain. This motif is often found in proteins that are involved in transcriptional regulation as well as in chromatin-regulatory complexes, and has some similarity to the DNA-binding domains

of myb-related proteins (Aasland *et al.*, 1996; Sterner *et al.*, 2002). Recent studies also indicate that SANT-containing regions of a number of co-repressors, including CoREST and SMRT, can bind and activate HDACs (Guenther *et al.*, 2001; You *et al.*, 2001). However, the exact function of the SANT domain in XMI-ER1 is still unknown.

Rather than performing a deletion of the whole domain, the SANT domain was analyzed for the most part using point mutations. In total, four constructs were used in the investigation of this domain. Two mutations were focused on the highly conserved tryptophan at the start of this region; one at a tryptophan located towards the end of the sequence; and the fourth was a deletion of five amino acids situated between the first and second helices within the domain. One recent study focusing on the SANT domain of Ada2 found the first tryptophan residue to be essential to the function of this domain in the protein (Sterner *et al.*, 2002). Two of the four XMI-ER1 SANT domain constructs included mutations of this same amino acid. Sterner *et al.* also demonstrated that the first half of the SANT domain in Ada2 could be directly linked to an interaction with or the recognition of chromatin (2002). In XMI-ER1, three of the SANT domain constructs can be mapped to this region, including $^{277}W \rightarrow A$, $^{277}W \rightarrow G$, and $\Delta^{292}YGKDF$. Nevertheless, injection of all four constructs yielded the same result. That is, like the ELM2 mutant discussed previously, they too caused the same defects seen with wild-type *Xmi-er1* injections. It therefore appears as though the mutations were not located in amino acids that were required for bringing about the abnormalities seen with *Xmi-er1* over-expression, despite comparisons with other SANT domain sequences from other proteins.

Similar results were obtained for injections of the construct containing the

mutated putative MEK phosphorylation site, a domain whose presence is predicted by numerous computer-assisted sequence analysis programs. Again, embryos developed abnormally and caused defects equivalent to those obtained for *Xmi-er1* injections. Thus, despite the changes that were made in this domain, the effects of over-expressing this construct were no different from the effects of over-expressing the wild-type sequence. These results suggest that this putative phosphorylation site is not associated with the abnormalities caused by *Xmi-er1* over-expression, and may not be a true phosphorylation site. Supporting this idea is the fact that the XMI-ER1 protein has never been shown to undergo phosphorylation and instead seems to be associated with other phosphorylated proteins in both its cytoplasmic as well as nuclear states (Luchman, unpublished results).

The final set of mutations were situated within the proline-rich motif located downstream of the SANT domain. In XMI-ER1, this is composed of the following sequence: PSPPP. Often, such regions are involved in binding SH3 domains of a protein that mediates interactions with a second protein. This binding would occur through one of the prolines (Ren *et al.*, 1993). However, the presence of a serine in this region made proline-directed phosphorylation another possibility. Investigation into the activity of this domain revealed that the proline-rich motif functions in the XMI-ER1 protein; that this region mediates the effects seen upon over-expressing wild-type *Xmi-er1*; and, that the activity of this region can be pinpointed to the first proline of this domain.

Once this was observed, the activity of these proline-rich domain constructs was investigated further in comparison with wild-type *Xmi-er1*. Analysis of the mesoderm induction activity for the proline-rich region constructs showed a similar reduction for

^{366}S→A, which, like *Xmi-er1*, causes abnormalities in embryos. However, the remaining two constructs, ^{365}*PS→AA* and ^{365}*P→A*, did not inhibit mesoderm induction activity in the same manner. These results confirm that the proline-rich domain is critical to the formation of abnormalities seen with the over-expression of *Xmi-er1* in *X. laevis* embryos. Further analysis of the effect these proline mutations have on the structure of the XMI-ER1 protein would complement this functional data well.

As for the future of this study, there is obviously a lot of work that has yet to be done in order to fully comprehend the role of *Xmi-er1* in developing *X. laevis* embryos. Nevertheless, the elucidation of the effects that this gene has upon over-expression and some of the tissues this affects are significant endeavours. In terms of the next step, doing the reverse study by knocking out this gene using RNAi or morpholino antisense technology could prove to be very exciting. This, together with the over-expression data, would help explain the various activities of endogenous XMI-ER1 in the embryo. Further analysis of the functional domains and the effects the protein has on additional gene expression and tissue formation would also be very valuable to the understanding of the FGF pathway in this organism. Analysis of molecular markers could paint a clearer picture of XMI-ER1 activity during development. The markers could be used to focus in on what is happening in the specific regions affected by *Xmi-er1* over-expression, such as *otx2* and *XlHbox1* for an anterior analysis, *Xhox36* or *Xhox3* for the posterior, and perhaps *MyoD* as a dorso-ventral mesodermal marker. As well, more work in this area could benefit current and ongoing studies of hMI-ER1 and its activity in human cancers.

References

Aasland, R, Stewart, AF, and Gibson, T. 1996. The SANT domain: a putative DNA-binding domain in the SWI-SNF and ADA complexes, the transcriptional co-repressor N-CoR and TFIIIB. *Trends in Biochemical Science* 21: 87-88.

Amaya, E., Musci, T. J., and Kirschner, M. W. 1991. Expression of a dominant negative mutant of the FGF receptor disrupts mesoderm formation in Xenopus embryos. *Cell* 66: 257-270.

Amaya, E., Stein, P. A., Musci, T. J., and Kirschner, M. W. 1993. FGF signalling in the early specification of mesoderm in Xenopus. *Development* 118: 477-487.

Berrada, W., Naya, A., Iddar, A., and Bourhim, N. 2002. Purification and characterization of cytosolic glycerol-3-phosphate dehydrogenase from skeletal muscle of jerboa (*Jaculus orientalis*). *Mol. Cell. Biochem.* 231: 117-127.

Carballada, R., Yasuo, H., and Lemaire, P. 2001. Phosphatidylinositol-3 kinase acts in parallel to the ERK MAP kinase in the FGF pathway during Xenopus mesoderm induction. *Development* 128: 35-44.

Chang, C. and Hemmati-Brivanlou, A. 1998. Cell fate determination in embryonic ectoderm. *J.Neurobiol.* 36: 128-151.

Christen, B. and Slack, J. M. 1999. Spatial response to fibroblast growth factor signalling in Xenopus embryos. *Development* 126: 119-125.

Christian, J. L. and Moon, R. T. 1993. Interactions between *Xwnt8* and Spemann organizer signaling pathways generate dorsoventral pattern in the embryonic mesoderm of *Xenopus*. *Genes Dev.* 7: 13-28.

Cohen, G., Ren, R., and Baltimore, D. 1995. Modular Binding Domains in Signal Transduction Proteins. *Cell* 80: 237-248.

Conlon, F. L., Sedgwick, S. G., Weston, K. M., and Smith, J. C. 1996. Inhibition of Xbra transcription activation causes defects in mesodermal patterning and reveals autoregulation of Xbra in dorsal mesoderm. *Development* 122: 2427-2435.

Cornell,R. A., Musci, T. J., and Kimelman, D. 1995. FGF is a prospective competence factor for early activin-type signals in *Xenopus* mesoderm induction. *Development* 121: 2429-2437.

Cox, W. and Hemmati-Brivanlou, A. 1995. Caudalization of neural fate by tissue recombination and bFGF. *Development* 121: 4349-4358.

Curran, K. L. and Grainger, R. M. 2000. Expression of activated MAP kinase in Xenopus laevis embryos: evaluating the roles of FGF and other signaling pathways in early induction and patterning. *Dev.Biol.* 228: 41-56.

Dale, L., Howes, G., Price, B., and Smith, J. 1992. Bone morphogenic protein 4: a ventralizing factor in early *Xenopus* development. *Development* 115: 573-585.

Dale, L. and Slack, J. M. W. 1987. Regional specification within the mesoderm of early embryos of *Xenopus laevis. Development* 100: 279-295.

Dale, L., Smith, J. C., and Slack, J. M. 1985. Mesoderm induction in Xenopus laevis: a quantitative study using a cell lineage label and tissue-specific antibodies. *J.Embryol.Exp.Morphol.* 89: 289-312.

Ding, Z., Gillespie, L. L., and Paterno, G. D. 2003. Human MI-ER1 alpha and beta function as transcriptional repressors by recruitment of histone deacetylase 1 to their conserved ELM2 domain. *Mol.Cell Biol.* 23: 250-258.

Eimon, P. M. and Harland, R. M. 1999. In *Xenopus* embryos, BMP heterodimers are not required for mesoderm induction, but BMP activity is necessary for dorsal/ventral patterning. *Developmental Biology* 216: 29-40.

Elinson, R. P. and Rowning, B. 1988. A transient array of parallel microtubules in frog eggs: Potential tracks for a cytoplasmic rotation that specifies the dorso-ventral axis. *Developmental Biology* 128: 185-197.

Fisher, M. E., Isaacs, H. V., and Pownall, M. E. 2002. eFGF is required for activation of XmyoD expression in the myogenic cell lineage of Xenopus laevis. *Development* 129: 1307-1315.

Gilbert, Scott F. Developmental Biology, 1997. Sunderland, Sinauer Associates, Inc.

Gillespie, L.L., Paterno, G.D., Mahadevan, L.C., and Slack, J.M.W. 1992. Intracellular signalling pathways involved in mesoderm induction by FGF. *Mechanisms of Development* 38: 99-108.

Godsave, S., Isaacs, H. V., and Slack, J. M. 1988. Mesoderm-inducing factors: a small class of molecules. *Development* 102: 555-566.

Gospodarowicz, D. 1974. Localisation of a fibroblast growth factor and its effect alone and with hydrocortisone on 3T3 cell growth. *Nature* 249: 123-127.

Gospodarowicz, D. 1987. Isolation and characterization of acidic and basic fibroblast growth factor. *Methods Enzymol.* 147: 106-119.

Gospodarowicz, D., Neufeld, G., and Schweigerer, L. 1986. Molecular and biological characterization of fibroblast growth factor, an angiogenic factor which also controls the proliferation and differentiation of mesoderm and neuroectoderm derived cells. *Cell Differ.* 19: 1-17.

Gospodarowicz, D., Rudland, P., Lindstrom, J., and Benirschke, K. 1975. Fibroblast growth factor: its localization, purification, mode of action, and physiological significance. *Adv.Metab Disord.* 8: 301-335.

Green, J. B. A. and Smith, J. C. 1990. Graded changes in dose of *Xenopus* activin A homologue elicit stepwise transitions in embryonic cell fate. *Nature* 347: 391-394.

Guenther, M., Barak, O., and Lazar, M. 2001. The SMRT and N-CoR corepressors are activating cofactors for histone deacetylase 3. *Mol.Cell.Biol.* 21: 6091-6101.

Harland, R. 1991. In situ hybridization: an improved whole-mount method for Xenopus embryos. *Methods Cell. Biol.*36: 685-695.

Harland, R. and Gerhart, J. 1997. Formation and function of Spemann's organizer. *Annu.Rev.Cell Dev.Biol.* 13: 611-667.

Hartley, R. S., Lewellyn, A. L., and Maller, J. L. 1994. MAP kinase is activated during mesoderm induction in Xenopus laevis. *Dev.Biol.* 163: 521-524.

Hayata, T., Tanegashima, K., Takahashi, S., Sogame, A., and Asashima, M. 2002. Overexpression of the secreted factor Mig30 expressed in the Spemann organizer impairs morphogenic movements during *Xenopus* gastrulation. *Mechanisms of Development* 112: 37-51.

Heasman, J. 1997. Patterning the Xenopus blastula. *Development* 124: 4179-4191.

Heasman, J., Ginsberg, D., Geiger, B., Goldstone, K., Pratt, T., Yoshida-Noro, C., and Wylie, C. 1994. A functional test for maternally inherited cadherin in *Xenopus* shows its importance in cell adhesion at the blastula stage. *Development* 120: 49-57.

Hemmati-Brivanlou, A. and Melton, D. 1992. A truncated activin receptor inhibits mesoderm induction and formation of axial structures in *Xenopus* embryos. *Nature* 359: 609-14.

Herman, M., Ch'ng, Q., Hettenbach, S., Ratliff, T., Kenyon, C., and Herman, R. 1999. EGL-27 is similar to a metastasis-associated factor and controls cell polarity and cell migration in *C. elegans*. *Development* 126: 1055-1064.

Isaacs, H. V. 1997. New perspectives on the role of the fibroblast growth factor family in amphibian development. *Cell Mol.Life Sci.* 53: 350-361.

Isaacs, H. V., Pownall, M. E., and Slack, J. M. 1994. eFGF regulates Xbra expression during Xenopus gastrulation. *EMBO J.* 13: 4469-4481.

Isaacs, H. V., Pownall, M. E., and Slack, J. M. W. 1998. Regulation of Hox gene expression and posterior development by the *Xenopus* caudal homologue Xcad3. *EMBO J.* 17: 3413-3427.

Jones, C.M., Kuehn, M., Hogan, B., Smith, J., and Wright, C. 1995. Nodal-related signals induce axial mesoderm and dorsalize mesoderm during gastrulation. *Development* 121: 3651-3662.

Jones, C. M. and Smith, J. C. An Overview of Xenopus Development, 1995. Totowa, Humana Press Inc.

Jones, E. A. and Woodland, H. R. 1989. Spatial aspects of neural induction in *Xenopus laevis*. *Development* 107: 785-791.

Joseph, E. M. and Melton, D. A. 1997. *Xnr4*: A *Xenopus* nodal-related gene expressed in the Spemann Organiser. *Developmental Biology* 184:367-372.

Joseph, E. M. and Melton, D. A. 1998. Mutant Vg1 ligands disrupt endoderm and mesoderm formation in *Xenopus* embryos. *Development* 125: 2677-2685.

Kao, K. R. and Elinson, R. P. 1988. The entire mesodermal mantle behaves as Spemann's organizer in dorsoanterior enhanced *Xenopus laevis* embryos. *Developmental Biology* 127: 64-77.

Kessler, D. S. and Melton, D. A. 1994. Vertebrate embryonic induction: mesodermal and neural patterning. *Science* 266: 596-604.

Kimelman, D. and Griffin, K. 2000. Vertebrate mesendoderm induction and patterning. *Current Opinion in Genetics and Development* 10: 350-356.

Kimelman, D. and Kirschner, M. 1987. Synergistic induction of mesoderm by FGF and TGF-B and the identification of an mRNA coding for FGF in the early *Xenopus* embryo. *Cell* 51: 869-877.

Kintner, C. R. and Brockes, J. P. 1984. Monoclonal antibodies identify blastemal cells derived from dedifferentiating muscle in newt limb regeneration. *Nature* 308: 67-69.

Kofron, M., Demel, T., Xanthos, J., Lohr, J., Sun, B., Sive, H., Osada, S., Wright, C., Wylie, C., and Heasman, J. 1999. Mesoderm induction in Xenopus is a zygotic event regulated by maternal VegT via TGFbeta growth factors. *Development* 126: 5759-5770.

Kroll, K. and Amaya, E. 1996. Transgenic *Xenopus* embryos from sperm nuclear transplantations reveal FGF signaling requirements during gastrulation. *Development* 122: 3173-3183.

Kuhl, M. 2002. Non-canonical Wnt signaling in Xenopus: regulation of axis formation and gastrulation. *Semin.Cell Dev.Biol.* 13: 243-249.

Kwan, K., and Kirschner, M. 2003. *Xbra* functions as a switch between cell migration and convergent extension in the *Xenopus* gastrula. *Development* 130: 1961-1972.

Larsson, H., Klint, P., Landgren, E., and Claesson-Welsh, L. 1999. Fibroblast growth factor receptor-1-mediated endothelial cell proliferation is dependent on the Src homology (SH) 2/SH3 domain-containing adaptor protein Crk. *J.Biol.Chem.* 274: 25726-25734.

Lee, M., Heasman, J., and Whitman, M. 2001. Timing of endogenous activin-like signals and regional specification of the *Xenopus* embryo. *Development* 128: 2939-2952.

Lerchner, W., Latinkic, B., Remacle, J., Huylebroeck, D., and Smith, J.C. 2000. Region-specific activation of the *Xenopus Brachyury* promotor involves active repression in ectoderm and endoderm: a study using transgenic frog embryos. *Development* 127: 2729-2739.

Luchman, H. A., Paterno, G. D., Kao, K. R., and Gillespie, L. L. 1999. Differential nuclear localization of ER1 protein during embryonic development in *Xenopus laevis*. *Mechanisms of Development* 80: 111-114.

Maeno, M., Ong, R., Suzuki, A., Ueno, N., and Kung, H. 1994. A truncated bone morphogenic protein-4 receptor alters the fate of ventral mesoderm to dorsal mesoderm: the roles of animal pole tissue in the development of ventral mesoderm. *Proc.Natl.Acad.Sci.USA* 91: 10260-10264.

Manes, M. E. and Elinson, R. P. 1980. Ultraviolet light inhibits gray crescent formation in the frog egg. *Wilhelm Roux Arch. Dev. Biol.* 189: 73-76.

Manetti, F., Corelli, F., and Botta, M. 2000. Fibroblast growth factors and their inhibitors. *Curr.Pharm.Des* 6: 1897-1924.

McDowell, N. and Gurdon, J. B. 1999. Activin as a morphogen in Xenopus mesoderm induction. *Semin.Cell Dev.Biol.* 10: 311-317.

Mohammadi, M., Honegger, A., Rotin, D., Fischer, R., Bellot, F., Li, W., Dionne, C., Jaye, M., Rubinstein, M., and Schlessinger, J. 1991. A tyrosine-phosphorylated carboxy-terminal peptide of the fibroblast growth factor receptor (Flg) is a binding site for the SH2 domain of phospholipase C-gamma 1. *Mol.Cell.Biol.* 11: 5068-5078.

Molenaar, M., van der Wetering, M., Oosterwegel, M., Perterson-Maduro, J., Godsave, S., Korinek, V., Roose, J., Destree, O., and Clevers, H. 1996. XTcf-3 transcription factor mediates b-catenin-induced axis formation in *Xenopus* embryos. *Cell* 86: 391-399.

Moon, R. T. and Kimelman, D. 1998. From cortical rotation to organizer gene expression: toward a molecular explanation of axis specification in Xenopus. *Bioessays* 20: 536-545.

Musci, T. J. Amaya E. and Kirschner, M. W. 1990. Regulation of the fibroblast growth factor receptor in early *Xenopus* embryos. *Proc.Natl.Acad.Sci.USA* 87: 8365-8369.

Newport, J. and Kirschner, M. 1982. A major developmental transition in early *Xenopus* embryo: I Characterization and timing of cellular changes at the midblastula stage. *Cell* 30: 675-686.

Newport, J. and Kirschner, M. 1984. Regulation of the cell cycle during early Xenopus development. *Cell* 37: 731-742.

Nieuwkoop, P. D. 1969. The formation of mesoderm in urodelean amphibians. I. Induction by the endoderm. *Wilhelm Roux' Arch.EntwMech.Org.* 162: 341-373.

Nieuwkoop, P. D. Normal Table of Xenopus Laevis (Daudin), 1994, New York, Garland Publishing, Inc.

Northrop, J. and Kimelman, D. 1994. Dorsal-ventral differences in *Xcad-3* expression in response to FGF-mediated induction in *Xenopus*. *Dev.Biol.* 161: 490-503.

Ong, S., Guy, G., Hadari, Y., Laks, S., Gotoh, N., Schlessinger, J., and Lax, I. 2000. FRS2 proteins recruit intracellular signaling pathways by binding to diverse targets on fibroblast growth factor and nerve growth factor receptors. *Mol.Cell.Biol.* 20: 979-989.

Park, E. K., Warner, N., Mood, K., Pawson, T., and Daar, I. O. 2002. Low-molecular-weight protein tyrosine phosphatase is a positive component of the fibroblast growth factor receptor signaling pathway. *Mol.Cell Biol.* 22: 3404-3414.

Paterno, G. D., Li, Y., Luchman, H. A., Ryan, P. J., and Gillespie, L. L. 10-10-1997. cDNA cloning of a novel, developmentally regulated immediate early gene activated by fibroblast growth factor and encoding a nuclear protein. *J.Biol.Chem.* 272: 25591-25595.

Paterno, G. D., Mercer, F. C., Chayter, J. J., Yang, X., Robb, J. D., and Gillespie, L. L. 1998. Molecular cloning of human *er1* cDNA and its differential expression in breast tumours and tumour-derived cell lines. *Gene* 222: 77-82.

Post, J. N., Gillespie, L. L., and Paterno, G. D. 7-27-2001. Nuclear localization signals in the Xenopus FGF embryonic early response 1 protein. *FEBS Lett.* 502: 41-45.

Powers, C. J., McLeskey, S. W., and Wellstein, A. 2000. Fibroblast growth factors, their receptors and signaling. *Endocr.Relat Cancer* 7: 165-197.

Pownall, M. E., Tucker, A. S., Slack, J. M. W., Isaacs, H. V. 1996. *eFGF, Xcad3* and Hox genes form a molecular pathway that establishes the anteroposterior axis in *Xenopus*. *Development* 122: 3881-3982.

Ren, R., Mayer, B., Cicchetti, P., and Baltimore, D. 1993. Identification of a Ten-Amino Acid Proline-Rich SH3 Binding Site. *Science* 259: 1157-1161.

Rowning, B, Wells, J, Wu, M, Gerhart, J, Moon, R, and Larabell, C. 1997. Microtubule-mediated transport of organelles and localization of b-catenin to the future dorsal side of *Xenopus* eggs. *Proc Natl Acad Sci USA* 94: 1224-1229.

Ryan, P. J. and Gillespie, L. L. 1994. Phosphorylation of phospholipase C gamma 1 and its association with the FGF receptor is developmentally regulated and occurs during mesoderm induction in Xenopus laevis. *Dev.Biol.* 166: 101-111.

Schulte-Merker, S. and Smith, J. C. 1995. Mesoderm formation in response to *Brachyury* requires FGF signaling. *Curr.Biol.* 5: 62-67.

Slack, J. M. 1991. The nature of the mesoderm-inducing signal in Xenopus: a transfilter induction study. *Development* 113: 661-669.

Slack, J. M. and Forman, D. 1980. An interaction between dorsal and ventral regions of the marginal zone in early amphibian embryos. *J.Embryol.Exp.Morphol.* 56: 283-299.

Slack, J. M. W., Darlington, B., Heath, J., and Godsave, S. 1987. Mesoderm induction in early *Xenopus* embryo by heparin-binding growth factors. *Nature* 326: 197-200.

Smith, J. C. 1993. Mesoderm-inducing factors in early vertebrate development. *EMBO J.* 12: 4463-4470.

Smith, J. C., Conlon, F. L., Saka, Y., and Tada, M. 2000. Xwnt11 and the regulation of gastrulation in Xenopus. *Philos.Trans.R.Soc.Lond B Biol.Sci.* 355: 923-930.

Smith, J. C., Price, B. M., Green, J. B., Weigel, D., and Herrmann, B. G. 1991. Expression of a Xenopus homolog of Brachyury (T) is an immediate-early response to mesoderm induction. *Cell* 67: 79-87.

Smith, J. C. and Slack, J. M. W. 1983. Dorsalization and neural induction: properties of the organizer in *Xenopus laevis*. *J.Embryol.exp.Morph.* 78: 299-317.

Sokol, S. 1996. Analysis of Dishevelled signalling pathways during Xenopus development. *Curr. Biol.* 6: 1456-1467.

Solari, F., Bateman, A., and Ahringer, J. 1999. The *Caenorhabditis elegans* genes *egl-27* and *egr-1* are similar to MTA1, a member of a chromatin regulatory complex, and are redundantly required for embryonic patterning. *Development* 126: 2483-2494.

Song, J. and Slack, J. M. 1994. Spatial and temporal expression of basic fibroblast growth factor (FGF- 2) mRNA and protein in early Xenopus development. *Mech.Dev.* 48: 141-151.

Sterner, D., Wang, X., Bloom, M., Simon, G., and Berger, S. 2002. The SANT domain of Ada2 is required for normal acetylation of histones by the yeast SAGA complex. *The Journal of Biological Chemistry* 277: 8178-8186.

Sterner, D. E. and Berger, S. L. 2000. Acetylation of histones and transcription-related factors. *Microbiol.Mol.Biol.Rev.* 64: 435-459.

Sun, B., Bush, S., Collins-Racie, L., LaVallie, E., DiBlasio-Smith, E., Wolfman, N., McCoy, J., and Sive, H. 1999. derriere, a TGF-b family member required for posterior development in *Xenopus*. *Development* 126: 1467-1482.

Takahashi, S., Yokota, C., Takano, K., Tanegashima, K., Onuma, Y., Goto, J., and Asashima, M. 2000. Two novel nodal-related genes initiate early inductive events in *Xenopus* Nieuwkoop center. *Development* 127: 5319-5329.

Tannahill, D., Isaacs, H. V., Close, M. J., Peters, G., and Slack, J. M. 1992. Developmental expression of the Xenopus int-2 (FGF-3) gene: activation by mesodermal and neural induction. *Development* 115: 695-702.

Teplitsky, Y., Paterno, G.D., and Gillespie, L.L. 2003. Proline^{365} is a critical residue for the activity of XMI-ER1 in *Xenopus* embryonic development. *Biochemical and Biophysical Research Communications* 308: 679-683.

Vincent, J. P., Oster, G. F., and Gerhart, J. C. 1986. Kinematics of gray crescent formation in *Xeopus* eggs. The displacement of subcortical cytoplasm relative to the egg surface. *Developmental Biology* 113: 484-500.

Vonica, A., and Gumbiner, B. 2002. Xygotic Wnt activity is required for *brachyury* expression in the early *Xenopus laevis* embryo. *Developmental Biology* 250: 112-127.

Wade, P. A., Gegonne, A., Jones, P. L., Ballestar, E., Aubry, F., and Wolffe, A. P. 1999. Mi-2 complex couples DNA methylation to chromatin remodelling and histone deacetylation. *Nat.Genet.* 23: 62-66.

Wallingford, J., Sater, A., Uzman, J., and Danilchik, M. 1997. Inhibition of morphogenic movement during *Xenopus* gastrulation by injected sulfatase: Implications for anteroposterior and dorsoventral axis formation. *Dev. Biol.* 187: 224-235.

Weeks, D. L. and Melton, D. A. 1987. A maternal mRNA localized to the vegetal hemisphere in Xenopus eggs codes for a growth factor related to TGF-beta. *Cell* 51: 861-867.

White, R., Sun, B., Sive, H., and Smith, J.C. 2002. Direct and indirect regulation of *derriere*, a *Xenopus* mesoderm-inducing factor, by VegT. *Development* 129: 4867-4876.

Xue, Y., Wong, J., Moreno, G., Young, M., Cote, J., and Wang, W. 1998. NURD, a novel complex with both ATP-dependent chromatin remodeling and histone deacetylase activities. *Molecular Cell* 2: 851-861.

You, A., Tong, J. K., Grozinger, C. M., and Schreiber, S. L. 2001. CoREST is an integral component of the Co. *Proc Natl Acad Sci U.S.A* 98: 1454-1458.

Zhan, X., Plourde, C., Hu, X., Friesel, R., and Maciag, T. 1994. Association of fibroblast growth factor receptor-1 with c-Src correlates with association between c-Src and cortactin. *J.Biol.Chem.* 269: 20221-20224.

Zhang, J., Houston, D. W., King, M. L., Payne, C., Wylie, C., and Heasman, J. 8-21-1998. The role of maternal VegT in establishing the primary germ layers in Xenopus embryos. *Cell* 94: 515-524.

Zhang, L., Yang, S., and Huang, Y. 2003. Evidence for disaggregation of oligomeric G(o)alpha induced by guanosine-5-3-O-(thio)triphosphate activation. *Biochemistry* 68: 121-128.